Regenerating Pulmonary Vascular Endothelium of Tissue-Engineered Lungs using Endothelial Progenitor Cells and Acellular Scaffolds

A Thesis

SUBMITTED TO THE FACULTY OF

THE UNIVERISTY OF MINNESOTA

BY

Ifeolu A. Akinnola

IN PARTIAL FULFILLMENT OF THE REQUIREMENTS

FOR THE DEGREE OF

DOCTOR OF PHILOSOPHY

UNDER THE MENTORSHIP OF

Angela Panoskaltsis-Mortari, PhD

October 2021

Acknowledgement

I would like to start by thanking my advisor, Dr. Angela Panoskaltsis-Mortari. You took a chance on a bright-eyed student, pushed me to excel in both research and professional aspirations, and believed in my growth and drive throughout my graduate years. To my former and current lab members, I thank you all for your insight, support, and comradery. Carolyn, Haylie, Zach, and Caleb, thank you for all of your help and friendship during my graduate training. Looking back, whether it was a time of excitement or frustration, I couldn't imagine going through graduate school without you all. I would like to thank the VHL, Osborn, and Blazar labs for all their help for providing samples and suggestions for my projects.

I would like to thank the students, faculty, and admins from the Integrative Biology and Physiology graduate program for their support and inclusiveness. In addition to the program and department, I would like to thank the Stem Cell Institute, the Stem Cell Biology T32, Dr. David Ingbar, and the Dinnaken fellowship for their support, both professional and financial, of my graduate training. To Drs. Jop van Berlo, Rita Perlingerio, James Dutton, and Greg Vercelloti, I would like to thank you all for being part of my thesis committee and providing me insight and encouragement.

I would like to thank the UMN Medical Science Training Program, Dr. Yoji Shimizu, and my entering class of 2015. The program has provided me with an amazing opportunity to be creative and achieve goals beyond my imagination prior to my entry and provided me with likeminded colleagues who have made me feel at home in the Midwest. Yoji, you gave me an opportunity and insight from my time in undergrad back in Maryland, and always assured me that my goals were within reach no matter how difficult it may have seemed.

Finally, I would like to thank my family and friends from both graduate and medical school. To my parents and siblings, you all have supported me throughout my career and reminded me of all I had accomplished along the way. To Em and Nat, I couldn't have asked for better friends (or roommates) during my undergraduate and graduate years. I earnestly don't think I would have enjoyed my time in Minnesota half as much without you two. In addition, thank you to all of my friends for the adventures throughout Minnesota, bonding over our graduate experiences, and encouragement throughout my graduate years, I look forward to making more amazing memories with you all.

Dedication

I dedicate this thesis to my family and loved ones.

To my parents, Solaide and Stephen, your love and support have allowed me to come this far and continue forward.

Abstract

Terminal lung diseases damage the organ through substantial irreversible changes to its architecture, leading to a suboptimal level of function. For this patient population, lung transplantation is the primary curative method to re-obtaining their previous quality of life. Relative to other whole organs used for transplant, the acquisition of transplantable lungs is low, resulting in a large deficit of lungs available for patients on the transplant list. Ongoing efforts towards creating functional organs from acellular scaffolds has the potential to address the deficit of lungs. The regeneration of a functional vasculature within acellular organ and tissue scaffolds is a necessity for their overall longevity and function. Current efforts in engineering transplantable lungs with long-term functionality are hindered due to vascular related complications within the newly generated organ. In over to overcome these limitations, improvements in re-endothelialization of scaffolds and acellular tissue are required. The studies described in this thesis provide valuable insight towards characterization of pulmonary endothelial progenitors and cells for re-endothelization, understanding the interaction between endothelial progenitors and vessel-specific extracellular matrices, and the potential for using iPSC-derived angiogenic hemangioblasts for developing vascular endothelium. Within both *in vitro* culture and acellular murine lung matrices, we have successfully characterized a highly proliferative rat pulmonary endothelial progenitor capable of re-endothelialization of the vasculature without site preference and can be used as a model for identifying progenitors in humans that are suitable for tissue engineering and clinical applications. We continued our efforts by using label-free liquid chromatography-mass spectrometry (LC/MS) analysis of decellularized porcine pulmonary vessels to compare the diversity and abundance of various extracellular matrix (ECM) proteins. The data generated from our LC/MS analysis can be used for future quantitative proteomic analyses. The decellularized ECM from both pulmonary arteries and veins were both used to evaluate

their effect on endothelial progenitor maturation, and we were able to detect increase expression of endothelial genes from cells cultured in ECM hydrogels. Finally, we developed a protocol to differentiate human iPSCs into angiogenic hemangioblasts. These differentiated cultures contained sub-populations of $CD31^{+}/VEGF2^{+}$ and VE-$Cadherin^{+}/CD73^{+}$ cells. The outcomes from this study will provide guidance for future experiments and insight on characterizing both endothelial progenitors for re-endothelialization and proteomic analysis of pulmonary vasculature ECM.

Table of Contents

List of Figures

Chapter 2: Engineering Functional Vasculature in Decellularized Lung Depends on Comprehensive Endothelial Cell Tropism

List of Tables

Chapter 2: Engineering Functional Vasculature in Decellularized Lung Depends on Comprehensive Endothelial Cell Tropism

Chapter 1

Background, Objective and Project Aims

Background

Basic Lung Anatomy and Physiology

Within mammalian respiratory systems, the highly vascularized lungs serve as the site of oxygen exchange between the atmosphere and circulating blood (Suresh and Shimoda, 2016; Jain et al., 2021). Breathing – the cyclic process of exhalation and inhalation – removes oxygen depleted air from and brings in oxygen rich air to the lungs. During inhalation the diaphragm and intercostal muscles contract, increasing the size of the thoracic cavity and decreasing pressure within the cavity. As the pressure within the thoracic cavity falls below atmospheric pressure, a negative pressure gradient is created and forces air into the body, starting in the upper respiratory airways (i.e., nasal cavity, pharynx, and upper trachea) and directly into the lower respiratory airways. The lower airways begin with the lower part of the trachea, which branches into the two main bronchi – one entering each lung (Powers and Dhamoon, 2021).

Once in a lung, bronchi continue to split into smaller branches, eventually forming smaller bronchioles, and by the 16^{th} generation of branches, they form terminal bronchioles. This region of the lower respiratory airway, from the trachea to the terminal bronchioles, is known as the conducting zone – where gas exchange between the airspace and blood has yet to occur. The next portion of the lower respiratory airway, known as the transitional and respiratory zones, begins with the respiratory bronchioles, alveolar ducts, and finally ending with air sacs known as alveoli – the primary site of external gas exchange. Though external gas exchange can occur throughout the transitional and respiratory zones, it is more pronounced within the alveoli, or alveolar sacs, as they have the highest density of capillaries and largest combined surface area, measured between 75 and 130 m^2 (Knust et al., 2009; Murray, 2010; Molnar and Gair,

2015). As the diaphragm and intercostal muscles relax, the size and pressure of the thoracic cavity is re-set, and air is forced out of the lungs.

Pulmonary circulation begins with the ejection of oxygen-depleted blood from the right ventricle of the heart into the large pulmonary artery. Initially following the large primary and secondary bronchi as it emerges from the lung hilus, the pulmonary artery quickly branches as it moves to the distal portions of the lung, reaching the regions where gas exchange occurs. Within human lungs, the pulmonary artery forms over 15 generations of branches, each sprouting at various angles within the lung (Townsley, 2012). These arterial branches eventually form into the thinly walled, pulmonary capillaries. The walls of alveoli are covered in the pulmonary capillaries, allowing red blood cells flowing through the vessels to release CO_2 into and take-up O_2 from the alveolar air space. The surface area of the pulmonary capillaries nearly reaches the same levels as the alveoli, also measured at over 100m^2 within a healthy adult (Murray, 2010).

The pulmonary blood-gas barrier, also known as the alveolar-capillary barrier, is located at the interface of alveoli and capillaries. On the alveolar side is the epithelium, primarily formed by type I alveolar cells, thinly stretching along the internal wall of the air sacs. On the vascular side is the continuous pulmonary endothelium, formed by endothelial cells, maintaining the barrier membrane of the vessel. Separating the two cellular layers is the relatively thick basement membrane formed of extracellular matrix proteins, primarily type IV collagen (West, 2009; Weibel, 2017; Leiby et al., 2020).

After external gas exchange occurs, oxygen-rich blood is carried from the pulmonary capillaries into the larger pulmonary veins. Though these veins don’t form the same number of branch generations as the pulmonary arteries, they similarly merge as the course from the distal areas of the lungs, towards the hilus, merging into the primary pulmonary vein and finally, into the left atria. Now within the left side of the heart, the

oxygen-rich blood will quickly be pumped into the aorta from the left ventricle, and throughout the rest of body's cardiovascular system, delivering oxygen and nutrients to other bodily tissues and organs.

Without the continuous process of breathing and external gas exchange, tissues and organs would be quickly depleted of oxygen. Once hypoxia has set in, cellular function will quickly begin to go awry, followed by organ system failure. Amongst its role in other important bodily functions (e.g., blood pressure control, pH balance, protection against infection), its central role in respiration alone establishes the lung as a vital organ.

Severe Lung Disease and Shortage of Lungs for Transplant

Individuals burdened with a progressive lung disease (i.e., interstitial lung diseases, chronic obstructive pulmonary disease, cystic fibrosis, pulmonary vascular diseases) that result in extensive adverse remodeling of their lung structure develop what is known as end-stage lung disease. Once end-stage lung disease has developed, there is minimal lung function left for the afflicted individual and the only curative measure is to undergo a lung transplant (Ohata and Ott, 2000; Del Sorbo et al., 2014). Since 1963, lung transplantation has been used to treat end-stage lung disease and has since increased in efficacy. Despite being a necessary treatment for the livelihood of individuals with end-stage lung disease, there is a severe shortage of lungs for transplant (Del Sorbo et al., 2014). The recovery rate of donor lungs ranges between 15% and 25% - the lowest among all major transplantable organs. In addition, 10% of patients on the lung transplant list die before a lung is available for them to undergo the procedure (Young and Dilling, 2019). Patients who obtain a donor lung face post-operative complications related to extra-pulmonary organ condition, organ rejection, and chronic immunosuppression (Kotloff and Thabut, 2011). According to the International Society

for Heart and Lung Transplantation, between 2000 and 2008, the median survival of a patient after transplant was only 5.7 years (Thabut and Mal, 2017).

Tissue Engineering Lungs Through Decellularization and Recellularization

Acellular tissues retain complex architecture and mechanics, in addition to tissue specific molecules that support recellularization. In the context of lung decellurization, we of the Panoskaltsis-Mortari lab group have developed an efficient protocol for the decellularization of lungs, providing us with a decellularized lung scaffold (DLS) that maintains its extracellular matrix (ECM) components and 3-D ultrastructure. Multiple bioengineering groups have repeatedly shown that the ultrastructure and ECM makeup of scaffolds play a significant role in the differentiation and maintenance of the local stem and progenitor cells (Davis and Senger, 2005; Daly et al., 2012; Crabbe et al., 2015; Ren et al., 2015).

While singular and mixtures of ECM proteins are commercially available for 2D and 3D cell culture, there has been a large increase in the number of biomedical research groups utilizing ECM acquired from decellularized tissue for their studies. Tissue decellularization is the process of removing cellular and genomic material by using a combination of physical, chemical, and/or enzymatic approaches. This leaves behind a biological scaffold that retains the ECM proteins and intricate structure of the original tissue/organ(Gilbert et al., 2006; Crapo et al., 2011).

Decellularization has been in use as early as the 1980s when porcine aortic valves were dissected and decellularized prior to implantation into healthy sheep as a pulmonary valve replacement (O'Brien et al., 1999). Decellularization became more prominent in the 2010s as a way to provide the complex, but necessary physical and biological environment for cells in order to recreate artificial tissue. In addition, decellularized tissue

can undergo different modifications and processing in order to be used in various applications, such as hydrogel formation or coating culture dishes (Claudio-Rizo et al., 2016; Saldin et al., 2017; Sackett et al., 2018; Giobbe et al., 2019).

Decellularization processes need to be tailored to the specific tissue in order to prevent any difficulties in reseeding scaffold for tissue regeneration. Triton X-100 and sodium deoxycholate (SDC) are common detergents used to create acellular tissue, and are usually preferred over harsher detergents, such as sodium dodecyl sulfate (SDS) and CHAPS in order to maintain scaffold architecture and structural proteins (O'Neill et al., 2013; Stabler et al., 2016b). Even if the organ is the same, differences between species can result in differences in the final relative ECM components, such as elastin, despite using the same protocol (O'Neill et al., 2013; Balestrini et al., 2016). At times, even SDC can cause difficulty when reseeding scaffolds, but reductions in concentrations have been beneficial in allowing EC seeding and ingrowth of scaffolds (Simsa et al., 2018; Liu et al., 2019). If not used as a scaffold, the tissue can be broken down further through a mixture of enzymatic, mechanical, and chemical processes to create a heterogeneous mixture of the original ECM components. This new mixture can be used as "ink" for biofabrication purposes or used for formation of a hydrogel, whether alone or with other agents to aid in desired shapes and other physical properties.

The current tools within tissue engineering (e.g., bioprinters, material casting) are unable to achieve the resolution needed to recreate the microstructures and topography observed within either native tissue or ECM scaffolds, including the intricate vascular ECM (Bishop et al., 2017). Decellularized scaffolds used as a starting point for the regeneration of the original tissue or organ are often seeded with primary ECs and EPCs to initiate re-endothelization (Crapo et al., 2011; Bonvillain et al., 2013; Song et al., 2013; Xu et al., 2019). In addition, without further enzymatic or chemical modifications of ECM

scaffolds, there is a preservation of binding sites for EC and other cells that are important for regeneration and maturation of endothelium. Several research groups, including ours have observed the benefits in using EPCs and combination EC seeding of acellular lung scaffolds (Ren et al., 2015; Gilpin et al., 2016; Scarritt et al., 2018; Akinnola et al., 2021). Differential expression of integrins amongst ECs led to phenotypic preference for certain binding sites and vascular regions. Re-endothelization of ovine pericardium scaffolds with ovine ECs has been useful in recreating an endothelium with cobblestone morphology and the ability to handle increasing levels of pressure, similar to that of its native counterpart (Mogaldea et al., 2019).

Vasculature Endothelium and Endothelial Cells

Endothelium cells, and their surrounding tissue, varies depending on which tissue and part of the vasculature is being observed (McCarron et al., 2017). While endothelial cells are generally flat, reaching below 1μm distally and 3μm at the nucleus, arterial endothelial cells are typically thicker than their venous counterparts (King et al., 2004a; Aird, 2007). In addition to thickness, arterial endothelial cells are longer and narrower than the relatively shorter and wider venous endothelial cells due to being exposed to a higher shear stress and flow rate. The long axis of arterial endothelial cell typically aligns with the direction of blood flow. Unlike arterial or venous endothelium, capillary endothelium is given one of three classifications: continuous, fenestrated, or sinusoidal (Pries and Kuebler, 2006; McCarron et al., 2017).

Continuous capillaries completely surround the lumen of the vessel, only allowing for diffusion of the smallest and most hydrophobic molecules. Continuous capillaries are often associated with pericytes, which helps by strengthening barrier permeability and regeneration. These capillaries can be found within the nervous system, skeletal muscle, the heart, and lung (Pugsley and Tabrizchi, 2000; Weibel, 2016). Fenestrated capillaries

are found in tissues where the primary function is either absorption, filtration, or excretion of larger molecules (e.g., small intestines, kidneys, endocrine glands) (Okada et al., 2017; Jourde-Chiche et al., 2019; Dumas et al., 2021). These capillaries are aptly named due to numerous fenestrae or pores (70-100 nm) that are seen throughout the endothelium. At the bottom of these pores are non-membranous diaphragms that are ~5nm in thickness and made of membrane glycoprotein. Finally, the sinusoidal capillaries that are found in organs where there is high traffic of serum proteins and cells in and out of the vasculature. Such organs with sinusoidal capillaries include the liver, bone marrow, and spleen. The endothelium here is described as having an incomplete basement membrane and larger gaps that span 100-200 nm in diameter (Gross, 1992; Sorenson and Brelje, 2014).

The vascular endothelium is the innermost layer of all blood vessels (i.e., the tunica intima), lining every portion of the cardiovascular system (Stary et al., 1992; Sandoo et al., 2010; Rajendran et al., 2013). A monolayer composed primarily of endothelial cells (ECs), the vascular endothelium is involved in multiple regulatory functions such as coagulation, vascular tone, angiogenesis, blood flow, inflammatory response, and barrier permeability. Without proper regeneration of a fully functional endothelium, it can be expected that newly engineered tissues will quickly become dysfunctional and deteriorate, diminishing their overall therapeutic potential. One of the major limitations of tissue-engineered vascular grafts is thrombosis due to suboptimal cell coverage of the endothelium (Pashneh-Tala et al., 2016). Without sufficient cellular coverage of the endothelium, exposed regions of the basement membrane are opportunistic sites for clot formation. In addition, without enough endothelial and supporting cells, the endothelium lacks a sufficient barrier to prevent fluid leakage.

Extracellular Growth Factors and Vesicles

Growth factor (GF) secretion and detection is essential to the development and function of all cells. Within the embryonic mesoderm, migrating mesodermal cells are stimulated by vascular endothelial growth factor (VEGF) via VEGF receptor 2 (VEGFR2) and become angioblasts. These VEGFR2 positive cells in the embryo are fated to become angioblasts and form blood islands. Blood island eventually fuse and form the initial extraembryonic vascular network (Risau and Flamme, 1995; Choi et al., 1998; Ferkowicz and Yoder, 2005; Mammoto and Mammoto, 2019). Whether they are being used in paracrine or autocrine signaling, growth factors must be secreted into the extracellular space before binding to targets on the cell membrane. ECM proteins may also bind to growth factors that are important for angiogenesis and the regulation of endothelium. Laminins contain heparin binding domains that are able to bind to various isoforms of VEGF (Ishihara et al., 2018; Mammoto and Mammoto, 2019). Fibronectin, which plays key roles in cell adhesion and wound healing (Pankov and Yamada, 2002), has also been shown to have VEGF binding sites located on its N and C terminus (Wijelath et al., 2002; Marchand et al., 2019). LN and FN are just two of many ECM proteins that are able to bind to GFs, that can later bind to membrane proteins of ECs. This property of ECM provides researchers with an opportunity to advance current studies addressing GF-cell interaction within 3D cultures by developing methods to slowly deliver GFs to ECs in culture by using GF-enriched ECM embedded with GFs prior to seeding (Meng et al., 2019). ECM materials and GFs can be modified to increase or decrease binding to one another (Martino et al., 2015). This in turn can lend itself to creating synthetic matrices with heparin or chondroitin sulfate molecules to help in delivery of FGF-2, a stimulator of EC proliferation and vessel repair (Liu et al., 2007;

Martino et al., 2015; Seo et al., 2016). This can play a role in wound healing by using GF enriched ECM hydrogels.

In addition to GFs, extracellular vesicles (EVs) exist in the extracellular space as another mode of intercellular signaling for regulating processes such as immune response, senescence, and proliferation (De Jong et al., 2014). EVs are produced by cells and contain a mixture of RNAs, lipids, proteins, and other small cellular materials. EVs can originate from endosomes or plasma membranes, and are known as exosomes and microvesicles, respectively (Raposo and Stoorvogel, 2013). Exosomes have been hypothesized to help regenerate the endothelium by stimulating proliferation, de-differentiation, and even endothelial-to-mesenchymal transition (Baruah and Wary, 2019). ECs can integrate microvesicles from other ECs and endothelial progenitor cells (EPCs) in order to trigger angiogenesis, survival, and proliferation (Deregibus et al., 2007). Exosomes from EPCs and human umbilical vein endothelial cells (HUVECs) have been shown to enhance early stage re-endothelization in rat models after undergoing injury to the endothelium of the carotid artery (Hu et al., 2019). While most EVs are found in culture supernatant and biological fluids, another type, known as matrix-bound nanovesicles (MBVs), has been recently discovered and is embedded within the ECM scaffold (Huleihel et al., 2016). MBVs contain biologically active microRNA and have demonstrated their ability to modify macrophage phenotype (Huleihel et al., 2016) and prevent damage of axon degeneration of ganglion cells post ischemic injury (van der Merwe et al., 2019). While these studies with MBVs have shown a positive effect on immune and neural cells, they both used MBVs derived from porcine urinary bladder matrix and have not shown the effect of MBVs on ECs. EVs as a whole are currently poorly understood, and much work is needed to discover the positive and negative effects of MBVs on the endothelium.

ECM Proteins and Endothelial Regeneration

The process of engineering new tissues, whether it is the reconstruction of an entire heart or formation of a skin flap for implant, is complicated and has need for improvement. For the majority of newly developed tissues, regeneration of the vasculature is a necessity. Creation of high-functioning vasculature is vital for tissues and organs. The vasculature serves as a delivery system for oxygen, nutrients, cells, and biochemical signals, in addition to its role in the removal of toxins and waste. Though vessels may vary in size, layers, and biomechanics, they all share one crucial component: an endothelium.

Accounting for up to 60% of the tunica intima within some vessels, the ECM serves as an environment for local deposition of important nutrients and signals, cellular migration, and waste accumulation (Stary et al., 1992). Previous reviews have reported, in extensive detail, the current understanding encompassing ECM and angiogenesis. These reviews summarized important ECM proteins in relation to angiogenesis, classifying them as either pro-angiogenic or anti-angiogenic (Sottile, 2004; Cheresh and Stupack, 2008; Neve et al., 2014). While many proteins play a role in forming new blood vessels, the major groups of ECM proteins that are known to affect angiogenesis are collagen, laminins, proteoglycan, fibronectin, and thrombospondin (Sottile, 2004; Neve et al., 2014; Mongiat et al., 2016; Marchand et al., 2019). Many of these proteins that directly affect angiogenesis can be found in the basement membrane (BM). As part of the BM, these major proteins often interact closely with each other and ECs, playing a role in cellular adhesion, migration, proliferation, apoptosis, and tube formation (Mongiat et al., 2016; Calle et al., 2017; Marchand et al., 2019).

Collagens (Col) are a family of large, structural, ECM proteins that are abundant throughout tissues and organs. Within the vascular ECM alone there are several types of

collagens as well as related functions. Types I, III, IV, XV, and XVIII are the most abundant forms of collagen within vascular tissue. Type 1 collagen (Col I) can activate the mitogen-activated protein (MAP) kinase pathway in ECs, stimulating their survival (Mongiat et al., 2016). Col I also induces ECs to change cellular shape through suppression of cyclic AMP dependent protein kinase A (PKA). This change in EC morphology results in actin fiber re-organization (Mongiat et al., 2016).

Col IV, along with laminins, heparan sulfate proteoglycans and fibronectin, account for a large proportion of the BM (Marchand et al., 2019). Col IV is arguably the most important collagen within BM. In a study comparing the angiogenic potential of four different commercial microvascular ECs, it was the ECs that had increased secretion of Col IV that displayed full *in vitro* angiogenic capabilities within 30-days of culture (Bahramsoltani et al., 2014). The triple-helix of Col IV is crucial for EC adhesion and migration along the BM. While Col IV has also displayed a necessity for the formation and stabilization of microvessels (Marchand et al., 2019), certain portions of Col IV (i.e. α1, α2, and α3) can be enzymatically cleaved in order to release fragments with anti-angiogenic properties (i.e. arresten, canstatin, and tumstatin, respectively) (Maeshima et al., 2002; Sudhakar et al., 2003; Mongiat et al., 2016). It has been revealed that the anti-angiogenic effects of arresten work through the heterodimeric α1β1 integrin in order to downregulate VEGF-induced proliferation and migration of EC (Colorado et al., 2000). On the other hand, canstatin, which has been linked to a decrease in endothelial migration and tube formation, induces EC apoptosis through down-regulation of FLIP, an anti-apoptotic protein (Kamphaus et al., 2000).

In addition to Col IV, types XV and XVIII both have non-collagenous domains that can inhibit angiogenesis (Petitclerc et al., 2000) and EC migration (Mongiat et al., 2016), though the presence of Col XV within mice has been shown to stabilize microvessels

(Mongiat et al., 2016). The anti-angiogenic protein endostatin can be derived from the NC1 domain of either Col XV or Col XVIII through proteolytic cleavage. The NC1 domain cleaved from the larger collagens is trimeric and also has anti-angiogenic properties before being cleaved further into the monomeric endostatins. Col XVIII-derived NC1 or endostatin inhibits endothelial migration within 3D culture.

Providing support and elastic recoil tissue, elastin is another major ECM component in vasculature, especially in medium and large arteries (Hayden et al., 2005). Elastin can be synthesized by both ECs and vascular smooth muscle cells as either the amorphous component or the microfibrillar component. Both components makeup elastic fibers, which can be found in both the tunica intima and media of vessels (Greenlee et al., 1966; Stary et al., 1992). Despite its importance within vasculature, elastin is often not viewed as a major component of capillary BM (Hayden et al., 2005). The absence of elastin from the BM can be appreciated in the glomerular tufts of kidneys. As intraglomerular hypertension develops, the glomerular capillaries are unable to stretch and rebound from the increase in pressure, leading to thickening of the BM (Sterzel et al., 2000).

In relation to endothelial cells, elastin can affect their function and proliferation through elastin derived peptides (EDPs). EDPs are formed when elastin is broken down into fragments by metalloproteases and other proteases during angiogenesis and vasculogenesis (Robinet et al., 2005). Elastin secreting cells also express elastin binding protein (EBP) that can bind to both elastin and EDPs, which can elicit various responses depending on the bound motif. Such responses to EDP binding include a change of intracellular calcium levels within

ECs which in turn affects vascular tone (Faury et al., 1998). Robinet et al showed that EBP binding a VGVAPG motif-containing peptide by ECs can trigger cell migration and tubulogenesis (Robinet et al., 2005).

Laminins (LNs) are heterotrimeric proteins with α,β, and γ chains, with isoforms 411, and 511 being the most prominent within the BM (Thyboll et al., 2002; Stenzel et al., 2011; Yousif et al., 2013; Marchand et al., 2019). LN 411 has an α4 chain that is known to regulate vascular density via endothelial Dll4/Notch signaling (Stenzel et al., 2011) as well as the deposition of other important BM proteins that interact with ECs (Thyboll et al., 2002). In fact, preventing synthesis of LN 411 via knockout of the α4 chain negatively impacted microvessels within mice due to malformed basement membranes(Thyboll et al., 2002). The α5 chain of LN 511 has an integral role in stabilizing VE-cadherin of endothelial adherens junctions, which affects endothelial shear stress response and permeability (Patarroyo et al., 2002; Di Russo et al., 2017; Song et al., 2017). In a previous study of recombinant human laminin isoforms, LN 511 was found to be associated with increased EC migration and adhesion when compared to LN 411 (Doi et al., 2002). Recently, the expression of *CXCR4*, a gene associated with angiogenic ECs, has been shown to be partly regulated by the interaction between α6 integrin and LN 511. When the production of LN 511 is decreased there is an inhibition of *CXCR4* expression, and in turn a decrease in endothelial sprouting and morphogenesis(Xu et al., 2020).

The basic structure of most proteoglycans (PGs) is a core protein with at least one covalently attached glycosaminoglycan (GAG) chain (Schaefer and Schaefer, 2010; Iozzo and Schaefer, 2015). Vascular PGs can have pro- or anti-angiogenic effects and are classified by location; extracellular, pericellular, and within the ECM (Lepedda et al., 2021). Pericellular PGs are closely associated with the surface of cells and are a part of

the BM. Most pericellular PGs, such as the multimodular perlecan, are heparan sulfate PGs (HSPGs) and can stimulate and regulate angiogenesis by binding to various growth factors (GFs) and presenting them to ECs (Iozzo and Schaefer, 2015; Mongiat et al., 2016; Marchand et al., 2019). Decorin and versican are extracellular chondroitin sulfate PGs (CSPGs) that have anti-angiogenic effects on ECs by sequestering GFs (i.e. VEGF, Insulin GF, FGF and PDGF) (Schaefer and Schaefer, 2010; Iozzo and Schaefer, 2015; Mongiat et al., 2016). Hyaluronan (HA) is structurally different from most PGs due to being a large GAG molecule lacking a core protein and can be found both intra- and extracellularly (Schaefer and Schaefer, 2010; Iozzo and Schaefer, 2015). HA is typically a large protein (>200 kDA) in the ECM but can be broken down to a low-molecular weight (< 200 kDa), especially in pathological states. While High-weight HA has been shown to have anti-angiogenic and immunosuppressive effects on endothelia, low-weight HA has been shown to stimulate inflammation, angiogenesis, tube formation, and EC proliferation/motility (Schaefer and Schaefer, 2010; Iozzo and Schaefer, 2015; Mongiat et al., 2016).

Fibronectin (FN) is a dimeric glycoprotein with variants that can be found either incorporated within an ECM or solubilized in plasma (Pankov and Yamada, 2002; Mongiat et al., 2016; Marchand et al., 2019). Within the BM, FN molecules are situated between ECs and pericytes, aiding in cell adhesion, development, migration, differentiation, and survival (Pankov and Yamada, 2002; Mongiat et al., 2016). FN expression is usually higher during embryonic development, wound healing, and tumor development. Notably, the RGD motif of FN has been shown to initiate EC survival and tube formation during tumor-associated angiogenesis (Tolsma et al., 1993; Kyriakides et al., 1998; Mongiat et al., 2016). In one study comparing the effect of Col I, FN, and gelatin coating on endothelial progenitor cells cultured *in vitro*, progenitors grown on FN

maintained a more immature endothelial phenotype compared to their Col and gelatin cultured counterparts as indicated by higher expression of CD133 and Tie-2. This led into improved *in vivo* angiogenesis when transplanted into rodent models as well as recruitment of endogenous cells in the formation of new vessels (Siavashi et al., 2016).

Thrombospondins are also glycoproteins found in the ECM, but in contrast to FN they are strong inhibitors of angiogenesis, typically preventing the effects of VEGF on EC(Lawler and Lawler, 2012; Mongiat et al., 2016). There are 5 known variants of TSP, but the most studied ones are TSP-1 and TSP-2. Despite promoting EC survival, *in vitro* and *in vivo* assays have shown that they prevent angiogenesis and neovascularization through inhibition of EC migration (Mongiat et al., 2016). In particular, TSP-1 has been observed to enact these effect through binding with CD36, a player in EC binding to the sub-endothelium and non-endothelial cells (Dawson et al., 1997, 1999).

Improving Endothelial Regeneration in Tissue-Engineered Lungs

Bioengineering whole organs, including lungs, with either allogenic or patient's cells would address the challenges associated with organ acquisition and post-operative complications. While tissue engineered constructs developed through biofabrication or bioprinting methods, one of leading methods for regenerating large tissues and organs is the process of decellularization and recellularization. Despite remarkable progress towards developing tissue-engineered lungs for transplant, failure of these lungs is often due to vasculature overload and hemorrhaging into alveoli, indicative of an endothelial lining that lacks integrity and function (Petersen et al., 2010; Doi et al., 2017). Because of these vascular complications, developing and evaluating new methods for reconstitution of the pulmonary vasculature would improve function and longevity of tissue-engineered lungs. A great starting point for improving vascular regeneration within tissue and organ scaffolds is to focus on the endothelium.

As stated above, decellularized tissue is rinsed to remove residual detergents and chemicals, and then used as a starting point for the regeneration of the original tissue or organ. For regeneration of the vasculature, scaffolds are often seeded with primary ECs and EPCs to initiate re-endothelization. Re-endothelization of ovine pericardium scaffolds with ovine ECs has been useful in recreating an endothelium with cobblestone morphology and the ability to handle increasing levels of pressure, similar to that of its native counterpart (Mogaldea et al., 2019). Ill-fitting decellularization processes for creating an acellular scaffold can result in subsequent difficulties during re-endothelization due to complications such as altered tissue architecture or residual detergents and chemicals within the scaffold that are cytotoxic. This can be seen whether re-endothelization of scaffolds takes place *in vitro* (i.e., culture ware, bioreactor) or *in vivo* (i.e., transplant of an acellular scaffold) (Liu et al., 2019).

Objective and Project Aims

Tissue engineering functional lungs is a dire need for patients that require a transplant. Though regenerating lungs from acellular scaffolds has made significant progress over the last decade, many of these have ultimately failed due to the physiological limitations of newly generated pulmonary vasculature, namely leakage from the vessels and spontaneous hemorrhage. The primary objective of this thesis was to address these concerns by investigating methods to improve reinstitution of pulmonary vascular endothelium. The studies presented in the following chapters focus on the characterization of proliferative endothelial progenitor cells found in the pulmonary vasculature, the vessel-specific effects that ECM components from pulmonary arteries and veins have on progenitor cells, and the potential of using hemangioblasts – a bipotent embryonic precursor cell for both endothelial and hematopoietic cells. Hemangioblasts can be differentiated from human induced

pluripotent stem cells, and may be able to serve as an additional cell source for regenerating vascular endothelium. The specific aims

Aim 1 (Chapter 2): Determine the endothelial cell specification needed to generate functional, patent pulmonary vasculature using acellular whole-lung matrices.

Aim 2 (Chapter 3): Compare pulmonary arterial and venous ECM proteins and observe how each affects endothelial progenitors as they become mature endothelial cells.

Aim 3 (Chapter 4): Determine the capacity of human-iPSC derived hemangioblasts to develop functional endothelium in acellular lung scaffolds.

The focus of Chapter 5, the summary and discussion of this dissertation, will be on the significance of characterizing endothelial progenitor cells and understanding their interaction with ECM components specific to the pulmonary arteries and veins. This chapter will also delve into how the findings from this thesis will affect the broader theme of creating tissue-engineered lungs and vasculature.

Chapter 2

Engineering Functional Vasculature in Decellularized Lungs Depends on Comprehensive Endothelial Cell Tropism

Ifeolu Akinnola[1], Daniel R. Rossi [2], Carolyn Meyer [2], Ashley Lindsey [3], Douglas R. Haase[4], Samuel Fogas [2], Michael J. Ehrhardt [2], Rachel E. Blue[4], Andrew. P. Price[2], Max Johnson[2], Diego F. Alvarez [3], Doris A. Taylor [5] and Angela Panoskaltsis-Mortari [2,6]

[1] MSTP, University of Minnesota Medical School, Minneapolis, MN, United States,
[2] Pediatric Blood and Marrow Transplantation and Cell Therapy, University of Minnesota, Minneapolis, MN, United States
[3] Internal Medicine and Center for Lung Biology, College of Medicine, University of South Alabama, Mobile, AL, United States
[4] University of Minnesota Medical School, Minneapolis, MN, United States
[5] RegenMedix, Houston, TX, United States
[6] Pulmonary, Allergy, Critical Care and Sleep Medicine, University of Minnesota, Minneapolis, MN, United States

Frontiers in Bioengineering and Biotechnology Vol. 9 Article 727869

Preface

Tissue engineering using decellularized whole lungs as matrix scaffolds began as a promise for creating autologous transplantable lungs for patients with end-stage lung disease and can also be used to study strategies for lung regeneration. Vascularization remains a critical component for all solid organ bioengineering, yet there has been limited success in generating functional re-endothelialization of most pulmonary vascular segments. We evaluated recellularization of the blood vessel conduits of acellular mouse scaffolds with highly proliferating, rat pulmonary microvascular endothelial progenitor cells (RMEPCs), pulmonary arterial endothelial cells (PAECs) or microvascular endothelial cells (MVECs). After eight days of pulsatile perfusion, histological analysis showed that PAECs and MVECs possessed selective tropism for larger vessels or microvasculature, respectively. In contrast, RMEPCs lacked site preference and repopulated all vascular segments. RMEPC-derived endothelium exhibited thrombomodulin activity, expression of junctional genes, ability to synthesize endothelial signaling molecules, and formation of a restrictive barrier. The RMEPC phenotype described here could be useful for identifying endothelial progenitors suitable for efficient vascular organ and tissue engineering, regeneration, and repair.

Introduction

The treatment of end-stage lung diseases requires lung transplantation, yet there is a severe shortage of available lungs for transplant. Roughly 20% of patients on lung transplant lists are removed before receiving a new lung due to death or becoming too ill to undergo the procedure (Ahya and Diamond, 2019). Tissue engineering using decellularized whole lungs as scaffolding might provide an opportunity to generate functional lungs for autologous transplant in patients for whom there is no other therapeutic alternative. Despite some advancements in lung tissue engineering (Petersen et al., 2010; Song et al., 2011; Calle et al., 2014; Ren et al., 2015; Balestrini et al., 2016), to date, the establishment of a functioning vasculature with low thrombogenicity and adequate barrier function has proven to be difficult, resulting in lung failure. Although synthetic vascular grafts are utilized clinically for simple vessels (Deutsch et al., 2009) current synthetic materials can mimic neither the anatomical placement of cells interacting at the air-liquid interface, the native mechanical properties of the lung, nor the complex organ compositional and micro-environmental cues needed for geospatial branching. Perfusion-based decellularization provides an alternative approach that preserves the lung's native architecture and extracellular matrix composition, overcoming these challenges (Price et al., 2010; Daly et al., 2012). Decellularized lungs provide the ideal biomimetic cues for appropriate cell localization, differentiation, and function. Such three-dimensional niches are conducive to physiological cell-matrix and cell-cell crosstalk, potentially enhancing the functionality and stability of engineered, transplantable organs.

Whole complex solid organ regeneration, while still in the early stages, has rapidly matured since the initial demonstration for the heart (Ott et al., 2008; Gilpin et al., 2016). Bioengineered lungs implanted in rats showed evidence of successful gas exchange for

up to 7 days (Song et al., 2011), and a similar method is being developed using a nonhuman primate model (Bonvillain et al., 2012). Bioengineered lungs have also been successfully implanted into large, non-primate mammals lasting up to 2 months, without acute rejection, where the implanted lung displayed continued growth and restoration of native microbiota (Nichols et al., 2018). While the longevity of a lung transplant depends on many different factors, the functionality of engineered grafts has faltered primarily from their susceptibility to thrombus formation and barrier leakiness (Petersen et al., 2010; Kurobe et al., 2012; Balestrini et al., 2016; Liu et al., 2018). In native tissues, the endothelium regulates hemostasis and thrombosis, forming a functional barrier that allows for selective permeability (Feletou and Vanhoutte, 2006; Aird, 2007). The primary goal of this study was to determine the endothelial cell specification necessary to generate functional, patent pulmonary vasculature using acellular whole lung matrices in bioreactor conditions. We show the identification of a pulmonary endothelial cell population from a single source that can overcome selective tropism, recellularize all vascular areas of an acellular lung scaffold, and provide a functional barrier.

Material and Methods

Animals: Male B10.BR mice were bred in-house at the University of Minnesota Research Animal Resources facility and used at 8–12 weeks of age. Sprague Dawley rats were purchased from Charles River Laboratory, housed at University of South Alabama, and used at 4 months of age. All experiments were approved by the Institutional Animal Care and Use Committees of the respective institutions.

Perfusion based decellularization of whole mouse lungs: Mouse lungs were decellularized as previously published (Price et al., 2010). Lungs were excised *en bloc* with the trachea and heart, and were perfused with sequential solutions of deionized water, 0.1% Triton X-100, 1% 3α,12α-dihydroxy-5β-cholanic acid sodium salt

(Na deoxycholate), 1 M NaCl, then 30 mg/ml porcine pancreatic DNase in 1.3 mM $MgSO_4$ and 2 mM $CaCl_2$, followed by a final rinse with sterile, deionized water. Cell removal was verified via 4′,6-diamidino-2-phenylindole (DAPI) immunofluorescence (Vector Labs) confocal microscopy (Olympus FV500) on cryosections of representative lungs processed at the same time for quality control purposes, as well as DNA quantitation using the PicoGreen Assay (Price et al., 2015). Decellularized scaffolds were maintained at 4°C in PBS containing pen/strep to maintain sterility.

Isolation and culture of rat endothelial cells: PAECs, MVECs, and RMEPCs were isolated from Sprague-Dawley rats and cultured as previously described (King et al., 2004b; Alvarez et al., 2008). For PAECs, the main pulmonary artery was dissected from the root to a second vessel generation and under sterile conditions placed in a 60 mm dish containing ice-cold DMEM (GIBCO). The vessels were inverted, the intima was scraped, and the collected cells were strained with a 20 μm filter (BD Biosciences). Harvested cells were transferred to a T75 flask, supplemented with DMEM enriched with 20% FBS (Hyclone) and 100 U/ml penicillin-100 μg/ml streptomycin (GIBCO) and were incubated at 37°C with 5% CO_2-21% O_2. For MVECs, the distal lung parenchyma was sliced, and the subjacent tissue was carefully dissected and placed in a 60-mm dish containing cold DMEM (4°C). Tissue was digested with type II collagenase (Worthington), rinsed with DMEM, transferred to a T75 flask, and incubated as described for PAECs. Cell culture medium was replaced with DMEM + 10% FBS and 1% penicillin/streptomycin and passages 5–7 were used for consecutive experiments. Cells were selected for homogeneity based on morphological appearance and tested by flow cytometry as described below. For RMEPCs, cells were selected after subjecting MVECs to a single-cell clonogenic assay as described (Alvarez et al., 2008). All cells were screened for *mycoplasma* (Lonza #LT07) and found to be negative.

Flow cytometry characterization of rat endothelial cells: PAECs, MVECs, RMEPCs were characterized by flow cytometry using a FACSCalibur (BD Biosciences) and analyzed with Cyflogic software. Cells were phenotyped using antibodies to rat CD31 (Abcam #ab28364), CD34 (BD Biosciences #341071), CD62P (Takara Bio #M062), CD104 (Millipore #AB 1922), CD146 (R&D Systems #FAB3250P), eNOS (Santa Cruz #sc654), VE-Cadherin (Santa Cruz #sc9989), VEGF (Santa Cruz #sc507), vWF (Affinity Biologicals #SARTW), and lectins from *Griffonia simplicifolia I and II* (GSI and GSII, EY Laboratories #F-2401-B-1 and #R2402-2), and *Helix pomatia* (HP, EY Laboratories #R3601-1 and F3601-1).

Gene expression: mRNA from recellularized lungs and cells grown in tissue culture flasks was analyzed using the RT2 Profiler PCR Array for Rat Tight Junctions (Qiagen, Valencia, CA). cDNA was generated using the RT2 First Strand Kit (Qiagen) following the product insert. Quantitative real-time PCR was performed on an ABI 7500 Real Time PCR System using the RT2 SYBR Green ROX qPCR MasterMix (Qiagen). Results were entered into the Ingenuity pathway analysis program (Ingenuity Systems, Inc.). Relative gene expression analyses of LDL-receptor, scavenger receptors and integrins was done by isolating total RNA from cells with TRIzol (Invitrogen, Carlsbad, CA), generating cDNA using the Superscript III First Strand RT PCR kit (Life Technologies), and qRT-PCR done using Taqman Universal PCR MasterMix (Life Technologies). For analysis, samples were only used in comparison if they met our cutoff criteria (i.e., CT values ≤ 35 and dCT Std Err ≤0.25). The probes used for these analyses were ordered from Life Technologies (Grand Island, NY) and listed in **Table 2.5**. For analysis of LDL-receptor and scavenger gene expression, samples from each cell line underwent serum starvation overnight prior to obtaining total RNA.

In vitro tube formation assay: Tube formation assays were performed as previously published (Chung-Welch et al., 1989). PAECs, MVECs, and RMEPCs were seeded at 4 × 10^4 cells per well, in triplicate, of a 24-well plate coated with 100 µL/cm^2 BD Matrigel (BD Biosciences) and incubated at 37°C, 5% CO_2. Cultures were imaged with a phase-contrast microscope (Leica) 2, 4, 8, and 24 h post-seeding.

Assessment of endothelial function: Dil-Ac LDL (1,1′-dioctacecyl-1,3,3,3′3-tetramethyl-indocarbocyanine perchlorate acetylated low density lipoprotein) uptake in PAECs, MVECs, and RMEPCs was measured in confluent cultures using previously published methods (Chang et al., 2009). Cultured cells were incubated with 10 µg/ml Dil-Ac LDL (ThermoFisher) for 4 h before analyzing for fluorescence at 550 nm (Leica). For reseeded lung scaffolds, 10 µg/ml Dil-Ac LDL was added to the bioreactor media 7 days after seeding to assess uptake. To prepare for histological analysis, lung constructs were inflated with PBS:OCT (1:3 ratio), embedded in OCT, frozen in liquid nitrogen and stored at -80°C. Cryosections (7 µm) were air dried, fixed with methanol (4°C) for 10 min and air dried for 30 min. Slides were then rinsed twice with PBS for 3 min, then with PBS-Tween 20 (0.2 M PBS, 0.05% Tween 20, pH 7.4) twice for 2 min before coverslipping with VectaShield mounting medium (Vector Labs) containing nucleic acid stain 4′,6-diamidino-2-phenylindole (DAPI) and imaged using a confocal microscope (Olympus FV500).

Bioreactor assembly: T-25 flasks were modified in sterile conditions. Holes were created through the vented filter cap and on the bottom of one wall just large enough to allow passage of 2 mm outer diameter Puri-Flex tubing (Masterflex) through both holes. This allowed for continuous circulation of liquid out from the bottom of the bioreactor, through an adjustable Masterflex pump, and back in through the cap, terminating with a 20-gauge x 1 ½″ disposable murine gavage needle (Cadence Science) serving as a

cannula for the heart/lung bloc. A hole was created in the right ventricular wall to allow insertion of the rubberized gavage needle tip to access the pulmonary trunk (main pulmonary artery).

Reseeding decellularized lungs with endothelial cells: The bioreactor set up, cell seeding protocol and assay endpoints are shown in **Figure 2.1A**. Decellularized lungs were perfused in a humidified bioreactor at 37°C/5%CO_2/21%O_2 with 25 ml PBS for 1 day (24 h), then with 25 ml of DMEM containing 10% FBS and 1% penicillin-streptomycin (complete media) for 1 day (24 h) prior to reseeding. Endothelial cells were washed with PBS and lifted from their tissue culture dish via 0.05% trypsin/EDTA, centrifuged for 5 min at ×2,000 g, and resuspended at 1 × 10^7 cells/ml. The cell suspension was filtered using a 40 μm pore mesh and loaded in a 3 ml luer lock syringe, for a total of 3 × 10^7 cells injected into each pair of decellularized lungs. The 20-gauge x 1 ½″ disposable gavage needle cannulating the decellularized heart/lung bloc was then attached to the syringe and placed in an automated syringe pump set at 0.6 ml/min. During the 5 min cell infusion, a 15 ml conical tube was placed under the lungs to collect flow for a final cell count and viability analysis. 25ml of fresh complete media was then added to each flask. After cell infusion, the gavage needle was removed from the luer lock syringe and attached to the bioreactor tubing. Air bubbles were avoided by priming the tubing before connections were made. The reseeded lungs were incubated in a humidified chamber at 37°C/5%CO_2/21% O_2 for 2 h prior to beginning vascular perfusion. Flow rates began at 1 ml/min on Day 3 (for 36 h), increased to 3 ml/min on Day 4 (for 36 h), increased again to 10 ml/min on Day 6 (for 72 h), and then slowed to 1 ml/min on Day 9 prior to the start of the acetylated LDL uptake or thrombogenicity assays. Media was replaced 24 h after cell seeding and then every 48 h thereafter. The lungs were then removed from the

bioreactor to be frozen. Frozen lungs were rinsed with PBS, infused with PBS:OCT (1:3 ratio), embedded in OCT, flash frozen in liquid N_2 and stored at −80°C.

H&E and Immunofluorescence staining of reseeded lungs: Frozen lung cryosections (7 μm) were prepared as described above. Sections were blocked with 10% normal horse serum for 30 min at room temp and incubated in the dark overnight at 4°C with 1 μg/ml rabbit-anti- VEGF (Santa Cruz #sc507) and sheep-anti-vWF (Affinity Biologicals #SARTW) primary antibodies. Sections were rinsed with PBS-Tween 20 before incubating 30 min at room temp with 1:1,000 Goat Anti-Rabbit IgG TRITC (Jackson #111-025-003) and Donkey Anti-Sheep IgG FITC (R&D Systems #F012F) secondary antibodies, then rinsed 3 times with PBS-Tween 20 for 2 min before coverslipping with VectaShield mounting medium (Vector Labs) containing DAPI. Absence of mouse cells was confirmed by negative PCR for murine GAPDH as described (Price et al., 2010).

Thrombomodulin activity assay: Measuring function of thrombomodulin (CD141) on endothelial cells was adapted from previously published studies (Calnek and Grinnell, 1998; Ibrahim and Ramamurthi, 2008; Robertson et al., 2014). Positive control lungs were excised from euthanized (sodium pentobarbital, 50 mg/kg) adult male B10.BR mice with the trachea and heart attached; after exsanguination via the right ventricle, the heart-lung bloc was perfused with PBS. After 7 days in bioreactor (Day 10), all lung (controls and reseeded) constructs were perfused for 15 min at 3 ml/min with 25 ml phenol red-free DMEM/F12. They were then perfused for 45 min at 1 ml/min with 4 ml phenol red-free DMEM/F12 plus human α-thrombin (0.1 U/ml) and human protein C (12 μg/ml). In triplicate, 100 μl was transferred to a 96-well plate and incubated for 5 min at 37°C with excess hirudin (6 U/ml) to inactivate the α-thrombin. S-2366 (Chromogenix) was added for a final concentration of 0.75 mM and incubated at room temperature for 5min before measuring absorbance at λ = 410 nm and λ = 490 nm (BIORAD Model

550). The relative absorbance was calculated by subtracting the mean acellular absorbance (λ = 410 nm from λ = 490 nm) from each sample.

Vascular permeability assay: To assess vascular barrier function in recellularized lungs, Evans blue (EB)-tagged bovine serum albumin (BSA) was perfused through the vasculature and measured using a near-infrared spectrophotometry method adapted from previously published studies (Lowe et al., 2010; von Drygalski et al., 2012). Decellularized and recellularized, and exsanguinated control mouse lung/heart blocs were weighed and perfused for 5 min with phenol red-free DMEM, then for 15 min with 0.4% EB-tagged BSA (EB-BSA) in phenol red-free DMEM, followed by a 5 min perfusion with 4% BSA in PBS before immersing and gently shaking in PBS as a final rinse. The hearts were then removed and weighed to obtain accurate lung weights for data normalization. EB-BSA content of each lung was then analyzed immediately using a Li-COR Odyssey scanner reading at 700 nm at a resolution of 169 μm and “Intensity” = 2. The lungs were scanned at three distinct focal planes (2, 3, and 4 mm) and the average of the three planes was then normalized to lung weight for a final measure of EB-BSA permeability.

In addition to evaluating EB-BSA permeability of recellularized lungs, isogravimetric and lung perfusion methods were used to recorded absolute change in weight of RMEPC-recellularized, decellularized and native mouse lungs. Gavage needles were inserted though the right ventricles in order to use the heart as conduit to the pulmonary vasculature. The trachea was then attached to an isometric force transducer (Harvard Apparatus) with a suture. 2 mm OD Masterflex tubing submerged in a 50 ml conical filled with PBS was primed and connected to the gavage needle while a P75 Hugo Sachs Elektronik pressure transducer (Harvard Apparatus) was added inline. A peristaltic pump was turned on to begin perfusion of the pulmonary vasculature with PBS. Every 5 min,

measurements from the pressure and force transducers were taken, followed by an increase in flow rate. This process continued until maximum flow rate from the pump was achieved. Data Acquisition ActiveX™ (DTx-EZ, Quick DataAcq) was used to record measurements from the pressure transducer. Results were recorded into Microsoft Excel, where average slope of each sample ($\Delta V_{Force}/\Delta V_{Pressure}$) and the average for each group was calculated.

Cytokine assays: Supernatants from endothelial cell cultures and effluent collected from decellularized and recellularized lungs (48 h collections) were assessed for levels of cytokines and soluble mediators that have been shown to play roles in angiogenesis, vascular integrity and permeability. Samples were evaluated for CXCL1, TIMP1, PAI1, and VEGF via the Luminex platform (Austin, TX) using rat-specific bead sets from Millipore (Billerica, MA) and data analyzed with BioPlex software (BioRad, Hercules, CA).

Statistical significance: Comparisons between control, decellularized, and recellularized lungs were analyzed by using one-way ANOVA using Tukey as a post-hoc test (R x64 2.15.0 statistical software). $p < 0.05$ was considered significant.

Results

Characterization of Pulmonary Endothelial Cells

All cultured rat pulmonary endothelial cells used in these studies were capable of *in vitro* tube formation in Matrigel as previously demonstrated (Alvarez et al., 2008). Functionality of the cultured rat endothelial cells was confirmed *in vitro* by demonstrating uptake of Dil-Ac LDL (**Figure 2.9**). In addition, PAECs, MVECs, and RMEPCs were assessed by flow cytometry to confirm the phenotypes perfused into the decellularized lungs. RMEPCs were negative for CD31 (PECAM-1), whereas PAECs and MVECs stained positively (**Figure 2.2**). RMEPCs expressed less CD62P (P-selectin), and more

CD146 (MUC18) when compared to PAECs and MVECs. Consistent with their endothelial phenotype, all cells displayed high levels of CD144 (VE-Cadherin) and eNOS, and lacked expression of CD34 (mucosialin) and CD45 (leukocyte common antigen). RMEPCs and MVECs were differentiated from their PAEC counterpart by their higher binding to lectins GSI, with low or negative binding to GSII and HPA, consistent with our previous report (Alvarez et al., 2008).

Gene expression of LDL-receptor, multiple scavenger receptors, as well as multiple integrin chains were assessed within PAECs, MVECs, and RMEPCs via qPCR within 2D cell culture. Fold change of genes for LDL-receptor and selected scavenger receptors (i.e., Scara1, Scara4, Scarf1 and Scarf2) were measured in both normal and serum starved conditions. Within both normal and serum starved conditions, all three pulmonary endothelial cell types had measurable expression of LDL-receptor, scavenger receptor class F, member 1 (Scarf1) and class F, member 2 (Scarf2). RMEPCs were the only cell type with measurable expression of Scara1 while PAECs were the only cell type with measurable expression of Scara4. For expression of selected integrin chains (i.e., αv, β1, β2, and β5), PAECs displayed the highest relative expression of αv, β1and β5. RMEPCs had the highest relative expression of β2 and virtually no expression of β1. Reported RQ values were normalized to fresh rat lung, which is comprised of multiple cell types, thus accounting for seemingly lower RQ values amongst some of our target genes.

From the assessment of endothelial markers and gene expression, we have established the overall phenotype of our RMEPCs as $CD31^{-}$, $CD45^{-}$, $CD144^{+}$, $eNOS^{+}$, $CD62P^{lo}$ cells with strong and weak binding to GSI and HPA, respectively. In addition, they have relatively higher gene expression of Scara1 and Itg-β2, compared to PAECs and MVECs.

Selective populations of endothelial cells and progenitor cells are necessary for segment-specific revascularization of decellularized lungs

PAECs, MVECs and RMEPCs were infused into the lung vasculature via the pulmonary artery trunk. Remarkably, when cells of arterial origin (PAECs) were used to reseed the tissue, only extra-capillary vessels were recellularized. In contrast, areas of lung that originally housed microvascular endothelium remained acellular. The reverse was seen when cells of microvascular origin (MVECs) were used to re-endothelialize the vasculature: cells were observed in microvasculature (capillaries) whereas extra-capillary vessels remained acellular. Interestingly, progenitor enriched endothelial cells (RMEPCs) had tropism for both larger vessel (i.e., extra-capillary) and microvascular (capillary) ECM and showed more matrix coverage when compared to lungs reseeded with PAECs or MVECs alone (**Figure 2.3A**). Importantly, RMEPCs displayed attachment within both extra-capillary and capillary vessels when compared to PAECs and MVECs after 8 days of incubation (**Figure 2.3A**). RMEPCs displayed widespread expression of VE-Cadherin/CD144–a major protein in establishing membrane permeability (**Figure 2.3B**). The detection of VE-Cadherin supports the use of RMEPCs to recreate a functional barrier membrane throughout the decellularized vasculature. Together, the data indicate that endothelial cells derived from the microvascular segments and enriched for progenitors can revascularize all pulmonary segments.

Revascularized Lung Scaffolds Retain Endothelial Cells that Maintain Functional Attributes

In **Figure 2.4**, decellularized mouse lungs reseeded with RMEPCs showed positive staining for PECAM-1 (CD31) and cytosolic vWF and VEGF after 8 days of incubation. This indicates that RMEPC possess the capacity to adopt a mature endothelial phenotype and retaining fundamental molecular cues for their functional behavior.

Binding to GSI and HPA lectins could not be used to distinguish endothelial subtypes since these lectins could also bind to decellularized lung ECM.

Figure 2.5A shows that decellularized mouse lungs reseeded and incubated for 7 days with rat PAECs, MVECs, or RMEPCs could take up Acetylated LDL. Thrombomodulin activity, relative to non-decellularized mouse lung controls (**Figure 2.5B**), was significantly increased in decellularized mouse lungs reseeded with RMEPCs compared with lungs reseeded with MVECs or PAECs or a combination of MVEC and PAECs (MV + PA). Collectively, these data demonstrate the extraordinary capacity of RMEPCs to generate endothelium barriers with functional behaviors.

RMEPC-reseeded decellularized lung scaffolds display enhanced repopulation and functional barrier properties

To demonstrate that decellularized lungs reseeded with rat RMEPCs could maintain a functional barrier, lungs (after 8 days incubation) were perfused with EB-tagged BSA for 5 min. After clearing the vasculature with PBS, lungs were imaged for near-infrared fluorescence that can detect any albumin-conjugated-Evans Blue dye leaking into the pulmonary interstitium and airway space. As shown in **Figure 2.5C**, intact control lungs displayed marginal vascular leak as evidenced by the low detection of extra-vascular albumin. In contrast, decellularized lungs exhibited substantial vascular leak as evidenced by the high levels of extra-vascular albumin detected. Decellularized lungs reseeded with RMEPCs demonstrated low vascular leak approximating that exhibited by intact control lungs, indicating significant re-endothelialization of the lung scaffold. Importantly, **Figure 2.5D** shows that lungs reseeded with RMEPCs respond to α-thrombin with an increase in vascular permeability, albeit higher than the response of intact normal lungs. Therefore, lungs re-endothelialized with RMEPCs not only generated barriers that restrict the movement of fluid and solutes from the vascular to

the interstitial space but formed a barrier that responds to a circulating agonist known to increase permeability.

Further evidence of tight barrier formation was obtained by measuring expression of tight junction and cell adhesion genes by qRT-PCR. Comparisons were made for RMEPCs grown to confluence vs. non-confluence in 2D tissue culture, those grown on decellularized lung ECM scaffolds versus 2D tissue culture, and versus rat PAEC and MVEC cells in 2D and on decellularized lung ECM in pulsatile flow conditions. **Figure 2.6** and **Table 2.1** show the top upregulated mRNAs in RMEPCs grown to confluence on plastic, with the highest being MAGI2, a gene that encodes for membrane-associated guanylate kinase inverted two protein. MAGI2 was further upregulated when RMEPC were grown on decellularized lungs under flow conditions. Growth on lung ECM also caused upregulation of several claudins as well as cadherin 5 (**Tables 2.2** and **2.3**). Since endothelial cells also respond to fluid flow and shear stress, mRNA expression of RMEPCs reseeded in decellularized lungs were compared in conditions of flow vs. no-flow (**Table 2.4**). In flow conditions, expression of many tight junction genes was downregulated compared to no-flow conditions (i.e., they were higher in no-flow), a finding that is consistent with the formation of mature junctions *in vivo*. **Figure 2.7** shows that in conditions of flow, expression of HIF-1a and caspase-3 mRNAs were decreased compared to no-flow conditions when RMEPCs were seeded on decellularized ECM, indicating that flow decreases apoptosis and hypoxia in the endothelial cells as expected.

To further evaluate the function of reseeded cells, effluents from PAEC-, MVEC- or RMEPC-infused matrices were examined for secreted vascular factors. **Figure 8A** shows that RMEPC-seeded matrices secreted higher levels of PAI-1, TIMP-1 and VEGF-A compared to those seeded with MVECs, PAECs, or MVECs + PAECs.

RMEPC-seeded lung scaffolds secreted levels of CXCL1 similar to PAEC-seeded scaffolds and were higher than those seeded with MVECs or MVECs + PAECs. Analysis of cell culture supernatants of these cells grown in tissue culture flasks (**Figure 8B**) showed that, within 2D culture, RMEPCs had the highest production of VEGF-A and TIMP-1, while levels of PAI-1 and CXCL1 were similar between RMEPCS and PAECs (and higher than MVECs). The discrepancies seen between cells grown in culture flasks versus those in reseeded lung scaffolds highlight the effect of ECM on signaling cytokine production in the three endothelial cell populations.

Final Conclusions and Discussion

We have described a pulmonary endothelial cell population generated from microvasculature that can functionally recellularize heterogeneous vascular segments of decellularized lung scaffolds. Perfusion of the vasculature with a pulsatile flow of endothelial populations enriched with progenitor cells assembles functional pulmonary vasculatures using a xenogeneic reseeding approach. Moreover, infused mature pulmonary microvascular endothelial cells consistently display selective tropism for their vascular segment of origin, whereas PAECs prefer to repopulate larger vessel conduits. Along with work conducted by other groups (Marcu et al., 2018; Scarritt et al., 2018), this observation indicates that engraftment into specific vascular segments is dependent on the endothelial cell phenotype when using mature endothelial cells. Importantly, infused endothelial progenitor cells were stable for up to 10 days post initial infusion and, under the flow conditions utilized, they retained functional endothelial attributes and developed functional restrictive barriers. Our findings provide the basis necessary for developing functional, autologous, transplantable lungs capable of gas exchange, proper hemodynamics, and incorporation into the host's circulatory system without thrombogenicity. In addition, the phenotypic characterization of cells capable of such re-

endothelialization could be useful for identifying endothelial progenitors suitable for efficient vascular organ and tissue engineering, regeneration, and repair.

Endothelial cells lining the pulmonary arteries, veins, and alveolar capillaries exhibit remarkable heterogeneity both in structure and in function. Ultrastructural analysis indicate that endothelial cells derived from the pulmonary artery (PAECs) reside in thicker basement membranes, display a bulging-like phenotype and possess cell to cell borders that are clearly distinguishable (King et al., 2004b; Aird, 2012; Przysinda et al., 2020). In contrast, pulmonary microvascular endothelial cells (MVECs) reside in thinner basement membranes, display a flatter phenotype, and overlap at the border with nearby cells forming what appear to be stronger junctional complexes when compared to their conduit vessel-residing relatives (King et al., 2004b; Aird, 2012). The structural differences are accompanied by significant differences in stress responses most of which have been studied in the context of inflammation and barrier restrictive properties. The clearly identifiable heterogeneity existing within the pulmonary circulation has been attributed to both environmental factors and epigenetic modifications. Exposure to high PCO_2, low PO_2 and relatively higher vascular pressure (when compared to other pulmonary vascular segments) demand unique adaptive processes in the endothelium lining pulmonary arteries while reciprocal exposures are seen in microvascular regions where gas exchange occurs (Aird, 2007). In addition, several epigenetic imprints have been described, in particular those which explain, at least in part, the enhanced replication competence of the microvascular endothelial cells when compared to their conduit-derived pulmonary artery counterparts (Alvarez et al., 2008; Clark et al., 2008).

Populations of resident endothelial cells enriched with progenitor cells have been previously described in the pulmonary circulation (RMVECs) (Alvarez et al., 2008). Compared to PAECs and MVECs, RMEPCs have longer telomeres, and a higher

proliferative capacity without evidence of transformation transelectrical membrane resistance. Furthermore, they exhibited the highest transepithelial membrane resistance (Alvarez et al., 2008). Our results demonstrated that those progenitor cells do not exhibit selective tropic abilities as shown by PAECs or MVECs but display a capacity to seed in any vascular segment. Considering our use of similar perfusion conditions, the data indicates that unique physical properties of the cells, specific expression of integrins, or other matrix-recognizing molecules are determinants for recognition of distinctive scaffold components that lure cells towards specific segments of the circulation. Similar work conducted with PAECs and MVECs, as well with HUVECs and pulmonary venous ECs, has shown similar limitations in vascular coverage and the need for combination seeding in order to achieve maximal coverage, including distal areas (Ren et al., 2015; Gilpin et al., 2016; Scarritt et al., 2018). Importantly, RMEPCs displayed an enhanced replicative competence (Alvarez et al., 2008) and/or enhanced adhesive ability which explains their remarkable vascular repopulation. Consequently, infusion of RMEPCs under the flow conditions described was able to generate a restrictive barrier with limited permeability for large solutes and detectable VE-cadherin, a major endothelial adhesion molecule, without the need for combination seeding.

Flow-seeding technology is necessary to perfuse the complete vasculature of decellularized whole organs (Walluscheck et al., 1996). Flow also induces physiological shear stress responses, which induces endothelium to shift from cobblestone morphology to align with the direction of flow, stabilizing endothelial-endothelial cell communications and promoting remodeling of focal adhesion sites (Davies et al., 1994; Malek and Izumo, 1996; Chiu and Chien, 2011; Adamson et al., 2013). While this technology is necessary for restoration of functional vasculature, there are numerous obstacles that are associated with seeding cells within acellular tissue and should be

consider by any research group studying tissue decellularization or recellularization. Harsh decellularization as well as improper storage (i.e. freezing, thawing) of acellular scaffolds can lead to disruption of components and architecture (Calle et al., 2016; Feng et al., 2020). During cell seeding of pulmonary vasculature, positioning of the scaffold (supine vs. prone vs. upright) and the physiological distribution of blood flow within the pulmonary vascular tree greatly affect distribution of cells within lobes (Stabler et al., 2016a). In order to prevent clots from disrupting complete organ decellularization and subsequent vascular recellularization, anticoagulants and thrombolytics are commonly employed to prevent and dissolve clots, respectively (Price et al., 2015; Doi et al., 2017). The method of seeding is another crucial factor in achieving high vascular coverage within acellular scaffolds. Recent reviews have stated the importance of using low cellular concentrations within large volumes, choosing gravity-dependent infusion over pump-dependent infusion, as well as seeding cells with both antegrade and retrograde perfusion to attain greater coverage throughout the entire vasculature of the acellular scaffold (Ohata and Ott, 2000; Robertson et al., 2014; Leiby et al., 2020). While we used pump-driven seeding in only the antegrade direction, we did not experience the seeding issues described above. This might be explained by our inclusion of priming the scaffolds with 24 h each of saline and media alone, and filtering of cell suspensions prior to reseeding to prevent clumping.

Our data show that, under continuous pulsatile flow, a significant proportion of RMEPCs was able to form a stable barrier for up to 8 days post initial infusion. Another benefit in the use of flow–perfusing conditions is the removal of any potentially thrombogenic gas nuclei within the lung tissue, as hydrostatic pressure has been shown to reduce the thrombogenicity of polytetrafluoroethylene vascular grafts (Ritter et al., 1989). Our data suggest that using native lung scaffolds as a substrate for cell attachment provides

sufficient binding to withstand pulsatile flow through the vasculature. We recognize that further hemodynamic studies are necessary for determining the optimal infusion conditions (rate, time, pressures) to obtain a pulmonary barrier similar to that observed *in vivo*.

Our results demonstrate that endothelial heterogeneity is required for bioengineering functional vasculature, consistent with *in vivo* findings (Belloni and Tressler, 1990; Sieminski et al., 2005; Verhamme and Hoylaerts, 2006; Stevens, 2011; Scarritt et al., 2018). All endothelial cells used for this study were able to attach and function on decellularized lung matrices, although RMEPC showed significantly greater attachment, maintenance of functional endothelial attributes (e.g., thrombomodulin activity, VEGF production), barrier restrictive properties, and a reduction of apoptotic signals in the presence of flow. Interestingly, RMEPC showed less CD31 expression than PAEC or MVEC *in vitro*. This may be explained, in part, by the heterogeneous nature of this particular primary endothelial lineage, which is enriched with progenitor cells not yet expressing migration adhesion molecules. In fact, among the tight junction and adhesion molecules we looked into (see **Table 2.3**), there were only a few that had a relatively higher gene expression within our RMEPCs. RMEPC have enhanced adherence to and maturation within multiple regions compared to PAEC and MVEC, apparently without much need for CD31 as seen in **Figure 2.2**. These data collectively lend evidence toward utilizing a single source-derived endothelial population that, after enrichment with progenitor cells, favors revascularization of each segment of the pulmonary circulation.

The qPCR results indicate that there are differences in the expression of genes for LDL-receptor and selected scavenger receptors (other proteins that play a role in the uptake of LDL) amongst the 3 cell types we studied. Based on information from public databases created from compiled murine endothelial cell transcriptomes (Goveia et al.,

2020; Kalucka et al., 2020), it was expected that similar expressions of genes for LDL-receptor, Scarf1, and Scarf2 would be found since LDL is an important nutrient for endothelial cells, and the class F scavenger receptors are classified as endothelial-specific (Patten, 2018). While public databases show a mixed expression of genes for αv, β1, β2, and β5 among all endothelial cell types, we found that the PAECs had relatively higher expression of all but β2, whereas our RMEPCs had the highest expression of β2, an integrin that forms adhesion proteins by binding to CD11 a-d and primarily seen amongst leukocytes (Fagerholm et al., 2019). While outside the scope of this study, more work is needed in both understanding the expression of these important proteins as they will further our understanding of supplying cells with proper nutrients during recellularization and insight into what sites they will be able to adhere to during the seeding step of regenerating tissue.

While differential tropism might indicate a difference in expression of integrins responsible for attachment to the ECM, we do not yet understand the molecular determinants that resulted in the endothelial cell recognition of specific vascular segments within the pulmonary circulation. Canonical homo- and hetero-topic interactions are ascribed to the engagement of integrins and the contribution of the endothelial cell glycocalyx. Based on our flow cytometry data of our markers of interest, there is little differential expression of cell surface adhesion molecules, though we were able to detect P-selectin, which is important for ECs and platelets during an inflammatory response. While GAGs play a role in cell adhesion to implantable grafts (Ibrahim and Ramamurthi, 2008), they may also allow for anatomically relevant attachment to decellularized native ECM, by providing native geospatial cues. This could be facilitated by glycosphingolipids, glycoproteins, or proteoglycans, which have all been documented as modulators of cell localization. If so, these terminal sugar residues would shift cell-

matrix binding toward common glycosylation motifs, instead of canonical integrin/collagen or laminin binding protein (LBP) within focal adhesions (that GAGs also modulate by conferring steric hindrance). Differential expression of saccharide-binding receptors, such as P-selectin, may explain the increased binding of the RMEPC. Alternatively, binding domains within ECM proteins favor a particular endothelial glycocalyx. Growth factors, cytokines, and chemokines trapped within native matrix may impact origin-specific endothelial cell-matrix binding. As with most physiological systems, there is likely a dynamic balance between these influences on cell adhesion and subsequent intracellular signal transduction through anchor proteins (Burgess et al., 2006; Schultz and Wysocki, 2009; Ishihara et al., 2018; Mammoto and Mammoto, 2019).

In summary, we have identified a single cell source that is capable of re-endothelializing the lung in a comprehensive manner providing a functional barrier. Furthermore, we have determined that endothelial cells that exhibit selective tropism are suboptimal for functional re-endothelialization of acellular lungs. Along with recent studies published by others we conclude that it is vital to include endothelial progenitors, such as RMEPCs, in the seeding process of decellularized lung scaffolds in order to improve endothelial function, barrier permeability, and coverage throughout the entire pulmonary vasculature (Ren et al., 2015; Nagao et al., 2016; Scarritt et al., 2018). Although future studies will help us understand the mechanism of the stochastic nature of lung microvascular EPCs in recellularizing the lung vascular extracellular matrix, it is apparent that our findings warrant moving ahead on determining their translational capacity for bioengineering, therapeutic applications, and understanding regeneration and repair for lungs and other vascularized organs

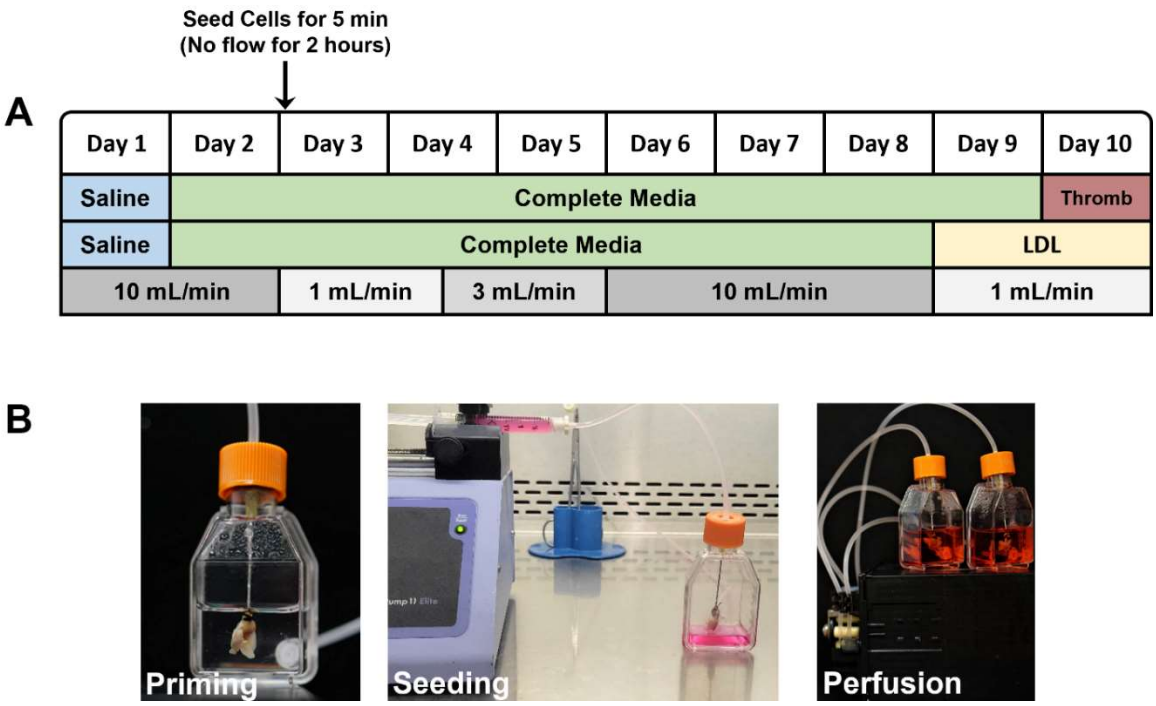

Figure 2.1 Bioreactor System and Timeline

(A) Flow chart outlining the reseeding protocol. LDL-uptake and Thrombogenicity assays were conducted on day 9 and 10, respectively. (B) Photographs showing assembled, modified tissue culture flask bioreactor with attached acellular mouse lung scaffold during priming with saline (left), injector pump seeding ECs into acellular scaffold via right ventricle (middle), and reseeded lung scaffolds with 25 ml of media in a closed loop system, attached to pulsatile pump (right)

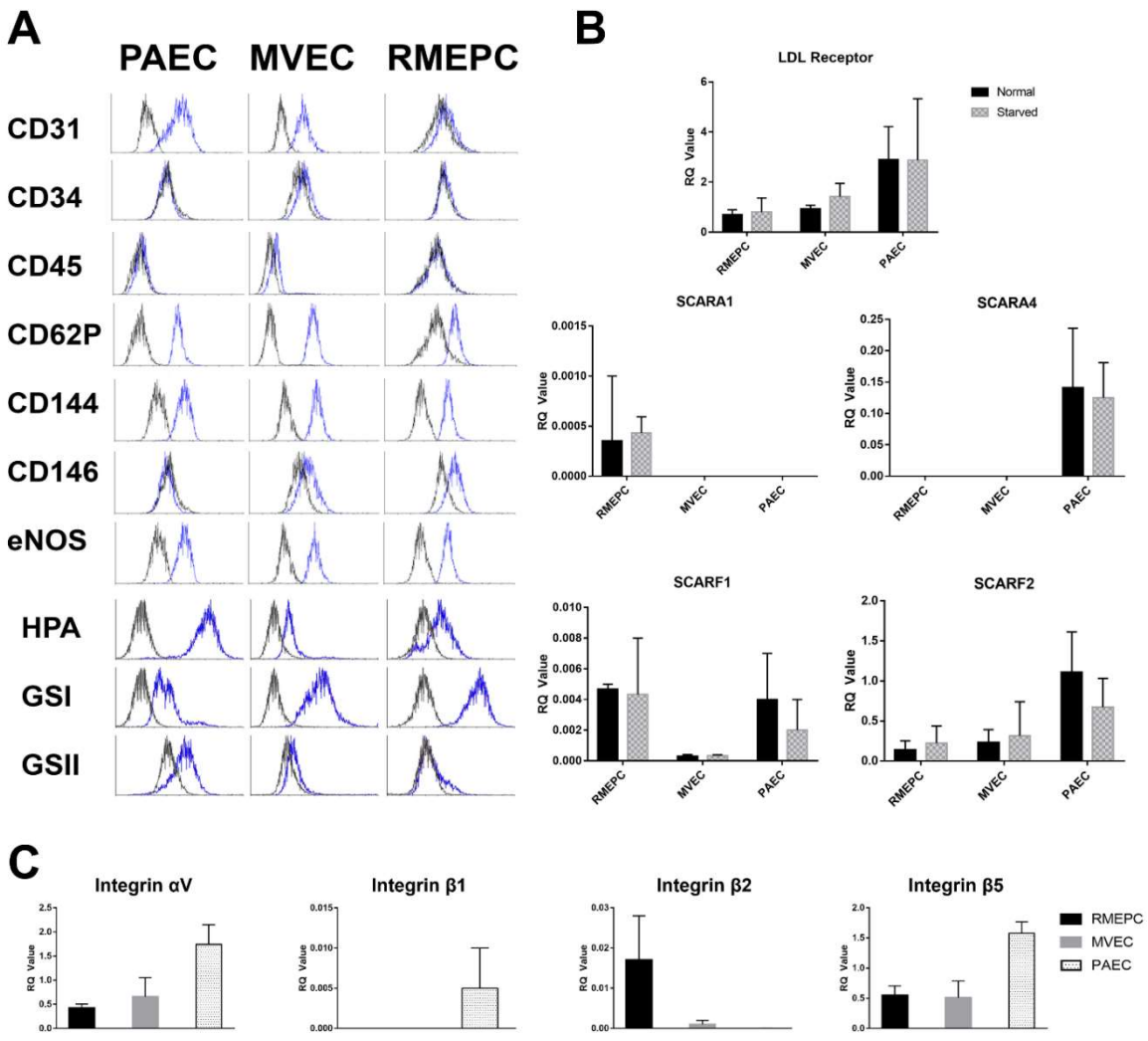

Figure 2.2 Characterization of Pulmonary Endothelial Cells (*in vitro)*

PAEC, MVEC, and RMEPC express representative endothelial cell associated markers and lectin binding properties as assessed via flow cytometry (A). In addition, gene expression of LDL-receptor, selected scavenger receptors, and selected integrin chains were assessed via qPCR (B, C). For qPCR data, n = 3 for each sample/condition.

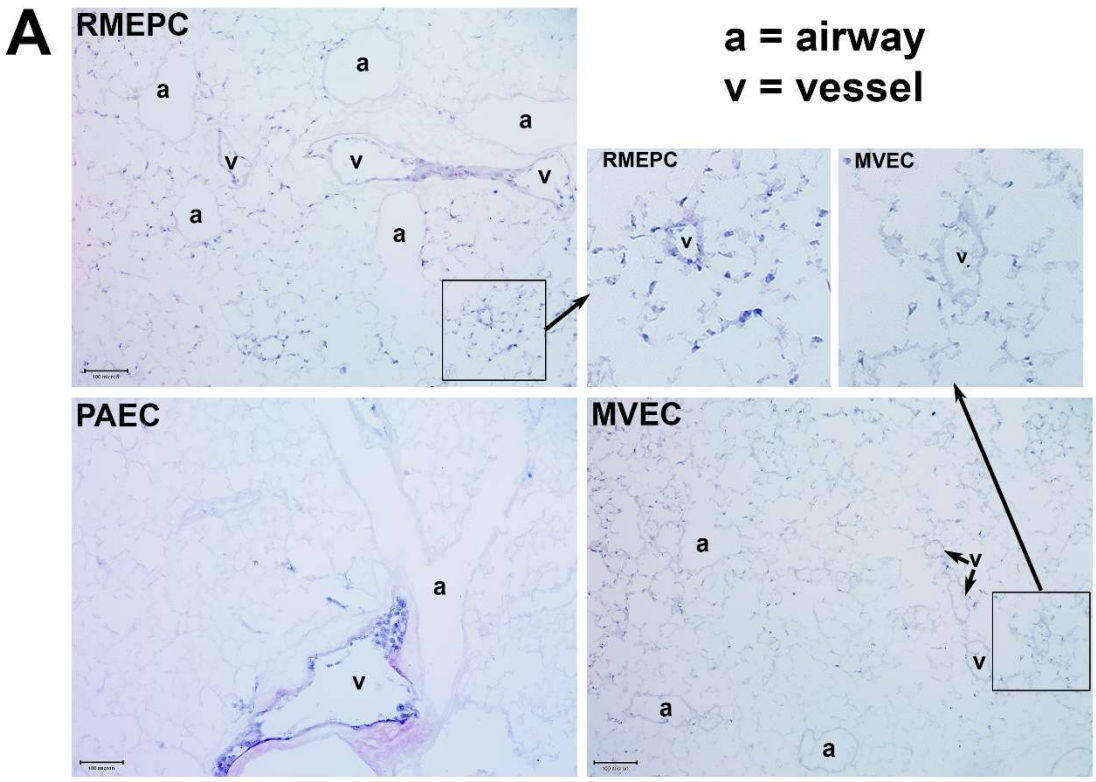
A
RMEPC
a = airway
v = vessel
RMEPC
MVEC
PAEC
MVEC
B
500 µm

Figure 2.3 Selective Tropism of Pulmonary Endothelial Cells

(A) MVEC and PAEC show selective tropism to their in vivo point of origin whereas RMEPC exhibit pan-tropism to ex vivo decellularized ECM vascular conduits. Representative H&E-stained cryosections (5 um) of decellularized whole lungs re-seeded with progenitor enriched microvascular cells (RMEPC), pulmonary arterial endothelial cells (PAEC), and microvascular (MVEC). All images are at ×100 magnification (×10 objective). Scale bar indicates 100 μm. Arrows indicate zoomed-in areas comparing engraftment of RMPEC to microvasculature and larger vessel, whereas MVEC engraftment is only in microvasculature. (B) Immunofluorescent image of a decellularized mouse lung lobe seeded with RMEPCs. Cryosection was stained for VE-Cadherin (red). Multiple images taken at ×40 objective magnification and stitched together. DAPI used to label cell nuclei (blue).

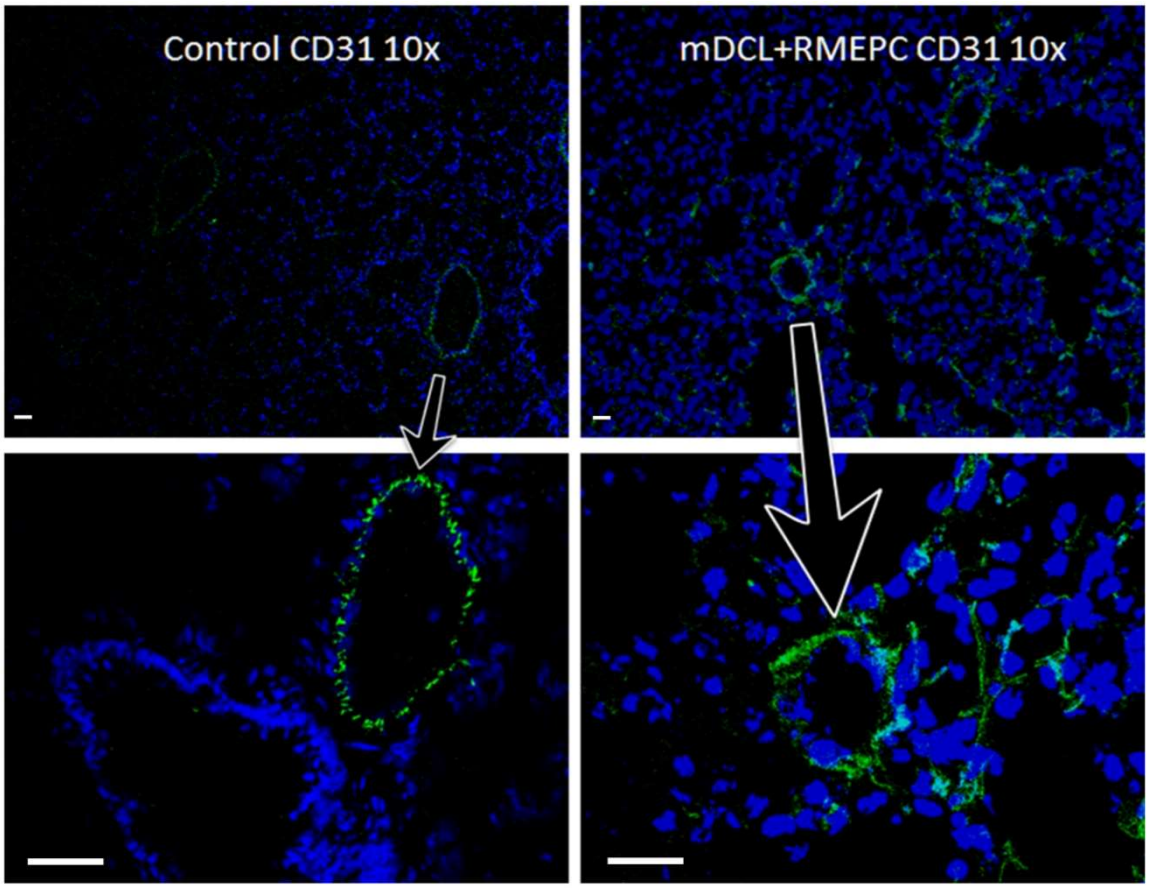

Figure 2.4 Maturation of RMEPCs within Decellularized Mouse Lung

RMEPC express endothelial markers after reseeding on decellularized mouse lungs. CD31/PECAM-1 expression (green) in rat lung control and recellularized lungs. Images taken at ×100 magnification, ×10 objective; DAPI nuclear stain in blue. Arrows point to zoomed areas. Scale bars set to 50 μm in each panel. Images taken by Daniel Rossi, MS.

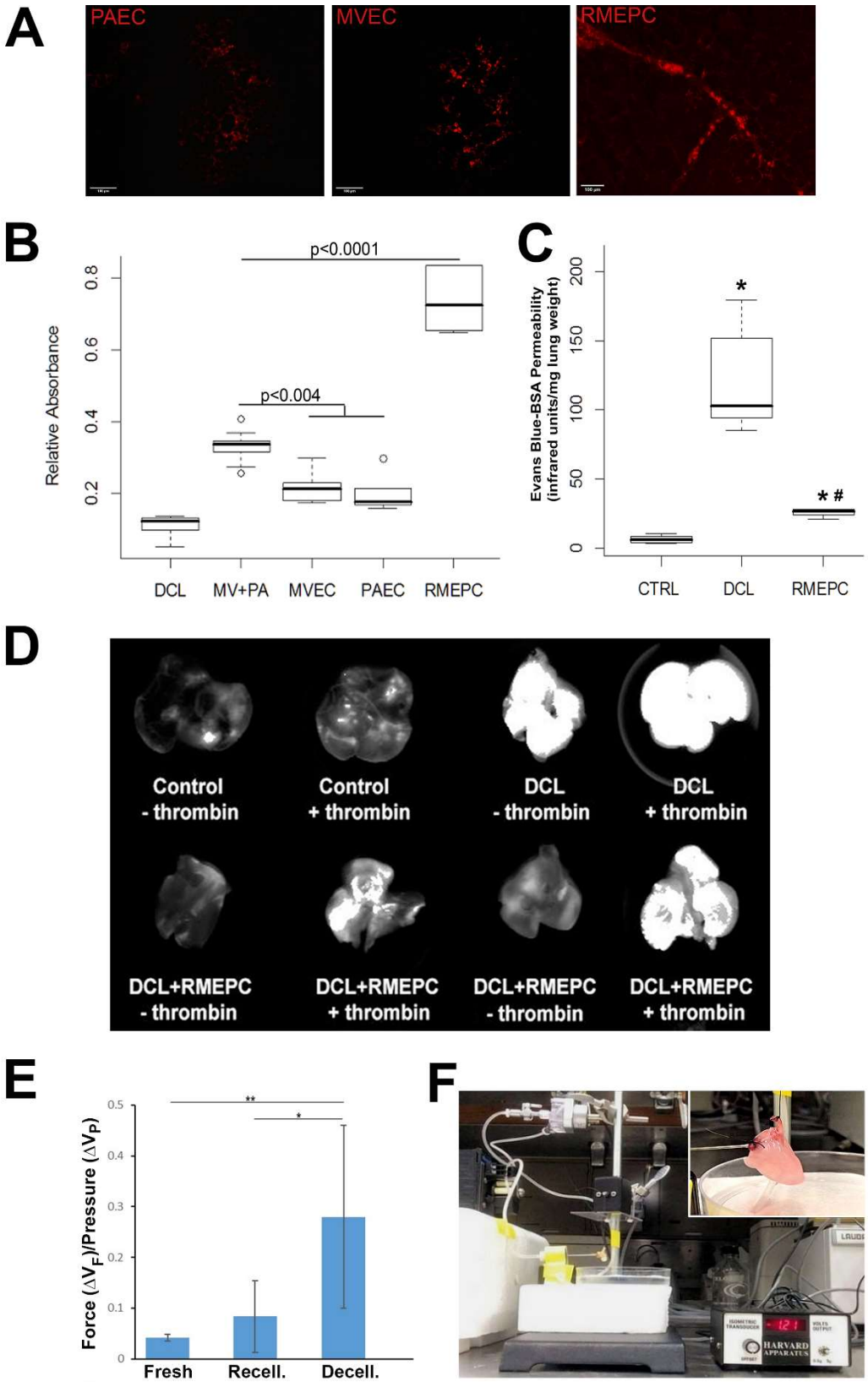
A
PAEC
MVEC
RMEPC
B
p<0.0001
p<0.004
Relative Absorbance
0.2
0.4
0.6
0.8
DCL
MV+PA
MVEC
PAEC
RMEPC
C
Evans Blue-BSA Permeability
(infrared units/mg lung weight)
0
50
100
150
200
*
* #
CTRL
DCL
RMEPC
D
Control
- thrombin
Control
+ thrombin
DCL
- thrombin
DCL
+ thrombin
DCL+RMEPC
- thrombin
DCL+RMEPC
+ thrombin
DCL+RMEPC
- thrombin
DCL+RMEPC
+ thrombin
E
Force (ΔV_F)/Pressure (ΔV_P)
0
0.1
0.2
0.3
0.4
0.5
**
*
Fresh
Recell.
Decell.
F
HARVARD
APPARATUS

Figure 2.5 Endothelial Functions of Pulmonary ECs and RMEPCs within Decellularized Mouse Lungs

Recellularized lungs are functional and maintain endothelial barrier integrity. (A) Uptake of Dil-Ac LDL in revascularized lungs. Cryosections (5 μm) viewed via confocal microscopy (Left–PAEC, Middle–MVEC, Right–RMEPC). (B) Thrombomodulin activity assay of recellularized lungs after 45 min perfusion with α-thrombin and protein C colorimetric activity was normalized to whole mouse lung controls (n = 6) and compared to decellularized lungs (DCL, n = 6), all other groups n = 3. (C) Vascular permeability of RMEPC-recellularized lungs (n = 4) compared to mouse lung controls (CTRL, n = 8) and decellularized lungs (DCL, n = 8) measured by near-infrared spectrophotometry of perfused Evans-blue-tagged albumin (EB-BSA). $^{*}p < 0.0000004$ vs. control; $^{*\#}p < 0.0004$ vs. decellularized lungs. (D) Representative whole lung near-infrared spectrophotometry of EB-BSA showing barrier integrity of RMEPC-recellularized lungs and increased permeability in response to thrombin (+). (E) Comparison of the average change in force (ΔV_F) gained per increase in pressure (ΔV_P) for native-fresh (n = 4), decellularized (n = 7), and RMEPC-recellularized (n = 6) mouse lungs (* indicates a *p*-value < 0.001). (F) Setup of isogravimetric experiment and insert of a close-up of heart/lung en bloc.

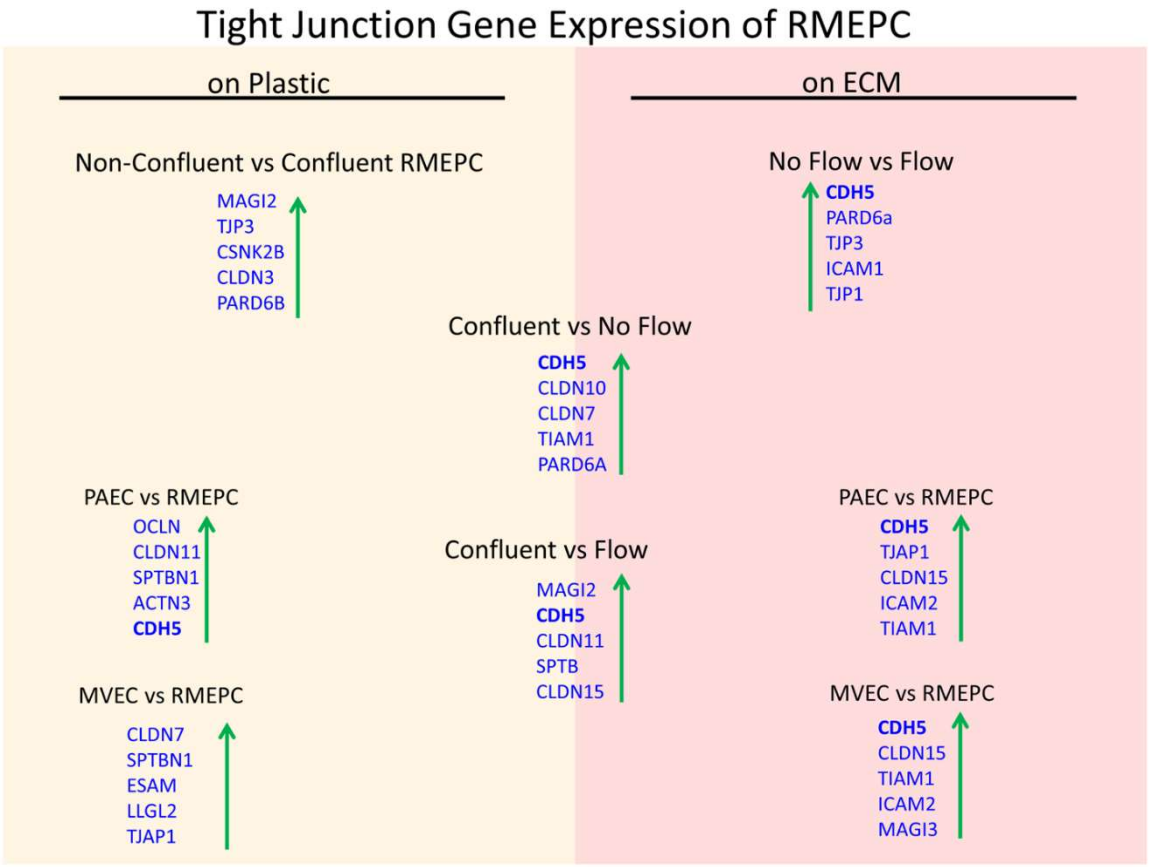

Figure 2.6 Tight Junction Gene Expression of RMEPC

Confluency, extracellular matrix, and no-flow conditions promote the highest expression of tight junction genes by RMEPCs. Top left shows the top upregulated tight junction genes in response to confluency on RMEPCs cultured on plastic. Bottom left shows the increase in genes in confluent RMEPCs compared to confluent PAECs and MVECs cultured on plastic. The right-hand side (red) shows day 7 gene expression when seeded by perfusion on decellularized mouse lung ECM. The bottom right shows the top tight junction genes upregulated in RMEPCs vs. PAECs and MVECs on ECM (with flow) after 7 days. The middle portion shows the increases in tight junction genes in RMEPC in conditions vascular flow and no-flow for 7 days compared to confluency on plastic. The far top right compares no-flow vs. flow of RMEPCs on ECM

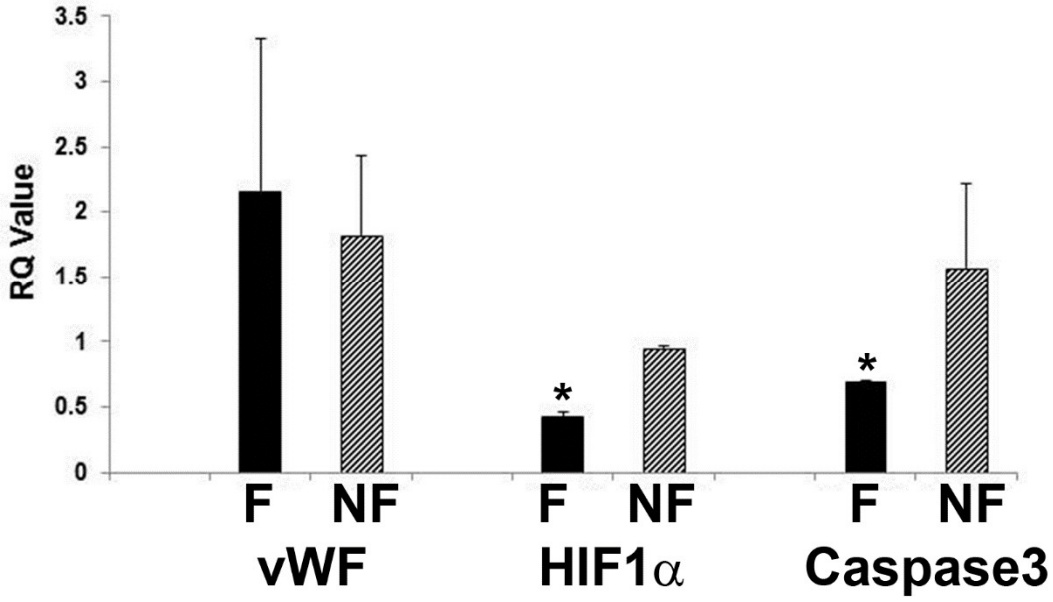

Figure 2.7 Addition of flow decreases hypoxic and apoptotic signals

Decreased apoptosis and hypoxic signal in RMEPC on ECM after 1 week in flow conditions. qRT-PCR for vWF, HIF-1a and caspase-3 are shown. F flow, NF no flow. *p = <0.05 for F vs NF (n = 3 per group)

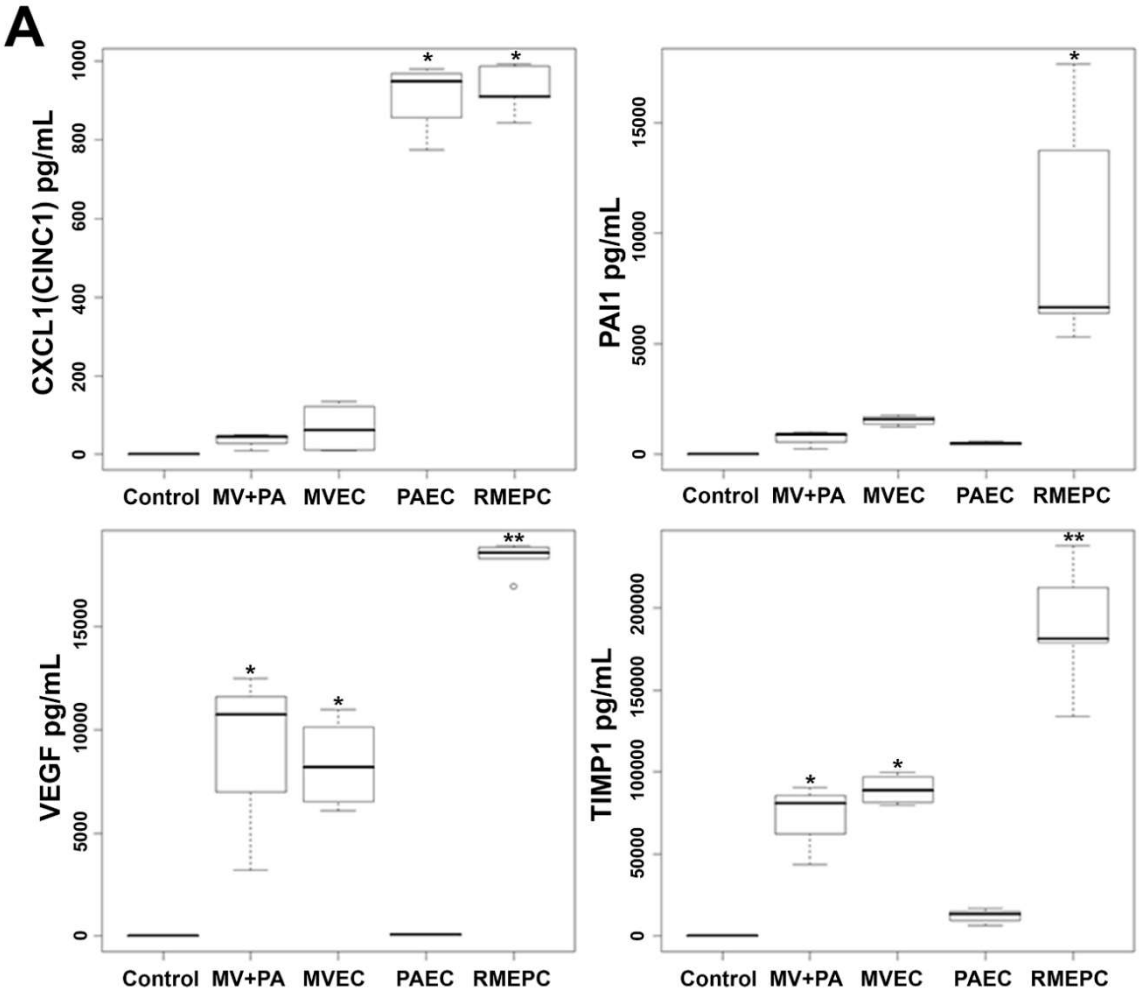
A
CXCL1(CINC1) pg/mL
0
200
400
600
800
1000
Control
MV+PA
MVEC
PAEC
RMEPC
PAI1 pg/mL
0
5000
10000
15000
VEGF pg/mL
0
5000
10000
15000
TIMP1 pg/mL
0
50000
100000
150000
200000
*
**

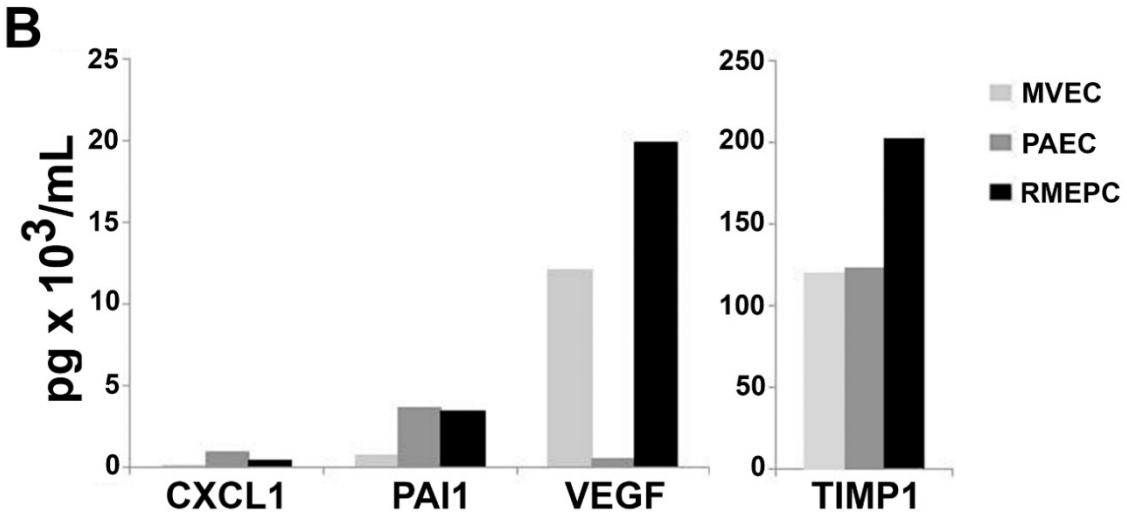
B
pg x 10^3/mL
0
5
10
15
20
25
0
50
100
150
200
250
CXCL1
PAI1
VEGF
TIMP1
MVEC
PAEC
RMEPC

Figure 2.8 Endothelial Cell Mediator Secretion

(A) Secretion of endothelial cell mediators from perfusate of decellularized lungs reseeded with RMEPC, MVEC, PAEC, or both MVEC and PAEC ("MV + PA"). "Control" indicates complete culture medium alone. Perfusates were sampled from reseeded constructs at 48 hours post-seeding. Single asterisk (*) indicates $p < 0.05$ versus non asterisk, and double asterisk (**) groups. For all samples, n = 8, except for RMEPC where n = 10. (B) In vitro production of endothelial cell mediators after 48 h of 2D tissue culture in flasks. These single samples were run in duplicate with CV < 15%.

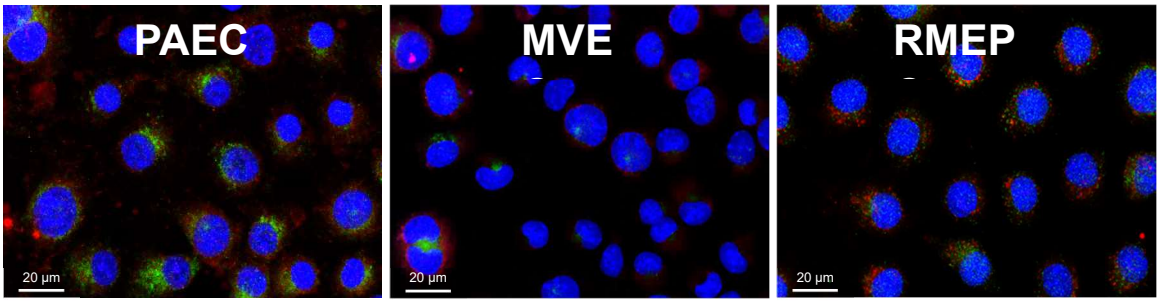

Figure 2.9 Uptake of Modified LDL *in vivo*

Ac-LDL uptake in vitro. Images were taken after overnight starvation and 4 hours of incubation with modified LDL at 400X magnification (40x objective lens). Blue: Nuclei; Green: VE-Cadherin; Red: Dil-acetylated-LDL. Scale bar = 20µm.

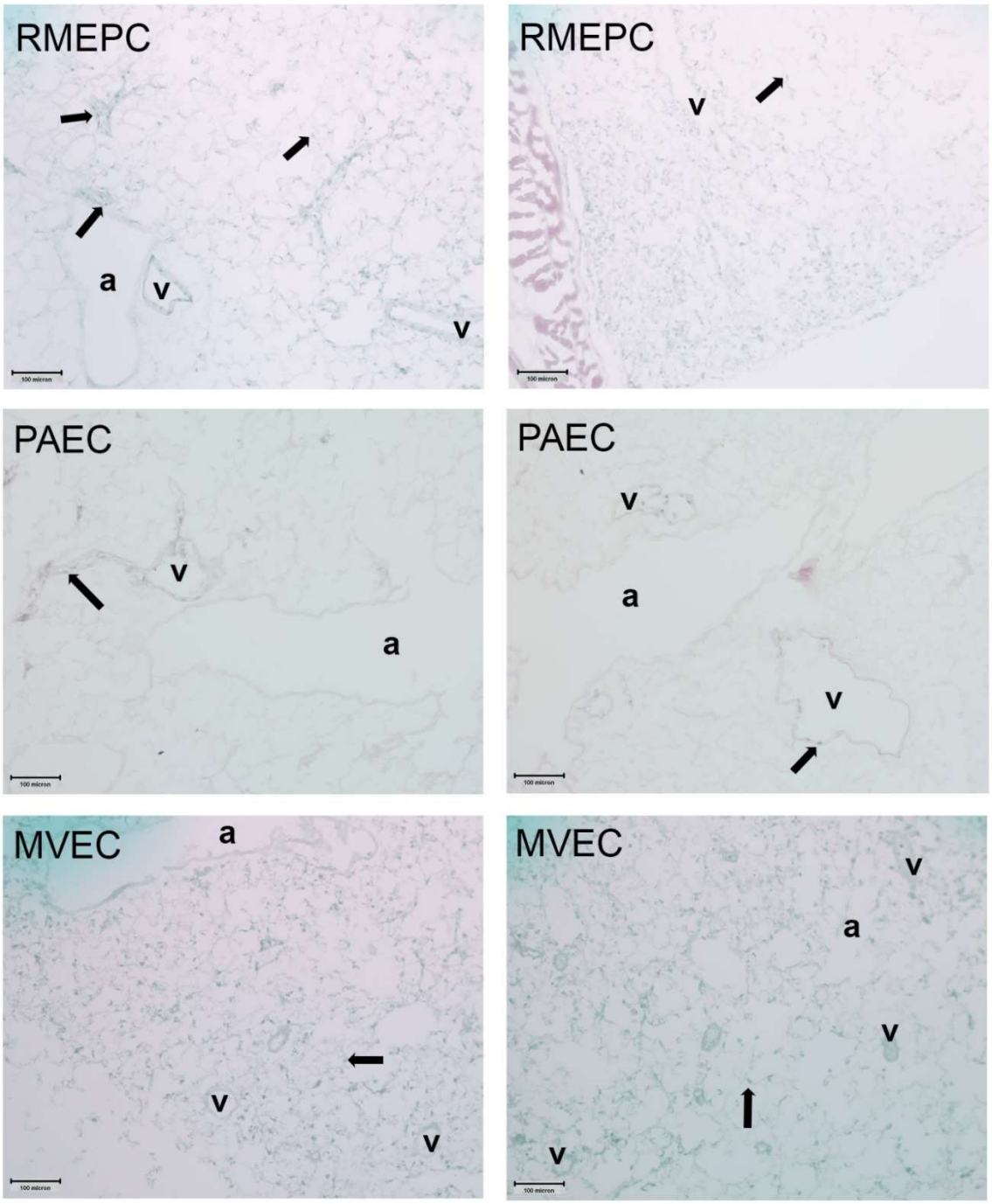

Figure 2.10 Additional Display of Selective Tropism

Additional H&E-stained cryosections of decellularized whole lungs re-seeded with either RMEPCs (top row), PAECs (middle row), or MVECs (bottom row). Images taken at 100X magnification (10X objective lens), with airways (a) and vessels (v) marked. Some examples of cells are indicated by arrows. Scale bar = 100μm.

Table 2.1 Tight Junction Array (Confluency Comparison)

Tight junction gene expression of RMEPC confluence on plastic vs non-confluence on plastic. Green=upregulation with confluence, red=downregulation with confluence

Symbol	Entrez Gene Name	Location	Plastic (confluent) vs Plastic (not confluent)
MAGI2	membrane associated guanylate kinase, WW and PDZ domain containing 2	Plasma Membrane	3.490
Tjp3	tight junction protein 3	Plasma Membrane	2.820
CSNK2B	casein kinase 2, beta polypeptide	Cytoplasm	2.440
CLDN3	claudin 3	Plasma Membrane	2.190
PARD6B	par-6 family cell polarity regulator beta	Plasma Membrane	2.130
ACTN1	actinin, alpha 1	Cytoplasm	1.940
LLGL1	lethal giant larvae homolog 1 (Drosophila)	Cytoplasm	1.840
CLDN11	claudin 11	Plasma Membrane	1.800
RHOA	ras homolog family member A	Cytoplasm	1.630
SMURF1	SMAD specific E3 ubiquitin protein ligase 1	Cytoplasm	1.620
LLGL2	lethal giant larvae homolog 2 (Drosophila)	Cytoplasm	1.600
TJAP1	tight junction associated protein 1 (peripheral)	Plasma Membrane	1.520
GSK3A	glycogen synthase kinase 3 alpha	Nucleus	1.480
F11R	F11 receptor	Plasma Membrane	1.400
CSNK2A2	casein kinase 2, alpha prime polypeptide	Cytoplasm	1.390
CDH5	cadherin 5, type 2 (vascular endothelium)	Plasma Membrane	1.370
SPTB	spectrin, beta, erythrocytic	Plasma Membrane	1.260
SYMPK	symplekin	Cytoplasm	1.240
CLDN18	claudin 18	Plasma Membrane	1.180
CTTN	cortactin	Plasma Membrane	1.160
YBX3	Y box binding protein 3	Nucleus	1.150
CLDN12	claudin 12	Plasma Membrane	1.140
ICAM1	intercellular adhesion molecule 1	Plasma Membrane	1.140
Cdk4	cyclin-dependent kinase 4	Nucleus	1.110
SPTBN2	spectrin, beta, non-erythrocytic 2	Cytoplasm	1.080
ILK	integrin-linked kinase	Plasma Membrane	1.050
ACTN4	actinin, alpha 4	Cytoplasm	1.030
TJP2	tight junction protein 2	Plasma Membrane	1.020
RAC1	ras-related C3 botulinum toxin substrate 1 (rho family, small GTP binding protein Rac1)	Plasma Membrane	-1.040
PARD6A	par-6 family cell polarity regulator alpha	Plasma Membrane	-1.100
GNAI2	guanine nucleotide binding protein (G protein), alpha inhibiting activity polypeptide 2	Plasma Membrane	-1.130

ICAM2	intercellular adhesion molecule 2	Plasma Membrane	-1.130
AMOTL1	angiomotin like 1	Plasma Membrane	-1.150
CDC42	cell division cycle 42	Cytoplasm	-1.250
CTNNB1	catenin (cadherin-associated protein), beta 1, 88kDa	Nucleus	-1.280
CSNK2A1	casein kinase 2, alpha 1 polypeptide	Cytoplasm	-1.470
ARHGEF2	Rho/Rac guanine nucleotide exchange factor (GEF) 2	Cytoplasm	-1.490
CLDN15	claudin 15	Plasma Membrane	-1.510
MARK2	MAP/microtubule affinity-regulating kinase 2	Cytoplasm	-1.590
CLDN19	claudin 19	Plasma Membrane	-1.620
VAPA	VAMP (vesicle-associated membrane protein)-associated protein A, 33kDa	Plasma Membrane	-1.630
TIAM1	T-cell lymphoma invasion and metastasis 1	Cytoplasm	-1.660
JAM3	junctional adhesion molecule 3	Plasma Membrane	-1.670
GSK3B	glycogen synthase kinase 3 beta	Nucleus	-1.730
PARD3	par-3 family cell polarity regulator	Plasma Membrane	-1.880
PRKCI	protein kinase C, iota	Cytoplasm	-2.170
EPB41L1	erythrocyte membrane protein band 4.1-like 1	Plasma Membrane	-2.810
MLLT4	myeloid/lymphoid or mixed-lineage leukemia (trithorax homolog, Drosophila); translocated to, 4	Nucleus	-2.890
MAGI3	membrane associated guanylate kinase, WW and PDZ domain containing 3	Cytoplasm	-2.930
SPTAN1	spectrin, alpha, non-erythrocytic 1	Plasma Membrane	-3.120
MPP5	membrane protein, palmitoylated 5 (MAGUK p55 subfamily member 5)	Plasma Membrane	-3.400
CASK	calcium/calmodulin-dependent serine protein kinase (MAGUK family)	Plasma Membrane	-3.750
ASH1L	ash1 (absent, small, or homeotic)-like (Drosophila)	Nucleus	-4.030
PTEN	phosphatase and tensin homolog	Cytoplasm	-4.080
SPTBN1	spectrin, beta, non-erythrocytic 1	Plasma Membrane	-4.120
TJP1	tight junction protein 1	Plasma Membrane	-4.560
MPDZ	multiple PDZ domain protein	Plasma Membrane	-5.950

Table 2.2 Tight Junction Array (ECM vs Plastic – No Flow)

Tight junction gene expression of RMEPC on lung ECM with no-flow vs confluence on plastic. Green=upregulation on ECM, red=downregulation on ECM

Symbol	Description	Fold Regulation
Cdh5	Cadherin 5	7695.13
Cldn10	Claudin 10	130.53
Cldn7	Claudin 7	104.90
Tiam1	T-cell lymphoma invasion and metastasis 1	102.48
Pard6a	Par-6 (partitioning defective 6,) homolog alpha (C. elegans)	48.12
Tjap1	Tight junction associated protein 1	40.09
Sptb	Spectrin, beta, erythrocytic	36.50
Cldn19	Claudin 19	36.23
Ocln	Occludin	33.43
Cldn18	Claudin 18	27.84
Cldn15	Claudin 15	20.36
Csnk2a1	Casein kinase 2, alpha 1 polypeptide	19.26
Icam1	Intercellular adhesion molecule 1	16.01
Actn4	Actinin alpha 4	11.97
Prkci	Protein kinase C, iota	11.94
Cdk4	Cyclin-dependent kinase 4	11.26
Cldn3	Claudin 3	9.74
F11r	F11 receptor	9.04
Amotl1	Angiomotin-like 1	8.86
Ctnnb1	Catenin (cadherin associated protein), beta 1	6.90
Sympk	Symplekin	5.83
MLlt4	Myeloid/lymphoid or mixed-lineage leukemia (trithorax homolog, Drosophila); translocated to, 4	5.04
Tjp1	Tight junction protein 1	4.43
Cttn	Cortactin	3.85
Pard6b	Par-6 (partitioning defective 6) homolog beta (C. elegans)	3.83
Magi3	Membrane associated guanylate kinase, WW and PDZ domain containing 3	3.70
Gsk3a	Glycogen synthase kinase 3 alpha	3.63
Jam3	Junctional adhesion molecule 3	3.56
Pard3	Par-3 (partitioning defective 3) homolog (C. elegans)	3.39
Ash1l	Ash1 (absent, small, or homeotic)-like (Drosophila)	3.14
Sptan1	Spectrin, alpha, non-erythrocytic 1	3.10
Gnai2	Guanine nucleotide binding protein (G protein), alpha inhibiting 2	3.09
Mark2	MAP/microtubule affinity-regulating kinase 2	2.83

Sptbn1	Spectrin, beta, non-erythrocytic 1	2.69
Ybx3	Cold shock domain protein A	2.10
Epb41l1	Erythrocyte membrane protein band 4.1-like 1	2.07
Cask	Calcium/calmodulin-dependent serine protein kinase (MAGUK family)	2.01
Smurf1	Similar to RIKEN cDNA 4930431E10	1.90
Cldn12	Claudin 12	1.78
Mpp5	Membrane protein, palmitoylated 5 (MAGUK p55 subfamily member 5)	1.75
Csnk2a2	Casein kinase 2, alpha prime polypeptide	1.72
Rhoa	Ras homolog gene family, member A	1.51
Icam2	Intercellular adhesion molecule 2	1.43
Csnk2b	Casein kinase 2, beta polypeptide	1.41
Llgl2	Lethal giant larvae homolog 2 (Drosophila)	1.31
Tjp2	Tight junction protein 2	1.20
Arhgef2	Rho/rac guanine nucleotide exchange factor (GEF) 2	1.19
Ilk	Integrin-linked kinase	1.02
Gsk3b	Glycogen synthase kinase 3 beta	-1.16
Tjp3	Tight junction protein 3	-1.18
Actn1	Actinin, alpha 1	-1.28
Rac1	Ras-related C3 botulinum toxin substrate 1	-1.48
Cdc42	Cell division cycle 42 (GTP binding protein)	-1.87
Mpdz	Multiple PDZ domain protein	-3.35
Pten	Phosphatase and tensin homolog	-3.79
Vapa	VAMP (vesicle-associated membrane protein)-associated protein A	-9.27

Table 2.3 Tight Junction Array (ECM vs Plastic)

Tight junction gene expression of RMEPC on lung ECM with flow vs confluence on plastic. Green=upregulation on ECM, red=downregulation on ECM

Symbol	Entrez Gene Name	ECM flow vs plastic
MAGI2	membrane associated guanylate kinase, WW and PDZ domain containing 2	8.910
CDH5	cadherin 5, type 2 (vascular endothelium)	7.950
CLDN11	claudin 11	6.130
SPTB	spectrin, beta, erythrocytic	5.080
LLGL1	lethal giant larvae homolog 1 (Drosophila)	3.280
Tjp3	tight junction protein 3	1.800
CLDN18	claudin 18	1.720
CLDN15	claudin 15	1.530
CLDN19	claudin 19	1.100
TIAM1	T-cell lymphoma invasion and metastasis 1	-1.050
PARD6A	par-6 family cell polarity regulator alpha	-1.080
F11R	F11 receptor	-1.240
CLDN3	claudin 3	-1.310
CDC42	cell division cycle 42	-1.370
CSNK2B	casein kinase 2, beta polypeptide	-1.700
RHOA	ras homolog family member A	-1.880
PTEN	phosphatase and tensin homolog	-2.020
VAPA	VAMP (vesicle-associated membrane protein)-associated protein A, 33kDa	-2.060
CASK	calcium/calmodulin-dependent serine protein kinase (MAGUK family)	-2.170
AMOTL1	angiomotin like 1	-2.240
JAM3	junctional adhesion molecule 3	-2.390
CLDN12	claudin 12	-2.750
CSNK2A1	casein kinase 2, alpha 1 polypeptide	-2.770
RAC1	ras-related C3 botulinum toxin substrate 1 (rho family, small GTP binding protein Rac1)	-2.800
SPTAN1	spectrin, alpha, non-erythrocytic 1	-2.860
ICAM1	intercellular adhesion molecule 1	-2.980
CSNK2A2	casein kinase 2, alpha prime polypeptide	-3.060
Cdk4	cyclin-dependent kinase 4	-3.100
GSK3A	glycogen synthase kinase 3 alpha	-3.130
YBX3	Y box binding protein 3	-3.300
ILK	integrin-linked kinase	-3.320
SPTBN1	spectrin, beta, non-erythrocytic 1	-3.540
PARD6B	par-6 family cell polarity regulator beta	-3.640

SMURF1	SMAD specific E3 ubiquitin protein ligase 1	-3.840
MPDZ	multiple PDZ domain protein	-3.940
LLGL2	lethal giant larvae homolog 2 (Drosophila)	-3.990
CTNNB1	catenin (cadherin-associated protein), beta 1, 88kDa	-4.040
ARHGEF2	Rho/Rac guanine nucleotide exchange factor (GEF) 2	-4.050
ICAM2	intercellular adhesion molecule 2	-4.130
PRKCI	protein kinase C, iota	-4.410
GSK3B	glycogen synthase kinase 3 beta	-5.110
GNAI2	guanine nucleotide binding protein (G protein), alpha inhibiting activity polypeptide 2	-5.120
MAGI3	membrane associated guanylate kinase, WW and PDZ domain containing 3	-5.180
PARD3	par-3 family cell polarity regulator	-5.900
MPP5	membrane protein, palmitoylated 5 (MAGUK p55 subfamily member 5)	-6.200
TJP2	tight junction protein 2	-6.800
TJP1	tight junction protein 1	-6.810
ACTN4	actinin, alpha 4	-7.310
ACTN1	actinin, alpha 1	-7.460
ASH1L	ash1 (absent, small, or homeotic)-like (Drosophila)	-7.610
MARK2	MAP/microtubule affinity-regulating kinase 2	-8.300
CTTN	cortactin	-8.410
MLLT4	myeloid/lymphoid or mixed-lineage leukemia (trithorax homolog, Drosophila); translocated to, 4	-10.130
SPTBN2	spectrin, beta, non-erythrocytic 2	-10.890
SYMPK	symplekin	-10.910
TJAP1	tight junction associated protein 1 (peripheral)	-12.170
EPB41L1	erythrocyte membrane protein band 4.1-like 1	-18.050

Table 2.4 Tight Junction Array (ECM – Flow vs No Flow)

Tight junction gene expression of RMEPC on lung ECM No-Flow vs Flow.

Green=upregulation in No-Flow

Gene Symbol	Description	Fold Reg
Cdh5	Cadherin 5	27.09
Pard6a	Par-6 (partitioning defective 6,) homolog alpha (C. elegans)	18.56
Tjp3	Tight junction protein 3	9.09
Icam1	Intercellular adhesion molecule 1	7.59
Cldn18	Claudin 18	6.88
Tjp1	Tight junction protein 1	6.07
Prkci	Protein kinase C, iota	5.61
Icam2	Intercellular adhesion molecule 2	5.49
Tiam1	T-cell lymphoma invasion and metastasis 1	5.45
Tjap1	Tight junction associated protein 1	5.24
Csnk2a1	Casein kinase 2, alpha 1 polypeptide	5.06
Sptan1	Spectrin, alpha, non-erythrocytic 1	4.59
Jam3	Junctional adhesion molecule 3	3.30
Mpp5	Membrane protein, palmitoylated 5 (MAGUK p55 subfamily member 5)	3.09
Cldn15	Claudin 15	2.98
MLlt4	Myeloid/lymphoid or mixed-lineage leukemia (trithorax homolog, Drosophila); translocated to, 4	2.85
Sptbn1	Spectrin, beta, non-erythrocytic 1	2.85
Cdk4	Cyclin-dependent kinase 4	2.41
Amotl1	Angiomotin-like 1	2.40
Ash1l	Ash1 (absent, small, or homeotic)-like (Drosophila)	2.36
Cttn	Cortactin	2.34
Ybx3	Cold shock domain protein A	2.14
F11r	F11 receptor	2.02
Actn4	Actinin alpha 4	2.01
Ctnnb1	Catenin (cadherin associated protein), beta 1	1.86
Magi3	Membrane associated guanylate kinase, WW and PDZ domain containing 3	1.74
Mpdz	Multiple PDZ domain protein	1.70
Sptb	Spectrin, beta, erythrocytic	1.64
Sympk	Symplekin	1.61
Gsk3b	Glycogen synthase kinase 3 beta	1.56
Arhgef2	Rho/rac guanine nucleotide exchange factor (GEF) 2	1.44
Gnai2	Guanine nucleotide binding protein (G protein), alpha inhibiting 2	1.41
Rac1	Ras-related C3 botulinum toxin substrate 1	1.38
Pard3	Par-3 (partitioning defective 3) homolog (C. elegans)	1.37
Smurf1	Similar to RIKEN cDNA 4930431E10	1.34
Pard6b	Par-6 (partitioning defective 6) homolog beta (C. elegans)	1.29

Epb41l1	Erythrocyte membrane protein band 4.1-like 1	1.27
Actn1	Actinin, alpha 1	1.26
Rhoa	Ras homolog gene family, member A	1.26
Gsk3a	Glycogen synthase kinase 3 alpha	1.25
Csnk2a2	Casein kinase 2, alpha prime polypeptide	1.25
Cask	Calcium/calmodulin-dependent serine protein kinase (MAGUK family)	1.24
Csnk2b	Casein kinase 2, beta polypeptide	1.14
Pten	Phosphatase and tensin homolog	1.13
Tjp2	Tight junction protein 2	1.07
Ilk	Integrin-linked kinase	-1.01
Mark2	MAP/microtubule affinity-regulating kinase 2	-1.03
Cdc42	Cell division cycle 42 (GTP binding protein)	-1.16
Llgl2	Lethal giant larvae homolog 2 (Drosophila)	-1.26
Cldn3	Claudin 3	-1.27
Vapa	VAMP (vesicle-associated membrane protein)-associated protein A	-1.47
Cldn12	Claudin 12	-1.61

Table 2.5 Additional Probes for Gene Expression

qPCR probes from Life Technologies (Grand Island, NY) used for additional gene expression experiments.

Target	Assay/Probe ID
Gapdh	Rn01775763_g1
Hif1a	Rn00577560_m1
Casp3	Rn00563902_m1
Vwf	Rn01492158_m1
Marco	Rn01408838_m1
Ldlr	Rn00598442_m1
Msr1 (Scara1)	Rn01488115_m1
Colec12 (Scara4)	Rn01531866_m1
Scarf1	Rn01470781_m1
Scarf2	Rn01404426_m1
Cd36 (Scarb3)	Rn00580728_m1
Itgav	Rn01485633_m1
Itgbl1	Rn01753534_m1
Itgb2	Rn01427948_m1
Itgb3	Rn00596601_m1
Itgb5	Rn01439348_m1

Chapter 3

Influence of Pulmonary Vasculature Extracellular Matrix Proteins on Endothelial Cell Fate: Arteries vs Veins

Ifeolu Akinnola[1] and Angela Panoskaltsis-Mortari [2,3]

[1] Integrative Biology and Physiology Graduate Program, University of Minnesota Medical School, Minneapolis, MN, United States,
[2] Pediatric Blood and Marrow Transplantation and Cell Therapy, University of Minnesota, Minneapolis, MN, United States
[3] Pulmonary, Allergy, Critical Care and Sleep Medicine, University of Minnesota, Minneapolis, MN, United States

Preface

Tissue extracellular matrices provide cells with adhesion sites and cues that mediate cell survival, proliferation, migration, differentiation, and function. As biomedical research advances towards developing new organs from acellular scaffolds, it is imperative to understand the effects of extracellular matrix (ECM) components on specific cells. For the re-endothelialization of acellular scaffolds, it is also necessary to understand the differences in the ECM composition of vessel types and how they influence endothelial cells and progenitors used to regenerate a functional endothelium. In this study, we present the early results of our proteomic analysis of decellularized porcine pulmonary arteries and veins in order to discern differences in ECM protein diversity and composition. Through label-free, mass spectrometry, we detected a higher diversity and abundance of ECM proteins within arterial ECM over venous ECM. In addition, we observed the effect of the ECM components from arteries and veins on endothelial progenitor cells through varied expression of selected endothelial genes.

Introduction

It is clear that whether being used in 3D bioprinting tissues, seeding and recellularization of acellular scaffolds, or creating a graft, extracellular matrix (ECM) components are a valuable asset in the regeneration of tissue and organs. The molecular structures of ECM components inherently provide signals to endothelial cells (ECs), influencing their proliferation, function, and survival. On a larger scale, their physical attributes can aid in robust 3D culture, and provide them with biomechanical cues to prepare cells for physiological levels of stress and strain. In addition, naturally occurring ECM components are easily degraded and modified by cells, serving as a flexible environment as migration and neo-angiogenesis occurs.

With their ability to bind growth factors and extracellular vesicles, ECM components can be primed prior to seeding cells. Novel immunologic and pharmacologic studies can take advantage of this environment to test immune and drug response of EC seeded ECM gels or scaffolds. In a similar fashion, previous age-related and disease-focused studies have capitalized on evaluating the differences between the effect of older or pathogenic ECM on ECs and subsequent re-endothelization. Studies from our research group with acellular lungs from young and aged mice revealed a decrease in laminin deposition by lung epithelial cells and fibroblasts (Godin et al., 2016). Many other groups have reported alterations to cell function and survival in the presence of aged or pathologic ECM (Damodarasamy et al., 2010, 2015; Sun et al., 2011; Scarritt et al., 2014; Rubiś et al., 2016; Woldhuis et al., 2020). Elucidating the differences in ECM composition, architecture, and integrity between heathy and pathogenic or young and aged ECM will aid in the selection and modification of tissues used in a research or clinical setting. Thorough understanding of the interaction between vascular ECM components and ECs, as well as endothelial progenitor cells (EPCs), will greatly advance tissue engineering of

endothelium as well as the greater vasculature. In turn, these advances will enable increased efficiency in creating new vessels and other tissue for clinical use.

The need to understand the interaction between ECM proteins and endothelial cells has grown as more tissue-engineered organs and grafts are being developed. One of the major drivers for elucidating these interactions is the limitations on size and viability of tissue-engineered constructs. Multiple groups have described failure of their new constructs (e.g., core necrosis, tissue edema, clot development, total-organ failure) and how they are directly related to inadequate vascularization and endothelium development (Petersen et al., 2010; Koffler et al., 2011; Doi et al., 2017; Gilbert-Honick and Grayson, 2020). For groups, such as our own, that are working towards the development of highly metabolic organs (i.e., tissue-engineered lungs for transplant), the re-institution of a fully functional vasculature is a necessity.

For the regeneration of endothelium, and preventing long-term vascular-related complications, endothelial cell type, scaffold architecture, growth factors, and ECM proteins must be taken into consideration. Many of these ECM proteins directly stimulate or inhibit ECs undergoing angiogenesis or neo-vasculogenesis, but the total protein composition varies among the different vessel types (i.e., arteries, veins, capillaries).

In the context of lung regeneration, previous proteomic studies have reported differences between whole organs of different ages and disease states, and even findings from analysis of airway ECM. Currently, there are limited studies providing insight on the differences in ECM composition between pulmonary vascular regions. In this study we used our experience in developing acellular scaffolds to begin a proteomic comparison between porcine pulmonary arteries and pulmonary veins. We then attempted to observe the effect of the decellularized ECM (dECM) on EPCs by using our rat pulmonary microvascular EPCs (RMEPCs) after 3-D *in vitro* cell culture. In short, our

main objective is to elucidate differences in ECM protein composition between different pulmonary vascular regions and detect in any genotypic difference in EPCs cultured in hydrogels with arterial or venous dECM particles.

Materials and Methods

Animals, Tissues, and Cells: Rat pulmonary arterial endothelial cells (PAECs), microvascular endothelial cells (MVECs), and the microvascular endothelial progenitor cells (RMEPCs) were acquired and provided to us by collaborator D. Alvarez as previously described (Alvarez et al., 2008; Akinnola et al., 2021) . Rat pulmonary venous endothelial cells (PVECs) were purchased from Cell Biologics (Chicago, IL, USA) and cultured on gelatin coated flasks as suggested by suppliers. Except for RMEPCs, all endothelial cells were cultured using Endothelial Cell Growth (ECG) Media and Supplement (R&D Systems). RMEPCs were cultured using DMEM (Gibco) enriched with 10% FBS (Hyclone) and 100 U/mL penicillin-streptomycin (Gibco). Cells were incubated at 37°C with 5% CO_2.

Porcine Lungs were provided by University of Minnesota collaborators of the Virtual Heart Lab. Pulmonary vessels were dissected from porcine lung lobes, approximately at the 3rd and 4th branch generations. Once excess parenchyma was removed, dissected vessels were separated into 50 mL conicals and flushed with multiple rinses of deionized water to remove residual blood and any clots.

Decellularizing Vessels: Freshly dissected and rinsed pulmonary vessels underwent decellularization based on previously published lab protocol (Price et al., 2010). Vessels were immersed in sequential solutions of deionized water, 0.1% Triton X-100, 1% 3α,12α-dihydroxy-5β-cholanic acid sodium salt (Na deoxycholate), 1 M NaCl, then 30 mg/ml porcine pancreatic DNase in 1.3 mM MgSO4 and 2 mM CaCl2, followed by a final

rinse with sterile, deionized water. Decellularization took place at 4°C on a bench rocker for constant agitation. Cell removal was verified with Quant-iT PicoGreen Assay dsDNA Assay (Invitrogen™) in a 96 well plate. 5 mg/mL of dry decellularized tissue in TE Buffer was used for each sample. Plate was analyzed using a Cytation3 Automatic Cell Imager and Plate Reader. Excitation and emission was set to 480 nm and 520 nm, respectively. Calculated DNA values were significantly below the accepted cutoff of 50 ng of double-stranded DNA per mg of dry weight set by previous studies (Crapo et al., 2011; Price et al., 2015). DNA standard and values for decellularized samples provided in **Figure 3.**8. Schematic of vessel decellularization is provided in **Figure 3.1A**.

Creation of decellularized ECM Powder: Decellularized arteries and veins were frozen overnight and then moved to a lyophilize for 3 days. Once lyophilized, tissue was either homogenized and used for DNA quantification (see above) or for milling. Tissue used for milling was minced and milled for 2-3 minutes in a cryomill (SPEX 6700 Freezer Mill) submerged in liquid nitrogen, resulting in decellularized ECM (dECM) powder.

ECM Sample Preparation: Arterial and venous dECM powder was reduced, alkylated, and then digested prior to submitting to the University of Minnesota Center for Mass Spectrometry and Proteomics (UMN-CMSP) in St. Paul, Minnesota. In a 1.5 mL tube, dECM powder was suspended in a solubilization buffer (6 M guanidine-HCl, 10 mM DTT, 40 mM chloroacetamide, 100 mM HCl) to a concentration of 5 mg/mL. ECM particles in the solution were further broken down using a probe sonicator for ~7 seconds per sample. Samples were then incubated for 30 minutes at 37°C for reduction and alkylation of disulfide bonds. Once cooled, samples were briefly spun down to collect condensation. Before pepsin digestion, Bradford assay was conducted on each sample. Aliquots of 50 µg of protein from each sample was taken. Solubilization buffer was used to bring all samples to the same volume. Porcine pepsin solution (1 mg/mL in

10 mM HCl pH ≤ 5) was added to each sample at a ratio of 1:50 enzyme: total protein. Samples were left at 37°C for overnight digest. 1 M NaOH was used to bring pH between 6 and 8, in order to inactivated pepsin and end digestion. Eppendorf SpeedVac was used to dry samples. Once dried, samples were stored at -80°C until sent to UMN-CMSP for further preparation and spectrometry.

Once received, samples were reconstituted in protein denaturing buffer (6 M guanidine hydrochloride, 0.5 M ammonium bicarbonate, 10% acetonitrile, and 5 mM TCEP) followed by brief vortexing. Samples were probe sonicated with a Branson Digital Sonifier 250 (Branson Ultrasonics, Danbury, CT) on ice at 30% amplitude for 5 sec. A 150ul aliquot of each sample was transferred to a PCT tube and run in a Barocycler NEP2320 (Pressure Biosciences, Inc., South Easton, MA). The barocycler cycled between 35 kpsi for 20 sec. and 0 kpsi for 10 sec. for 60 cycles at 37 °C. The PCT tube was uncapped and 200 mM iodoacetamide was added to a final concentration of 8 mM iodoacetamide, recapped, inverted several times, and incubated 15 minutes at room temperature. The samples were transferred to a new 1.5 mL microfuge Eppendorf Protein LoBind tube and centrifuged at 13000g for 10 minutes at 18°C. Two aliquots for each sample were taken for protein concentration determination by Bradford assay. A 10 ug aliquot of each sample was transferred to a new 1.5 mL microfuge tube and brought to the same volume with protein denaturing buffer plus 8 mM iodoacetamide. All samples were diluted five-fold with ultra-pure water, and then trypsin (sequencing grade, Promega, Madison, WI) was added in a 1:40 ratio of trypsin to total protein. Samples were incubated overnight for 16 hrs at 37 °C. After incubation the samples were acidified to pH 3 with 10% TFA. Samples were desalted with C18 STAGE tips (PMID: 12585499) and the eluted sample was dried down *in vacuo*.

Liquid Chromatography-Mass Spectrometry Analysis and Data Interpretation: We reconstituted the dried peptides in 97.9:2.0:0.1, H_2O:acetonitrile (ACN):formic acid (FA) and analyzed 10% of each peptide pool by capillary LC-MS with a Thermo Fisher Scientific, Inc (Waltham, MA) Dionex UltiMate 3000 system in-line with Orbitrap Fusion mass spectrometer (Thermo Fisher Scientific). We loaded peptides directly on-column in solvent A (99.9:0.1, H_2O:FA) at maximum pressure (800 bar). We separated peptides on a self-packed C18 column (Dr. Maisch GmbH ReproSil-PUR) 1.9 um, 120 Å C18aq, 100 um ID x 70 cm length at 55 °C with a biphasic gradient starting at 5% solvent B at a flow rate of 325 nl/minute. From the starting conditions, the gradient was increased to 10% solvent B by 3 minutes followed by an increase to 32% B by 58 minutes. The gradient was rapidly increased to 90% B by 60 minutes and held for 8 minutes. The gradient was returned to starting conditions of 5% B by 70 minutes and held for 7 minutes (total run length: 77 minutes). We employed 3-second cycle time data dependent acquisition method with the following MS parameters: ESI voltage 2.1 kV, ion transfer tube 275 °C; Orbitrap MS1 scan 120k resolution in profile mode from 380 – 1580 *m/z* with 50 msec maximum injection time, 125% (5E5) automatic gain control (AGC); MS2 triggered on the most abundant ions above 2E4 counts, 1.6 Da quadrupole isolation window, fixed HCD activation with 35% collision energy, Orbitrap detection with 50K resolution at 200 *m/z*, first mass fixed at 110 *m/z*, 86 msec max injection time, 5E4 AGC and 40 sec dynamic exclusion duration with +/- 10 ppm mass tolerance.

Peaks® Studio (Ma et al., 2003) 10.6 build 20201015 (Bioinformatics Solutions, Inc, Waterloo, ON CA) software package was used for interpretation of tandem MS (mass spectra) and protein inference. Search parameters were: Sus scrofa (Pig) [Taxon ID: 9823] FASTA protein database downloaded from UniprotKB on 20200918 concatenated with the common lab contaminant proteins from http://www.thegpm.org/crap/; parent

mass error tolerance 15.0 ppm; fragment mass error tolerance 0.05 Da; precursor mass search type monoisotopic; a non-specific, no enzyme search; variable modifications: methionine and proline oxidation, pyroglutamic acid conversion from glutamine, deamidation of asparagine, acetyl of the protein N-terminus ; fixed modifications carbamidomethyl cysteine; maximum variable modifications per peptide 2; false discovery rate calculation On.

Support for the detection of peptides plus adducts from each supporting tandem MS data was based on: 1) high confidence Peaks® Peptide Score (minimum -10 logP 30); 2) a minimum of 5 consecutive b- or y-type peptide fragment ions; 3) high precursor mass accuracy (<7 ppm); 4) supporting signature ion peaks for the site localization of the pertinent cysteine modification on one or more peptide fragments. Mass spectral data of 5 pulmonary arteries and 5 pulmonary veins, was obtained from UMN-CMSP core for further interpretation using Peaks® Studio software. Threshold for PTM results were set at a false discovery rate (FDR) of ≥ 25 and ≥ 2 unique peptides. After a manual NCBI Blast search of remaining “uncharacterized” proteins, identified proteins that passed both threshold and manual search were exported and organized by sample.

Creation of ECM Hydrogel: Arterial and venous dECM powder were sieved using a dry 100 micro nylon mesh to separate particles below and above 100 microns. Particles 100 micron and smaller were used for the formation of 10% ECM/GelMA hydrogels. For hydrogel formation, ECG media was added to a 50 mL conical wrapped in aluminum to protect from light. Lithium phenyl-2,4,5-trimethylbenzoylphosphinate (LAP) was added to media at 10 mg/mL. Methacrylated gelatin (GelMA, UMN Bioprinting Facility) was added to solution at 10% w/v. GelMA solution was then vortexed and incubated in 50°C water bath. Once the GelMA was dissolved, the solution was filtered using a sterile Millex-GV 0.22 µm syringe filter (Millipore®). For GelMA only hydrogels, RMEPCs were added at

750,000 cells/mL. For ECM hydrogels, sterile GelMA solution was added to either arterial or venous dECM powder at 10% w/v. ECM-GelMA solution was incubated again in the water bath and vortexed momentarily prior to added RMEPCs at the same concentration. Hydrogel-RMEPC solutions were then casted in 48-well plates at ~200µL. Once casted, the plate was exposed to UV-LED flood lamp for 15 second in activate LAP and solidify hydrogels. Once solidified, 0.4-0.5 mL of media was added to each well. RMEPC-seeded hydrogels were incubated for 7 days with a media change every 48 hours.

RNA Extraction and cDNA Synthesis: Cell from 2D culture were harvested using TrpyLE (Gibco) and neutralized with culture media. Cell suspension was transferred to 15 mL conicals for centrifugation. After centrifuging for 5 minutes at 300 rpm, supernatant was removed from each sample. 500 µL of TRIzol Reagent (Invitrogen) was added to each pellet and transferred to 1.5 Eppendorf tubes. For RMEPC seeded hydrogels, media was removed from wells, followed by 2 rinses with PBS. Gels were transferred into 1.5 mL Eppendorf tubes and 700 µL of TRIzol was added to each tube. Samples were homogenized for 1-2 minutes before being placed on ice. All samples were allowed to incubate in TRIzol for 5 minutes before adding chloroform. 200 µL of chloroform was added for every mL of TRIzol. RNA containing phase was separated by centrifuging samples at 12,000 g for 15 minutes at 4°C. Colorless, upper phase, containing RNA, was transferred to RNAse-free tube. The remainder of RNA extraction was carried out using a PureLink™ RNA Mini Kit (Invitrogen™). Once extracted, total RNA was stored at -80°C until cDNA synthesis. cDNA was created from samples using SuperScript™ III First-Strand Synthesis System (Invitrogen™) following kit protocols. All RNA samples used had a $^{260}/_{280}$ ratio above 1.8. Once synthesized, samples were stored at -20°C until use for gene expression

Gene Expression: Quantitative real-time PCR of samples was performed on an ABI 7500 Real-Time PCR System using TaqMan™ Gene Expression Master Mix (Applied Biosystems). Assay probes ordered from Life Technologies™ were used to target the follow genes: *KDR* (Rn00564986_m), *Efnb2* (Rn01756899_m1), *Ephb4* (Rn01481051_m1), *Nrp1* (Rn00595457_m1), *Car4* (Rn00569826_m1), *Etv2* (Rn01457547_g1), and *Gapdh* (Rn01775763_g1) as a housekeeping gene. Samples were run in triplicate.

Results

Proteomic Analysis of Arterial and Venous ECM

Pulmonary arterial and venous dECM (A-ECM and V-ECM) powder samples were further digested and solubilized before injection into the mass spectrometer. Samples were unlabeled to allow for non-selective detection of all solubilized peptides. Proteomic analysis revealed A-ECM samples (**Figure 3.3)** to have a more diverse collection of protein groups (28 ±1.0 vs 20 ±6.2) and on average, more detectable peptides amongst these groups (2154.2 ±541.7 vs 1055 ±449.0) than V-ECM samples (**Figure 3.4**). Within both A-ECM and V-ECM samples, the most abundant peptides were for elastin, collagen VI (Col VI), and actin groups. Col I and fibrillar collagen peptides were found to be more abundant in V-ECM samples than A-ECM samples.

Low-Abundant Proteins in Arterial and Venous ECM

Protein Groups composing of less than 2% of total detected peptides were classified as “Low-Abundant” proteins (LA-protein). LA-proteins from A-ECM samples (**Figure 3.5)** were once again more diverse than those of V-ECM samples (**Figure 3.6)**. LA-proteins of A-ECM samples also accounted for a larger percentage of total peptides than LA-proteins of V-ECM samples (10.38 ±1.8 vs 5.57 ±0.7).

3D culture of RMEPCs in ECM hydrogels increases expression of certain endothelial genes

Within hydrogels made containing dECM particles, we sought to evaluate the ability of ECM from pulmonary arteries and veins to drive endothelia progenitors towards an arterial or venous phenotype, respectively. After adding RMEPCs to of GelMA only, Arterial ECM (A-ECM), and Venous ECM (V-ECM) hydrogel solution (750,00 cells/mL), 200 µL of cell embedded solution was added to wells of a 48-well plate and crosslinked. GelMA only and ECM hydrogels were incubated for 7 days, with a media change every 48 hours. After the 7 days, RNA was extracted from constructs and used for cDNA synthesis and subsequent qPCR analysis. In addition to our hydrogels, RNA also extracted from rat pulmonary arterial endothelial cells (PAECs), venous endothelial cells (PVECs), and microvascular endothelial cells (MVECs) grown in 2D cultures for cDNA synthesis and qPCR analysis.

Our RMEPCs are a proliferative subset of cells extracted from the larger MVEC population, and all qPCR results were calibrated to MVECs. We used probes targeting the angiogenic growth factor *Efnb2*, venous endothelial gene *Ephb4*, *Nrp1*, *Kdr*, *Etv2*, and *Car4* (**Figure 3.7**). From our experiment, we were unable to detect expression of *Etv2* and *Car4*. RMEPCs cultured in both A-ECM and V-ECM hydrogels displayed higher expression of *Nrp1* compared to those in the GelMA-only group. Expression of both *Efnb2* and *Ephb4* were higher in RMEPCs in ECM hydrogels than both GelMA-only and 2D culture groups. Despite detection of *KDR* from 2D cultures of RMEPCs, we were unable to detect in any our RMEPC-hydrogel groups.

Final Conclusions and Discussion

Generating tissue-engineered organs and grafts requires in-depth understanding of the effects ECM components have on cells survival, proliferation, and function (Rozario and DeSimone, 2010; Hynes and Naba, 2012; Kular et al., 2014; Yi et al., 2017; Barallobre-Barreiro et al., 2020). We have already begun to see the importance of ECM components in engineering new vasculature (Neve et al., 2014; Marchand et al., 2019). While there is a general understanding to the ECM proteins that make up blood vessels (see **Figure 3.1**) there is still much that is unknown about the differences between arterial and venous ECM components. Considering the functional difference between vascular regions are intrinsically related to the differences in their endothelial cells and ECM compositions (dela Paz and D'Amore, 2009; Aird, 2012; Joddar et al., 2018) it is important to elucidate the effects of these regional differences as we continue to engineer new blood vessels. The importance of chamber specific ECM components from hearts has already been shown to drive cells to a region-specific phenotype in other studies (Cao et al., 2016; Mesquita et al., 2021).

After dissecting and decellularizing 5 arteries and 5 veins from porcine pulmonary vasculature, we were able to use the decellularized tissue conduct label-free mass spectrometry on for our proteomic analyses and create ECM hydrogels for 3D culture of RMEPCs. From our proteomic analysis, we observed that the most abundant peptides related to elastin Col VI, and actin. Of these, Col VI is interesting due to normally being distributed in the sub-epithelium of lungs and aiding in elastic and mechanical support (Bober et al., 2010). That being said, it has been suggested that Col VI interacts with multiple other collagens (e.g., types I, IV, and XIV) to support cell-ECM adhesion and migration (Howell and Doane, 1998; Lamandé et al., 2006; Gramann et al., 2009). Col IV is a major component of the endothelial basement membrane and directly interacts with endothelial cells. In addition to other endothelial interactions, proteolytic cleavage of Col

VI alpha chain produces a fragment protein known as endotrophin. Endotrophin can act independently, serving as a chemoattractant for macrophages and endothelial cells, especially in developing tumors. In addition, it stimulates endothelial migration and tubule formation *in vitro* (Park and Scherer, 2012; Chen et al., 2013). For tissue engineering purposes, integration of Col VI and endotrophin into ECM-derived scaffolds may aid in regeneration of endothelium through supporting cell migration and basement membrane support.

Actin, thought typically known for its interaction with the extracellular matrix, has been previously detected in the matrix of bovine aorta, chick embryo fibroblast, rat smooth muscle cells, and the vascular walls of vessels from various organs (Chen et al., 1978; Jones et al., 1979; Bach and Bentley, 1980; Accinni et al., 1983). Though we are uncertain of the specific isoform of actin detected in our samples, as well as its full binding capabilities, previous groups have described the ability to bind with angiogenin, a pro-angiogenic molecule, and the expression of actin on the surface of calf pulmonary arterial cells (Hu et al., 1993; Moroianu et al., 1993). Elastin is a major component of blood vessels, primarily in arteries as they typically have an internal and external elastic lamina. The elastic lamina is often indistinct, and sometimes absent, within pulmonary veins as they are not as elastic compared to the arteries that must absorb the pressure generated by the right ventricle (Michel, 1982; Gao and Raj, 2005). While elastin can be produced by ECs it is not viewed as an important basement membrane component (Greenlee et al., 1966; Stary et al., 1992; Hayden et al., 2005). If cleaved by extracellular proteases, elastin derived peptides can modulate EC function and proliferation by stimulating cell migration and tube formation (Robinet et al., 2005).

One of the primary difference we observed between A-ECM and V-ECM was that Col I and fibrillar collagen peptides were more abundant in V-ECM. Without robust direct

quantification methods, we cannot determine if this observation is relative to mass or an absolute difference in portions of Col I and fibrillar collagen. This is an important consideration as pulmonary veins are much thinner and have less mass than arteries of the same generation. Within canine lungs, the tunica media of pulmonary veins compromises 22-60% less of the wall than in pulmonary arteries (Michel, 1982). In addition, the subgroup of fibrillar collagens contains type I, II, III, V, XI, XXIV, and XXVII collagens (Bella and Hulmes, 2017). Mass spectrometry targeting each of these collagens would be necessary to elucidate the composition of fibrillar collagens in both arterial and venous ECM. Another fibrillar collagen, Col I is the most abundant collagen in the human body. In additional to various roles in a multitude of tissues, Col I supports EC survival through mitogen-activated protein kinase pathway stimulation and can indirectly induce intracellular actin-reorganization to change EC morphology (Mongiat et al., 2016). It has been observed that angiogenic effects of Col I on ECs is mediated through its interaction with α2β1 integrin of ECs, making it a protein of interest for bioengineers developing pro-angiogenic scaffolds and polymers (Twardowski et al., 2007; Turner et al., 2020).

While we did observe that “Low-Abundant” proteins made up a larger portion of the total detected peptides for A-ECM samples than V-ECM samples, we must acknowledge again that the overall diversity of protein groups and number of detected peptides was higher amongst A-ECM than V-ECM. In addition to the more prevalent protein groups, this provides us with a list of peptides to target in future proteomic studies of pulmonary vessels. With this we must acknowledge some of the other limitations of our experimental setup for this portion of our study. To start, not all of the ECM components are able to be solubilized within our solutions for subsequent injection and solubilization. This is a common limitation of mass spectrometry as we can only measure the soluble

fraction. This is even more pronounced as we used a label-free detection method while analyzing complex heterogenous samples. While the benefit of this method is the ability to detect any peptide within the soluble fraction, proteins that are more abundant within our samples (e.g., elastin, collagen) can easily mask the presence of any less abundant proteins. Finally, we were unable to conduct robust quantitative analysis on the data collected from our measurements. This includes normalizing the data between samples to account for instrument variability between injections as well as proportion of detected proteins relative to total. We believe that some of these limitations can be overcome with future experiments and data processing methods.

To begin evaluating the effect of arterial and venous ECM proteins on EPCs we cultured our RMEPCs in arterial and venous ECM-hydrogels and measured gene expression of several endothelial genes. Gene expression measurements were also taken for RMEPCs grown in GelMA only hydrogels as well as *in vitro* cultures of RMEPCs, PAECs PVECs, and MVECs. PAECs and PVECs were included as positive controls. We detected expression of *Ephb4*, which codes for a venous-specific EC receptor, and *Efnb2*, which codes for an angiogenic growth factor and ligand for Eph receptor B4, in all samples. Relative to both RMEPCs grown *in vitro* and in GelMA only conditions, there was an increase expression of both genes in RMEPC grown in A-ECM and V-ECM hydrogels. *Ephb4* was markedly increased in V-ECM conditions than A-ECM conditions, an indication that ECM from pulmonary veins are directing progenitor cells to a vessel-specific phenotype. This observation falls in line with previous reports classifying high expression of *Ephb4* and its related protein as a characteristic of venous ECs (Wang et al., 1998; Shin et al., 2001; Niklason and Dai, 2018). Though the mechanism behind is currently unclear, the interaction between ephrin-B2 ligand and EphB4 receptor has been established as a necessity for proper embryonic angiogenesis and endothelial

migration (Steinle et al., 2003; Kuijper et al., 2007; Luxey et al., 2011). Increased expression of both genes within EPCs when exposed to either A-ECM or V-ECM is a notable finding and provides additional insight in regenerating acellular ECM constructs.

Neuropilin-1 binds vascular endothelial growth factor (VEGF), coexpresses with VEGF receptor 2 (VEGFR2) in endothelial tip cells, and is an early marker of arterial endothelial cell differentiation (Herzog et al., 2005; Hsieh et al., 2008; Aspalter et al., 2015; Kim et al., 2018). Though expression levels were decreased relative to MVEC controls, we were able to detect *Nrp1* within RMEPCs in each condition. Extended culture of cells within A-ECM and V-ECM hydrogels may further increase of *Nrp1*. Future genomic experiments would benefit from evaluating the expression levels of other vessel specific genes, including but not limited to, the arterial specific *Ephb2*, *Cx40*, *Sox17*, *Nr2f2*, and *Nrp2* (Shin et al., 2001; Herzog et al., 2005; Shin and Anderson, 2005; You et al., 2005; Cui et al., 2015; Niklason and Dai, 2018). Unfortunately, we were unable to detect *Kdr*, the gene encoding for mature endothelial cell marker CD31, from RMEPCs cultured in any of our hydrogel conditions. We believe that this may require extended culture timelines as we have previously seen increased expression of CD31 in RMEPCs when seeded into acellular murine lung scaffolds and cultured within our bioreactor system (Akinnola et al., 2021).

While limited, this study provides insight on how differences in ECM components between arterial and venous segments of pulmonary vasculature effects the phenotype of endothelial cells. We have begun the in-depth investigation into the complex differences between the arterial and venous ECM proteins and how they may support endothelialization of ECM scaffolds and acellular tissue and further robust proteomic analysis can be done with proteomic data obtained from this study. Creation of ECM hydrogels embedded with EPCs provided a design for evaluating ECM effect on

progenitor cells and groundwork for genotyping cells after exposure to ECM particles in 3D culture. Finally, while we didn't detect expression of *Etv2*, an early regulator of endothelial differentiation, in any of our samples, this negative finding may be indicative of cells being exposed to sufficient oxygen in our hydrogels as ETV2 decreases after the gastrulation phase of embryogenesis and rises in the setting of hypoxia (Kataoka et al., 2011; Oh et al., 2015; Tsang et al., 2017; Van Pham et al., 2017; Wang et al., 2020). A benefit of not detecting *Etv2* is that our cells are able to avoid hypoxia within the current thickness of our gels, as central necrosis is a common occurrence in thicker 3D cultures. This is just one possibility and should be evaluated with future experiments incorporating higher cell concentrations and extended culture periods.

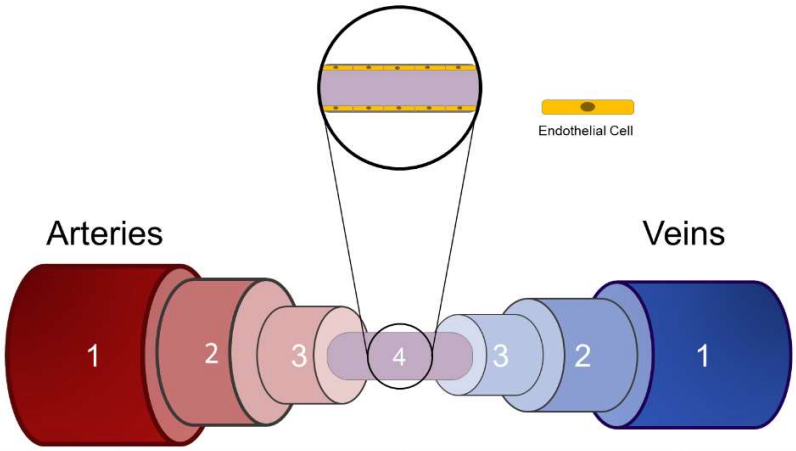

1. Basement Membrane	2: Tunica Intima	3: Tunica Media	4: Tunica Externa (Adventitia)
Collagen I/III/IV/XVIII	Collagen I/III	Collagen IV	Collagen IV
Laminin	Elastin	Fibronectin	Non-fibrillar Collagen
Versican	Fibronectin	Laminin	Laminin
	Laminin	Nidogen	Nidogen
	Proteoglycans	Proteoglycans	Proteoglycans
		Glycoproteins	Glycoproteins

Figure 3.1 Major ECM Proteins in Blood Vessels

Standard organization of four layers that compose blood vessels (arteries and veins) and important ECM proteins that are found in those respective layers.

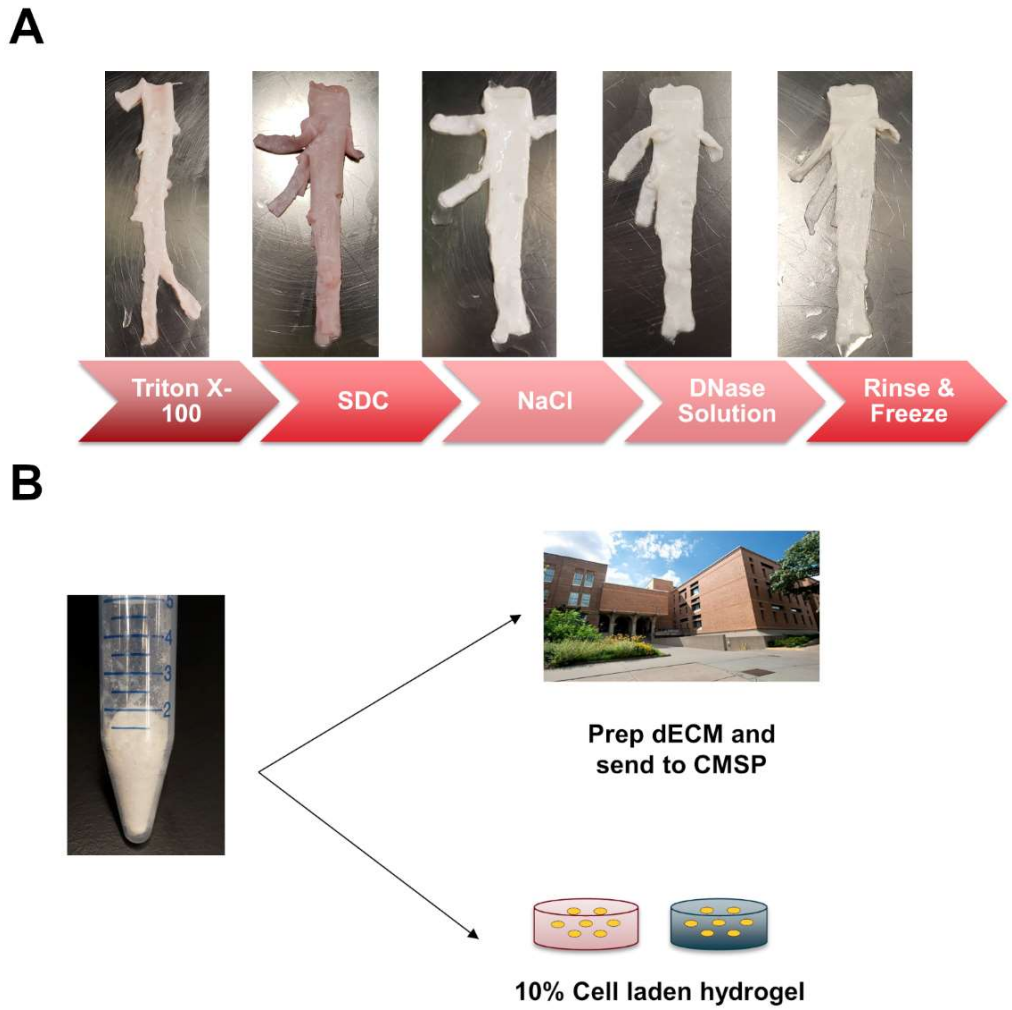

Figure 3.2 Vessel Decellularization and ECM preparation

A) Decellularization of a pulmonary artery following the process described in **Materials and Methods**. B) Milled dECM formed into a powder was used for proteomic analysis in collaboration with UMN-CMSP or used for formation of ECM hydrogels embedded with endothelial progenitor cells.

Figure 3.3 Composition of major ECM Proteins from Porcine Pulmonary Arteries

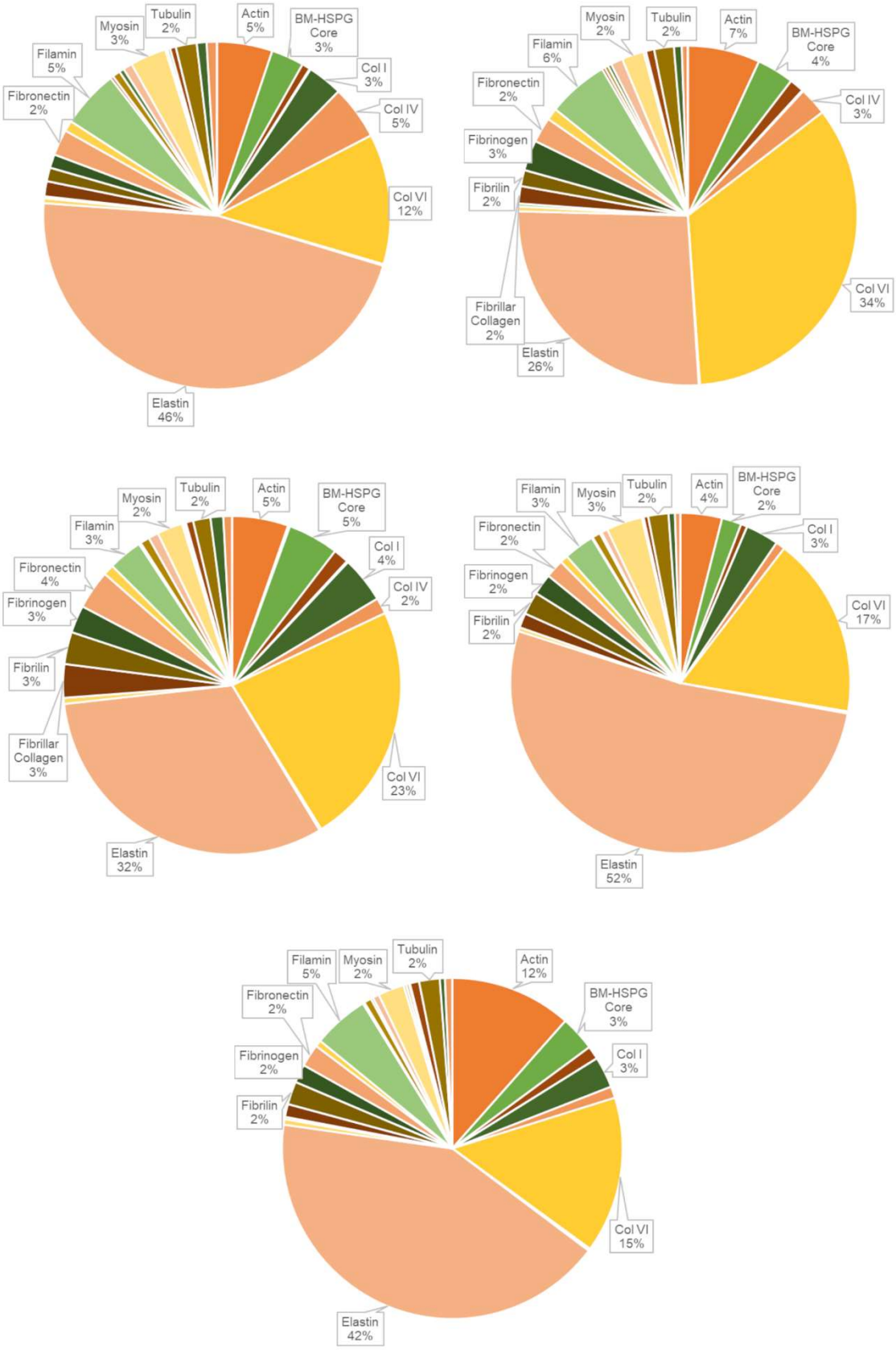

Figure 3.3 Composition of major ECM Proteins from Porcine Pulmonary Arteries

Liquid chromatography/mass spectrometry was used to analyze proteins within porcine pulmonary artery dECM samples. After further processing, charts for each of the 5 samples were created, detailing the percent composition of specific protein groups based detected peptides or their respective group. Labels were only added for protein groups that accounted for ≥ 2% of total detected peptides.

Figure 3.4 Composition of major ECM Protein from Porcine Pulmonary Veins

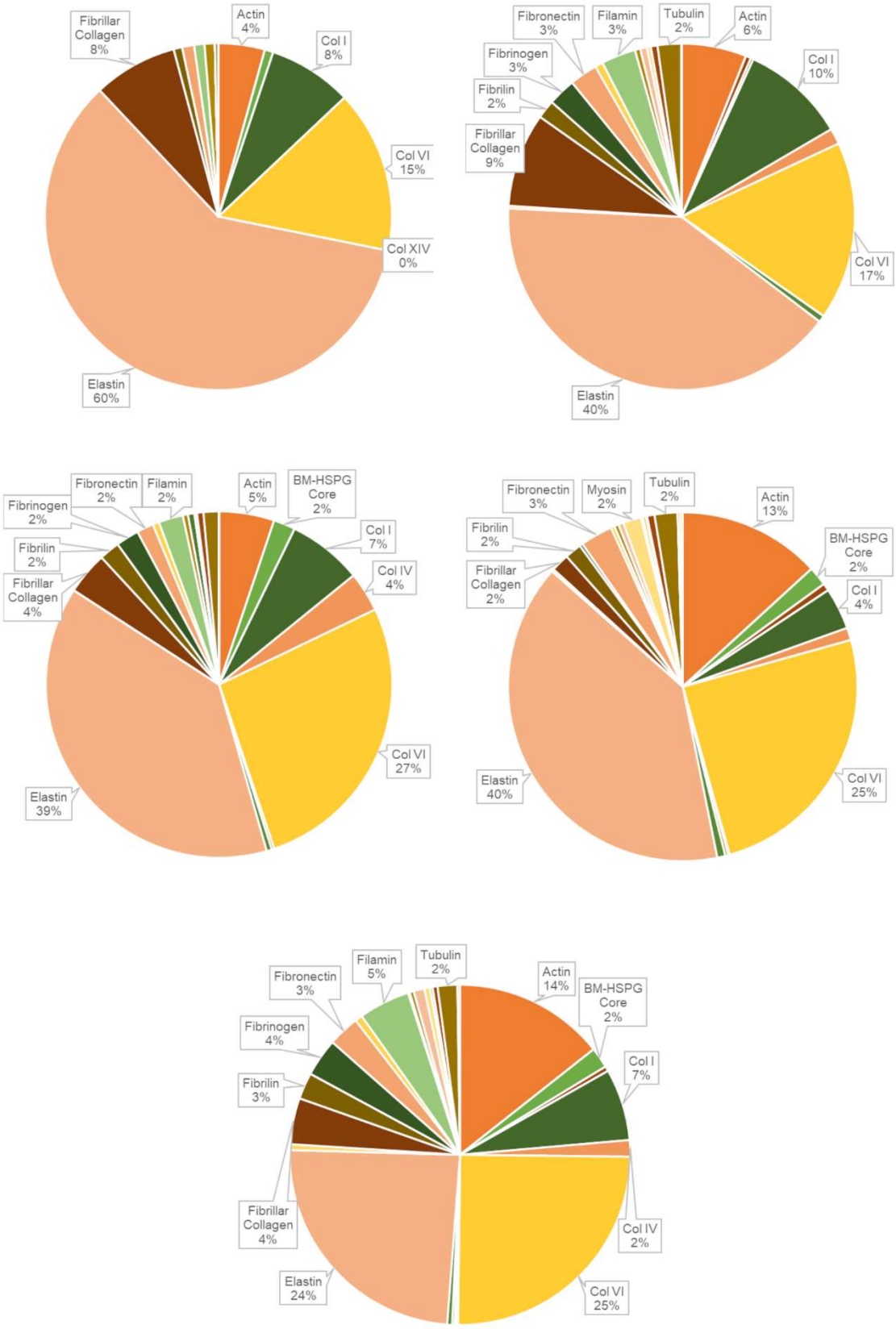

Figure 3.4 Composition of major ECM Protein from Porcine Pulmonary Veins

Liquid chromatography/mass spectrometry was used to analyze proteins within porcine pulmonary vein dECM samples. After further processing, charts for each of the 5 samples were created, detailing the percent composition of specific protein groups based detected peptides or their respective group. Labels were only added for protein groups that accounted for ≥ 2% of total detected peptides.

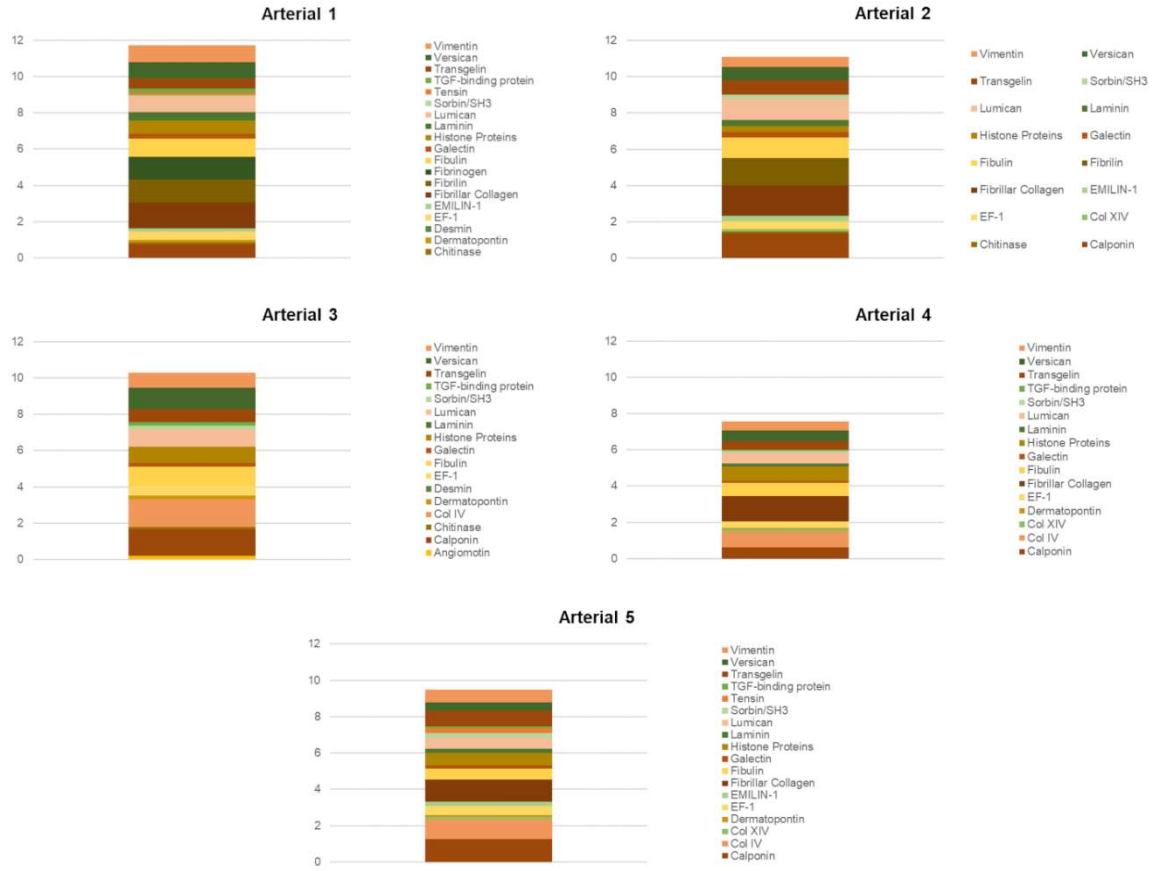

Figure 3.5 Low-Abundant Proteins in Pulmonary Artery ECM

Breakdown of protein groups from porcine pulmonary artery dECM samples that were measured to be < 2% of total peptides detected.

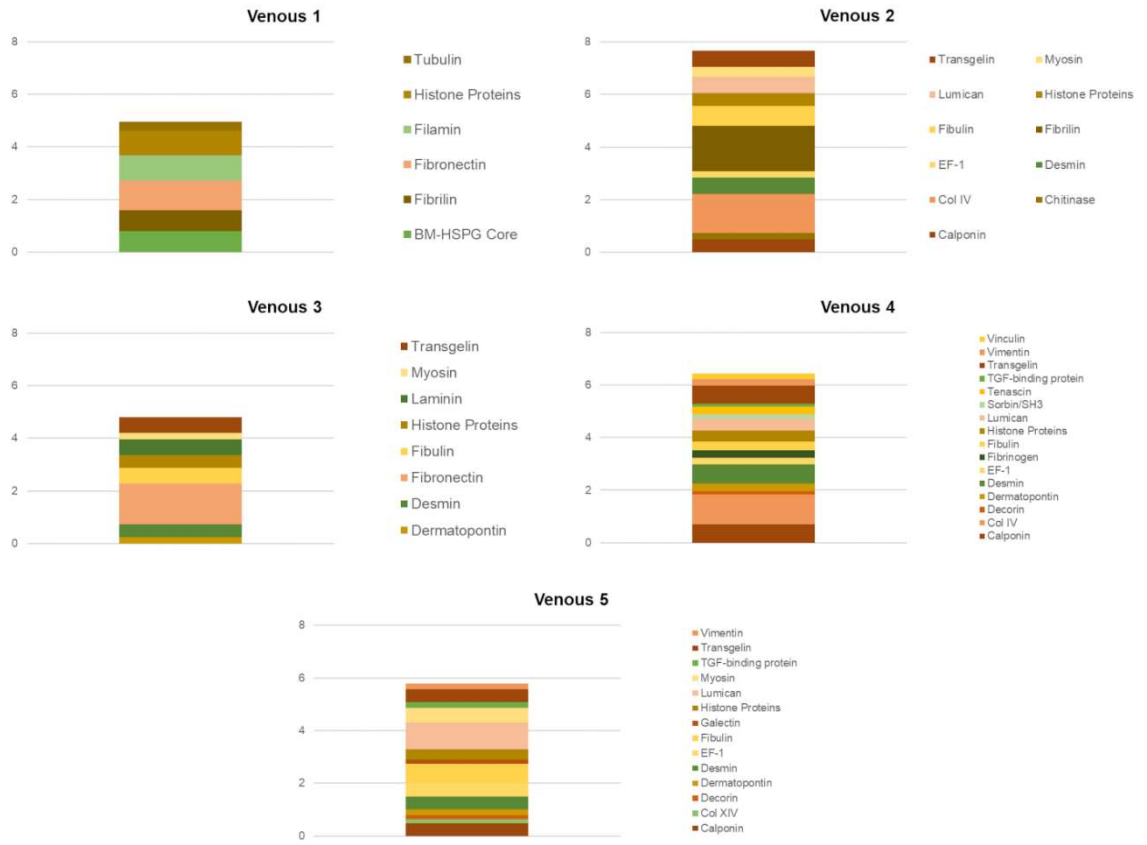

Figure 3.6 Low-Abundant Proteins in Pulmonary Vein ECM

Breakdown of protein groups from porcine pulmonary vein dECM samples that were measured to be < 2% of total peptides detected.

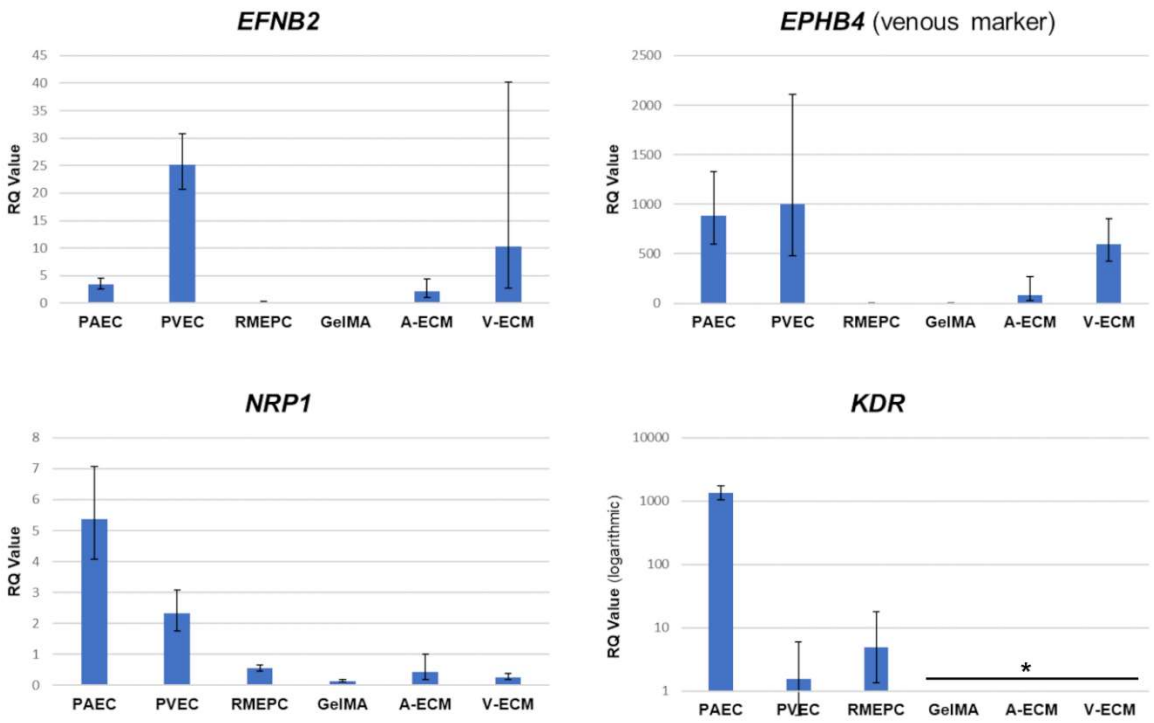

Figure 3.7 Gene Expression of EPCs cultured in ECM Hydrogels and Pulmonary ECs from 2D culture

Quantitative RT-PCR was used to detect expression of endothelial genes from 2D and 3D hydrogel cultures of ECs and EPCs. “PAEC”, “PVEC”, and “RMEPC” indicate ECs that were cultured in 2D/*in vitro*. “GelMA”, “A-ECM”, and “V-ECM” indicate 3D cultures of RMEPCs within hydrogel. *Efnb2*, *EPHB4*, and NRP1 were detected in all samples. *Kdr* was only detected in PAECs, PVECs, and RMEPCs. Data represent triplicates from one biological sample. “*****” denotes samples where gene expression was undetected.

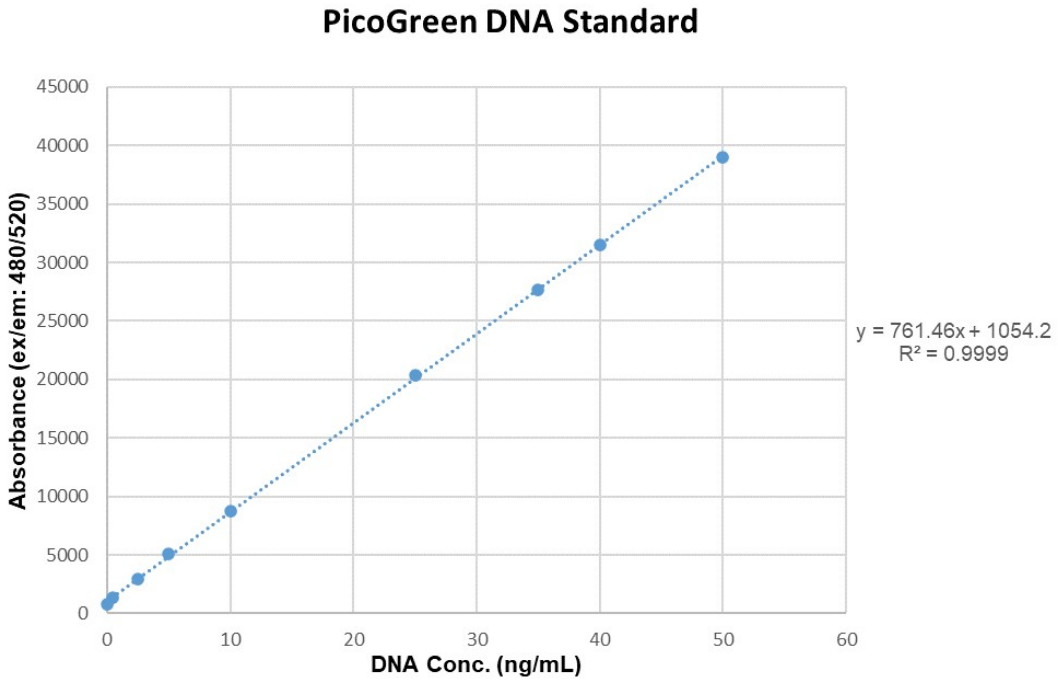

Arterial Samples	Absorbance (480/520)	Final Conc. (ng/mL)	Avg. Conc. (ng/mL)	DNA/wt. (ng/mg)
1	5138	10.7	**6.5**	**1.3**
2	3986	7.7		
3	1453	1.0		
Venous Samples	**Absorbance (480/520)**	**Final Conc. (ng/mL)**	**Avg. Conc. (ng/mL)**	**DNA/wt. (ng/mg)**
1	4776	9.8	**3.1**	**0.6**
2	1056	0.01		
3	854	-0.5		

Figure 3.8 DNA Quantification of Decellularized Vessels

Quant-iT™ PicoGreen assay was utilized to detect double-stranded DNA within decellularized pulmonary arteries and veins. Standard curve and samples were prepared in a 96-well plate and absorbance measured (ex/em: 480/520 nm). Standard curve provided above in addition equation and R^2 for trendline. N = 3 for each group, samples were run in triplicate.

Chapter 4

Differentiation of Hemangioblasts from human iPSCs and their Potential in forming new Endothelium

Ifeolu Akinnola[1] and Angela Panoskaltsis-Mortari [2,3]

[1] Integrative Biology and Physiology Graduate Program, University of Minnesota Medical School, Minneapolis, MN, United States,
[2] Pediatric Blood and Marrow Transplantation and Cell Therapy, University of Minnesota, Minneapolis, MN, United States
[3] Pulmonary, Allergy, Critical Care and Sleep Medicine, University of Minnesota, Minneapolis, MN, United States

Preface

Tissue engineering of grafts and organs is dependent on the establishment of a functional vascular network in order to break free from size limitations and improve recellularization and function of constructs. Vascularization of such constructs has often been accomplished with fully mature endothelial cells, such as HUVECs, though the field has moved towards the use of endothelial progenitors due to their proliferative potential over primary cells. Hemangioblasts are a bipotent hematopoietic-endothelial progenitor found in embryonic development that give rise to early vasculature. Previous studies with hemangioblasts have been limited and their potential in regeneration of endothelium within acellular 3D environments has yet to be evaluated. In this study, we developed a protocol for generating angiogenic hemangioblasts from human induced pluripotent stem cells. Post-differentiation, we identified both $CD31^{+}$/$VEGFR2^{+}$ and VE-$Cadherin^{+}$/$CD73^{+}$ subcultures. This process was dependent on transient hypoxic incubation, utilization of ECM glycoprotein tenascin-C, and growth factor supplementation. In addition to increased expression of several hematopoietic and endothelial genes, we observed our hemangioblasts adhering to the luminal wall of a hydrogel microchannel.

Introduction

The bioengineering of whole organs, such lung, from a patient's own cells would address the challenges associated with organ acquisition and post-operative complications. Our group has developed an efficient protocol for the decellularization of lungs, leaving us with a decellularized lung scaffold (DLS) that maintains its extracellular matrix (ECM) components and 3-D ultrastructure. Multiple bioengineering groups have repeatedly shown that the ultrastructure and ECM makeup of scaffolds play a significant role in the differentiation and maintenance of the local stem and progenitor cells (Davis and Senger, 2005; Daly et al., 2012; Crabbe et al., 2015; Ren et al., 2015). Recellularization and transplant of DLS in rat models is possible, but the new lungs fail after a short period post-transplant. Failure of the new lung is often due to vasculature volume overload and hemorrhaging into alveoli, indicative of an endothelial lining that lacks integrity and/or function (Petersen et al., 2010; Doi et al., 2017; Le et al., 2017). Because of these vascular complications (illustrated in **Figure 4.1**), I propose that developing and evaluating new methods for reconstitution of the pulmonary vasculature would improve function and longevity of these new lungs.

Hemangioblasts are progenitor cells found in the primitive streak of early embryos and give rise to both hematopoietic and endothelial cells (ECs). While their post-embryonic existence and characterization is debated heavily (Cao and Yao, 2011), some studies have shown postnatal hemangioblast (HBs) activity in maintaining local endothelium (Pelosi et al., 2002; Ramos et al., 2010; Sun et al., 2010). In addition to their postnatal presence and function, HBs can be differentiated into ECs in both *in vitro* and *in vivo* experiments (Amaya, 2013). A previous study detailed the ability of HB blast colonies to differentiate into endothelial cells and repair the endothelium of damaged mouse retinal vasculature (Lu et al., 2007). We plan to add onto previous HB studies by using them to

re-establish pulmonary endothelium in DLSs. Composition and ultrastructure of ECM scaffolds have been used to drive differentiation of stem and progenitor cells. Surface interactions with ECM components initiate differentiation of cells to their proper cell types while ultrastructure of scaffolds aids in the localization of terminally differentiated cells. With our lab's experience in creating DLS, and using them in the engineering of lungs, we are well-suited to create and evaluate HB-derived endothelium. In this study, our objective was to develop a reproducible differentiation protocol for generating HBs from human pluripotent stem cells. We then planned to characterize the hemangioblasts and evaluate their potential in seeding and growing within a luminal space.

Materials and Methods

Cell Culture: The human iPSCs used in this studied were vShiPs kindly provided by the Dr. James Dutton (Stem Cell Institute, University of Minnesota Medical School). vShiPs are clonally derived from PCBC16iPS cells (previously described by Ye et al. (Ye et al., 2013) that have been conditioned to grow on vitronectin in Essential 8™ media. Prior to differentiation, vShiPs were cultured on Synthemax® II (Corning®) – a vitronectin based coating protein. Human umbilical vein endothelial cells (HUVECs) were ordered from Angio-Proteomie (Boston, MA) and cultured in Endothelial Cell Growth Medium (R&D Systems).

Differentiation of iPSCs into Hemangioblasts: Protocol for differentiation of iPSCs into hemangioblasts, illustrated in **Figure 4.2**, was adapted from hematoendothelial development methods described by Uenishi et al. (Uenishi et al., 2014). Prior to differentiation, culture ware was coated with purified human tenascin-C (Millipore™). 0.5 µg/mL of tenascin-C was reconstituted in 1X PBS and filtered through a Millex-GV 0.22 µm syringe filter (Millipore®). Once culture ware surfaces were completely covered in sterile tenascin-C solution, they were allowed to sit overnight at 4°C overnight to

complete coating. vShiPs were harvested using Accutase® Cell Detachment Solution (BioLegend®) and seeded at 10,000 – 15,000 cells/cm^2 in Essential 8™ Media and 10μM Rock Inhibitor. After 24 hours, cells are switched IF9S media produced in-house (see **Table 1**) and supplemented with 50 ng/mL of bone morphogenetic protein 4 (BMP4), 50 ng/mL of basic fibroblast growth factor (FGF2), 15 ng/mL Activin A, and 2 mM of lithium chloride. After the media change, the culture is transferred to hypoxic incubation at 5% O_2. After 48 hours the media supplement is changed to 50 ng/mL of FGF2 and 50 ng/mL of vascular endothelial growth factor A (VEGF-A). After an additional 48 hours the culture is returned to normoxic incubation. After a final 48 hours the differentiation is complete, and cells can be used for further experiments.

Flow cytometry characterization of hemangioblasts: Human iPSC-derived hemangioblasts were characterized by flow cytometry using a FACSCalibur (BD Biosciences) and analyzed using FlowJo™ software. After harvesting cells were labeled using antibodies to human CD31 (BD Bioscience 555445), Apelin receptor (R&D Systems #FAB856A), CD73 (BD Biosciences 561014), CD144/VE-Cadherin (BD Biosciences #560411), VEGFR2 (BD Biosciences #560872).

Gene Expression

After harvesting, cell suspension was transferred to 15 mL conicals for centrifugation. After centrifuging for 5 minutes at 300 rpm, supernatant was removed from each sample. 500 μL of TRIzol Reagent (Invitrogen) was added to each pellet and transferred to 1.5 Eppendorf tubes. Samples were allowed to incubate in TRIzol for 5 minutes before adding chloroform. 200 μL of chloroform was added for every mL of TRIzol. RNA containing phase was separated by centrifuging samples at 12,000 g for 15 minutes at 4°C. Colorless, upper phase, containing RNA, was transferred to RNAse-free tube. The remainder of RNA extraction was carried out using a PureLink™ RNA Mini Kit

(Invitrogen™). Once extracted, total RNA was stored at -80°C until cDNA synthesis. cDNA was created from samples using SuperScript™ III First-Strand Synthesis System (Invitrogen™) following kit protocols. All RNA samples used had a $^{260}/_{280}$ ratio above 1.8. Once synthesized, samples were stored at -20°C until use for gene expression. Quantitative real-time PCR of samples was performed on an ABI 7500 Real-Time PCR System using TaqMan™ Gene Expression Master Mix (Applied Biosystems). Assay probes ordered from Life Technologies™:

Seeding Fibrin Channel:

Construction of microchannels within fibrin hydrogels was executed as previously described (Meng et al., 2019). Hydrogels were created using 10 mg/ml of human plasma fibrinogen (EMD Millipore) crosslinked with 0.5 U/mL of human plasma thrombin (Sigma) within IF9S media supplemented with FGF2 and VEGF-A. Prior to casting and crosslinking the hydrogels, metal pins with a 300-micron outer diameter were placed for to form microchannels. The pins were removed after fibrin crosslinking, leaving channels with a lumen size similar to that of the outer diameter of the pins.

Prior to harvesting, iPSC-derived hemangioblasts were labeled using Qtracker 525 (Invitrogen). 2 µL of labeled cell suspension (2.5 x10^4 cells) was injected into the microchannels. After 24 hours of culture, non-adherent cells were flushed out using fresh media. Cell-laden microchannels were cultured for 4 days prior to imaging using an EVOS Cell Imaging System.

Results

Tenascin-C supports differentiation of human-iPSCs into angiogenic hemangioblasts

Our modified protocol for differentiation of human iPSCs (hiPSCs) into hemangioblasts (**Figure 4.2**) was utilized on cell cultured on both Synthemax and human tenascin-C

(Ten-C).Originally, Ten-C was used by Uenishi et. al. for generation of hemangioblast and T-lymphoid cells. After modifying their protocol for generation of angiogenic hemangioblasts, we predicted that it would be possible to attempt differentiation of our hiPSCs on Synthemax and achieve generation of angiogenic hemangioblasts. After completion of the differentiation protocol, cultures were characterized for expression of endothelial markers via flow cytometry. Cultures were tested for double-positive expression of endothelial intercellular junction protein, CD31, and vascular endothelial growth factor receptor 2 (VEGFR2), as well as adhesion protein vascular endothelial cadherin (VE-Cadherin) and CD73. From our assessment of endothelial marker expression within subpopulations in both conditions, cell cultured and differentiated on Synthemax are unable to develop into angiogenic hemangioblast (HB) subpopulations (**Figure 4.3 A)**. Cells cultured and differentiated on Ten-C were able to develop CD31+/VEGFR2^{+} and VE-Cadherin^{+}/CD73^{+} subpopulations (**Figure 4.3 B**).

Tenascin-C is inefficient at differentiating hiPSCs into angiogenic hemangioblasts alone

After confirming that Ten-C could be used to differentiate hiPSCs into angiogenic hemangioblasts, we then assessed if Ten-C alone was sufficient for successful differentiation of cells compared to supplementation of culture media with growth factors. Ten-C has multiple fibronectin domains and an EGF-like domain that interact with integrins on cell membranes. The interactions between integrins and domains of Ten-C have been observed to stimulate cell proliferation and differentiation, as well as preventing cell death (Tucker et al., 1994). Ten-C was necessary in the previous experiment for generating angiogenic subpopulations, but we believed that it was not sufficient on its own to achieve the same level of success without additional growth factors. Two replicate hiPSC cultures underwent differentiation in parallel with only one receiving standard growth factor supplementation (i.e., BMP4, FGF2, Activin A, LiCl and

VEGF-A). While both cultures were able to partially differentiate into $CD31^{+}$/$VEGFR2^{+}$ and VE-$Cadherin^{+}$/CD73+subcultures, the absence of growth factors resulted in a less efficient development of angiogenic subcultures (**Figure 4.4**). The combination of Ten-C coating and growth factor supplementation is necessary for efficient generation of angiogenic subcultures of differentiated hiPSCs.

Human iPSC-derived Hemangioblasts have an increase in several endothelial and hematopoietic genes

Assessment of endothelial and hematopoietic gene expression of angiogenic hemangioblasts was carried out via quantitative real-time PCR (qPCR). Of the genes tested, we reported increases increase in *Cdh5, Hhex, Runx1, Sox7, and Tal1* when compared to undifferentiated hiPSCs (**Figure 4.5**). In particular, *Cdh5*, the gene encoding VE-Cadherin, had higher expression in hemangioblasts than in our HUVEC positive controls.

Human iPSC-derived HB can adhere and culture in fibrin vessels

Before being used for re-endothelialization of an acellular vascular lumen, endothelial cells and progenitors must be able to line the inner wall of the vessel. Using resources from the UMN Bioprinting facility and methods developed by Meng et al. 2019 (Meng et al., 2019), we developed a hydrogel microchannels for assessing the ability of HBs in adhering to the luminal wall (**Figure 4.6 A**). Before harvesting from Ten-C coated plates, cultures were labeled with green-fluorescent, cytoplasmic nanocrystals for easy detection. After injecting green-fluorescent cells into fibrin microchannel and a post-24-hour wash, cells were culture for 4 days before fading of fluorescent signal. **Figure 4.6 B** shows that cells were able to adhere and line the luminal wall of the microchannel. In addition, we observed potential modification of the hydrogel by the cells – another function of endothelial cells during angiogenesis and vasculogenesis.

Final Conclusions and Discussion

We have successfully adapted and utilized a differentiation protocol for creating angiogenic hemangioblast from human iPSCs. The success can be highly attributed to the use of Ten-C and supplementation of culture media with growth factors.

With our new protocol, we were able to generate $CD31^{+}/VEGFR2^{+}$ cells at a slightly higher rate than the original protocol (> 35% vs 30% of total population). In comparison to the original protocol, which was developed for the generation of hematopoietic progenitors, our group was able to amend the protocol to require less growth factors for supplementation. Ten-C is an ECM protein that is abundant during embryogenesis, primarily in neuroectodermal tissues and areas of high cellular turnover. Previous studies have shown that Ten-C is produced by multiple cell types (including ECs and fibroblasts) and is present in multitude of embryonic matrix tissue (Tucker et al., 1994; Zhao and Young, 1995). Of the various forms of tenascin protein, the Ten-C variant has a higher molecular weight, and is associated with regions of active tissue remodeling, cell migration, and proliferation (Tucker et al., 1994; Viale et al., 2002; Giblin and Midwood, 2015). One study investigating retinal ECs has revealed that the expression of Ten-C is inversely related to apoptosis, delaying the collapse of retinal EC capillary tubes via interactions with αVβ3 integrin (Castellon et al., 2002). Another study revealed a postnatal importance of Ten-C in cardiac angiogenic function. Ten-C was found to colocalize with endothelial progenitor cells (EPCs) that were heading to sites of cardiac angiogenic and that Ten-C double knockout mice were unable to vascularize cardiac allograft unlike the wildtype controls (Ballard et al., 2006). Despite being associated with numerous tissue types, there is much more work needed in understanding the effect of Ten-C on vasculature and endothelial cells.

We have also concluded that the success of generating angiogenic HB subcultures is highly dependent on both the use of Ten-C for coating as well as growth factor supplementation. Of these growth factor. While BMP4, Activin A, and LiCl were important in the early differentiation steps, FGF2 and VEGF-A were important for the majority of the process. This comes as no surprise as VEGF-A is inarguably the most important growth factor within the VEGF/PDGF family for the development and function of endothelial cells.

VEGFs are ligands for VEGF receptors 1 and 2 (VEGFR1, VEGFR2), and angiogenesis is heavily regulated through their interaction *in vivo* (Veikkola and Alitalo, 1999; Ferrara et al., 2003). VEGF binding to VEGFR2 specifically is known to be responsible for endothelial migration and angiogenesis by inducing phosphorylation of phosphatidylinositol 3-kinase and phospholipase C-γ (Gille et al., 2001). Within tissue engineering, VEGF can be used for enhancement of endothelial differentiation of human stem cells (Nourse et al., 2010).

BMP4 supports formation of immature vasculature from embryoid bodies (Boyd et al., 2017). The addition of BMP4 to embryonic stem cell cultures increases the commitment of cells towards endothelial lineage. This was concluded though detection of VEGFR2, VE-Cadherin, and CD31 (Goldman et al., 2009). Utilized with stem cell factor (SCF) and FGF2, BMP4 is able to differentiate human embryonic stem cells into colony forming cells, also known as hemangioblasts.

Uenishi et al found that addition of Activin A, BMP4, and LiCl consistently induced expression of APLNR, a mesodermal surface marker, and VEGFR2 during the early portion of their differentiation process. The addition of Activin A is supported as it one of many growth factors that drive the formation of the primitive streak and mesoderm development during embryogenesis (Gadue et al., 2005).

After our differentiation process, the hiPSC culture is now a heterogenous culture containing angiogenic HB. We observed that with subsequent culture after the process, the HB subculture can be taken over. Future work on would benefit from developing ways to maintain or increase the HB subculture over others. This may depend on if there is further addition or modification of current growth factors to cell media.

The q-PCR analysis of our heterogenous cultures revealed an increase in certain endothelial and hematopoietic genes including *Cdh5*, *Hhex*, *Runx1*, *Sox7*, and *Tal1*. *Tal1/Scl*, encodes for a basic helix-loop-helix family transcription factor that is necessary for the generation of hemangioblasts (Kallianpur et al., 1994; Liao et al., 1998; Serrado Marques et al., 2018). While not as essential as *Tal1* the homeobox gene *Hhex* works in parallel with *Tal1* during embryogenesis for endothelial and hematopoietic differentiation (Liao et al., 2000). *Cdh5* encodes for VE-Cadherin and is an early gene specific for vascular endothelial cells (Sumanas et al., 2005). *RUNX1*, in addition to *GATA2*, is another transcription factor involved in the formation of hemangioblasts (Goldman et al., 2009). *SOX7*, *SOX17* and *SOX18*, are important transcription factors in early vasculogenesis and endothelial differentiation. The vast majority of early ETV2+/FLK/VEGFR2+/CD41- EPC in embryonic mice express SOX7 (Yao et al., 2019). During development of the cardiac outflow tract, *Sox7* stimulates expression of VE-cadherin and prevents EC transition to mesenchymal cells (Lilly et al., 2017; Jiang et al., 2021). While we detected an overall increase in these genes in comparison to undifferentiated hiPSCs, only *Cdh5* had a higher expression in HB cultures than HUVECs. Future qPCR experiments could include switching differentiated cultures to a similar commercial endothelial growth media and observe whether or not there is a subsequent increase in gene expression to similar levels as HUVECs.

While we did not compare differentiation of cells with the inclusion and removal of hypoxic incubation, previous studies have shown the benefit of transient hypoxia for the recruitment of EPCs and stimulating angiogenesis. Hypoxia has been found to induces vessel maturation (Krock et al., 2011) and stimulate marrow EPCs and mesenchymal stem cells into becoming ECs by VEGF regulation (Conway et al., 2001; Liu et al., 2015). Hypoxic environments have also been observed in stimulating EPCs to produce VEGFR for detection of pro-angiogenic molecules (Conway et al., 2001; de la Puente et al., 2013). In addition, *Sox7* expression rapidly increases in ECs during hypoxia, indicating that this transcription factor plays a role in hypoxia-induced angiogenesis (Klomp et al., 2020).

Recent studies suggest that the stress-response transcription factor, nuclear erythroid 2-related factor (Nrf2), is an important player in post-hypoxia repair and angiogenesis. Nrf2 has been shown to be activated after ischemia and reperfusion to repair lung injury, promote angiogenesis in response to oxidative stress, and the survival and function of hind limb ECs in ischemia models (Florczyk et al., 2014; Wei et al., 2016; Chai et al., 2018; Guo and Mo, 2020).

Unfortunately, we were unable to obtain similar success in differentiation when scaling up our cultures. Our typical cell culture were grown within a maximum surface area of approximately 9.8 cm^2. During our attempts to scale up our cultures, thus increasing surface area, we had difficulty achieving the same level of efficiency suggesting that an increase in cell density hiPSCs may be needed at higher surface areas. Another consideration for this protocol is the financial cost of Ten-C for cell culture use, as there is a potential loss of protein during the filtering process, and it is difficult to obtain relatively affordable amounts of Ten-C for larger cell culture. One solution would be to use OP9 cells to establish an extracellular matrix coat, that includes Ten-C, as described

by Uenishi et al. This may be a necessary route for future efforts in scaling up production of angiogenic HBs.

In conclusion, we believe that this protocol can be effectively used in differentiating human iPSCs into becoming angiogenic hemangioblasts. Within the heterogenous culture, $CD31^{+}$/$VEGFR2^{+}$ and VE-$Cadherin^{+}$/CD73 subsets can be generated at an appreciable level. Further robust experiments should be conducted to detect the overlap between the two classifications and potentially provide a clearer classification for these angiogenic cells. Such experiments should expand the targets for flow to detect other potential cells types within the heterogenous culture (e.g., hematopoietic, mesenchymal, neuronal). Despite difficulty in generating a large quantity of cells for creating of vascular grafts or re-endothelialization of acellular scaffolds, iPSC-derived hemangioblasts have the potential to provide coverage to a luminal wall and potentially incorporated into an established vascular space as seen in previous studies.

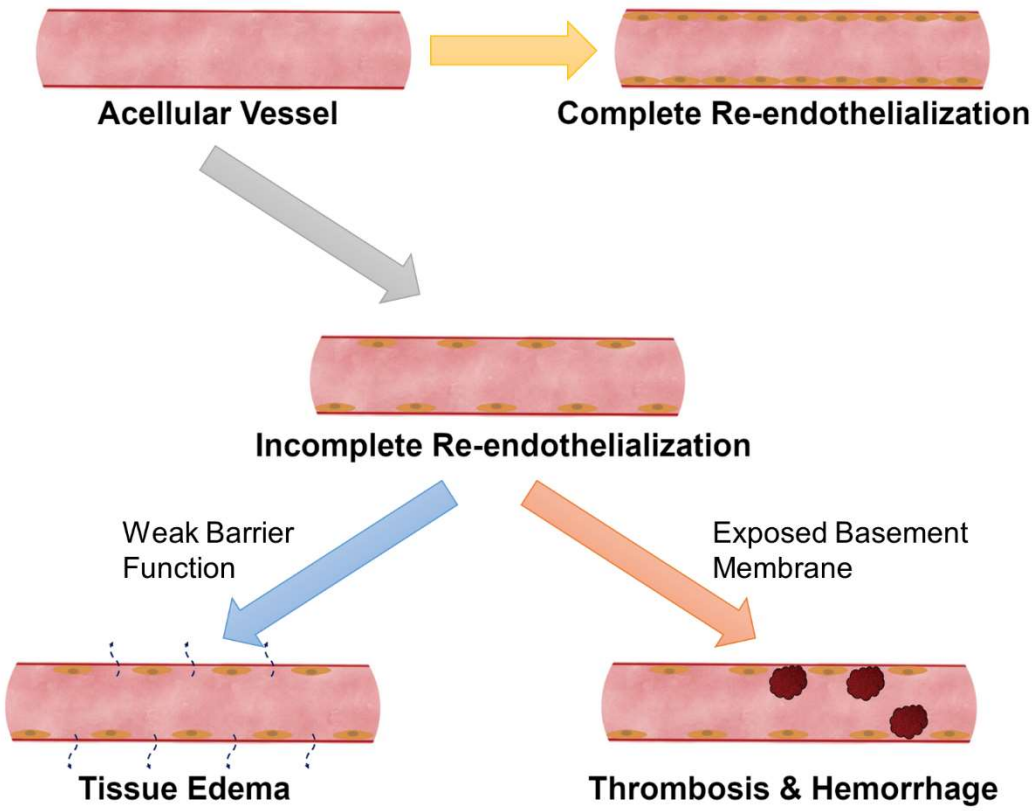

Figure 4.1 Complications in Regeneration of Endothelium

Illustration of common complications when regenerating the endothelium of tissue-engineered vessels. Without complete endothelial coverage the permeability barrier created by endothelial cells is unable to prevent leakage into the subendothelial space and outer lying tissue, resulting in edema. In addition, exposed regions of the basement membrane are opportunistic sites for spontaneous thromboses. Eventually, the accumulation of clots will lead to turbulent blood flow and spontaneous hemorrhage from the vessel.

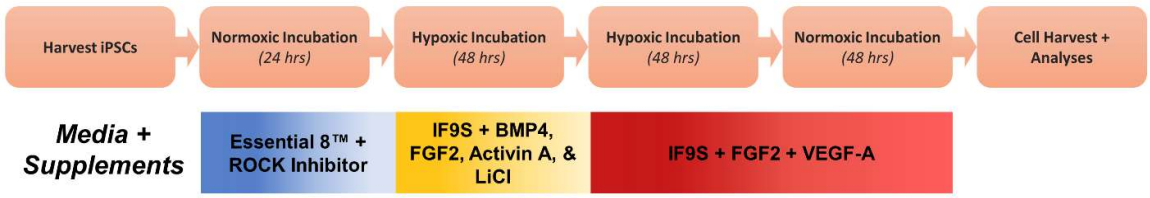

Figure 4.2 Schematic for differentiation of iPSCs into Hemangioblasts

Differentiation of human iPSC into heterogenous cultures containing angiogenic hemangioblasts is a 168-hour (7 day) process. After 24 hours, cultures are changed to IF9S media and hypoxic incubation (37°C, 5% O_2, 5% CO_2). After 96 hours (4 days) in hypoxic incubation, cultures are transferred back into normoxic incubation to allow cells to recover from hypoxia and for another 48 hours. After the 168 hours are complete, cells are used for further experiments and analyses. Supplementation to IF9S media during the differentiation process is provided at the bottom of the figure.

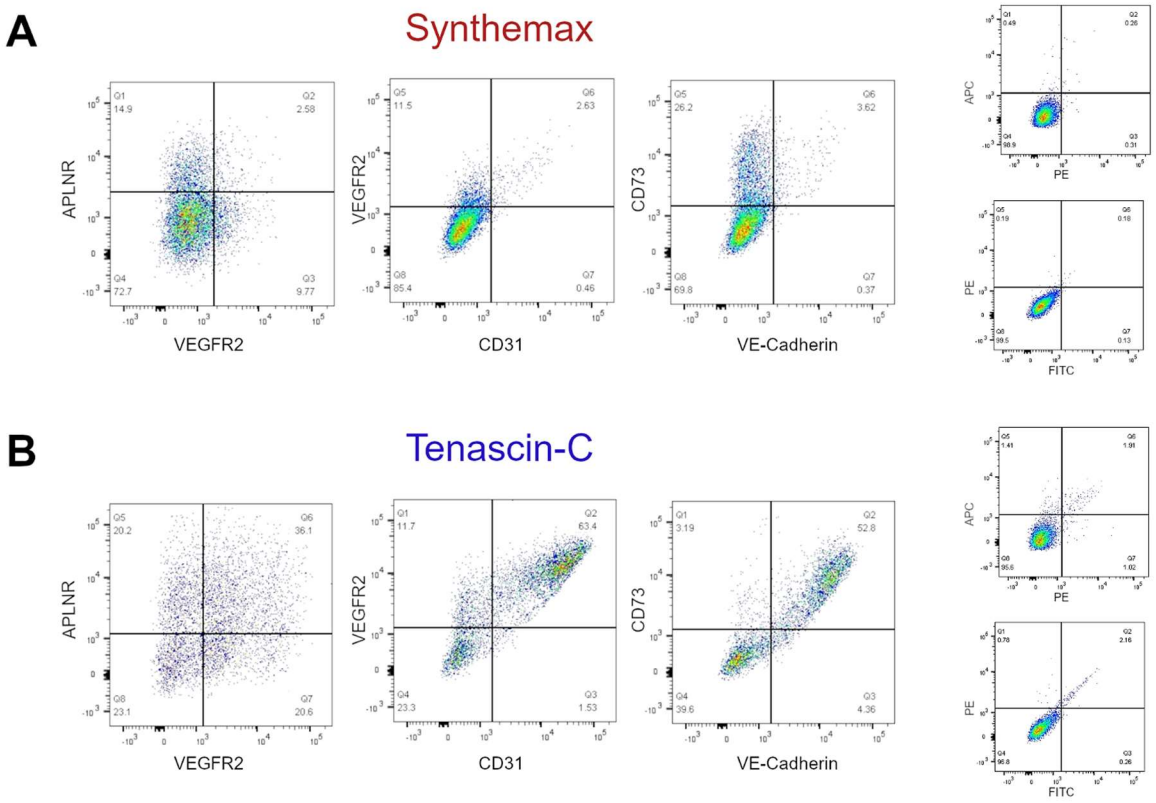

Figure 4.3 Differentiation of human iPSCs into Hemangioblasts: Synthemax vs Tenascin-C

We attempted to differentiate hiPSCs on both Synthemax and Ten-C coated culture into angiogenic hemangioblasts. Cultures were differentiated in parallel and flow cytometry was used to detect endothelial markers within the heterogenous culture. A) Synthemax was inefficient in generating double-positive subcultures after attempting differentiation. B) Ten-C was highly successful in generating subcultures that were double-positive for markers of EC and endothelial progenitors. Primarily the subculture that was $CD31^{+}/VEGFR2^{+}$. Negative control for each condition provided on the right of figure

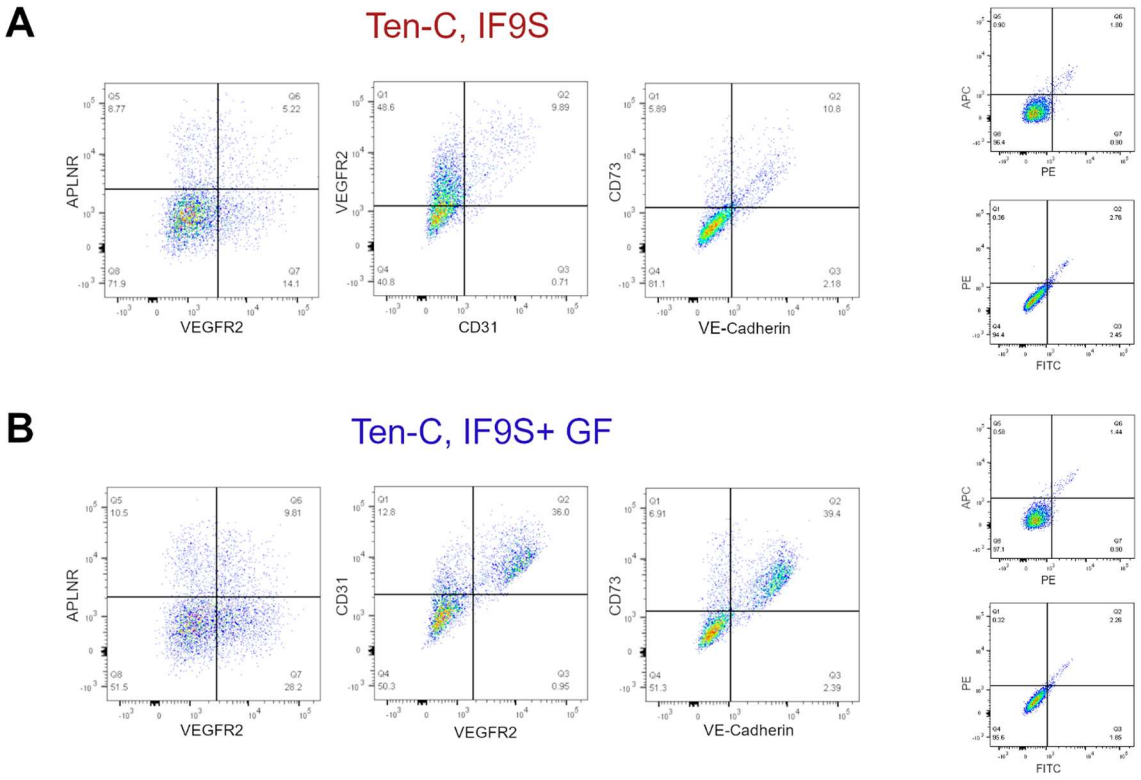

Figure 4.4 Differentiation of human iPSCs into Hemangioblasts: Absence and Supplementation of Growth Factors

We attempted to differentiate hiPSCs on Ten-C with both growth factor deficient (A) and supplemented (B) media. Cultures were differentiated in parallel and flow cytometry was used to detect endothelial markers within the heterogenous culture. We failed to detect substantial $CD31^{+}/VEGFR^{+}$ subcultures and minimal $VE\text{-}Cadherin^{+}/CD73^{+}$ subculture in cells differentiated without growth factors.

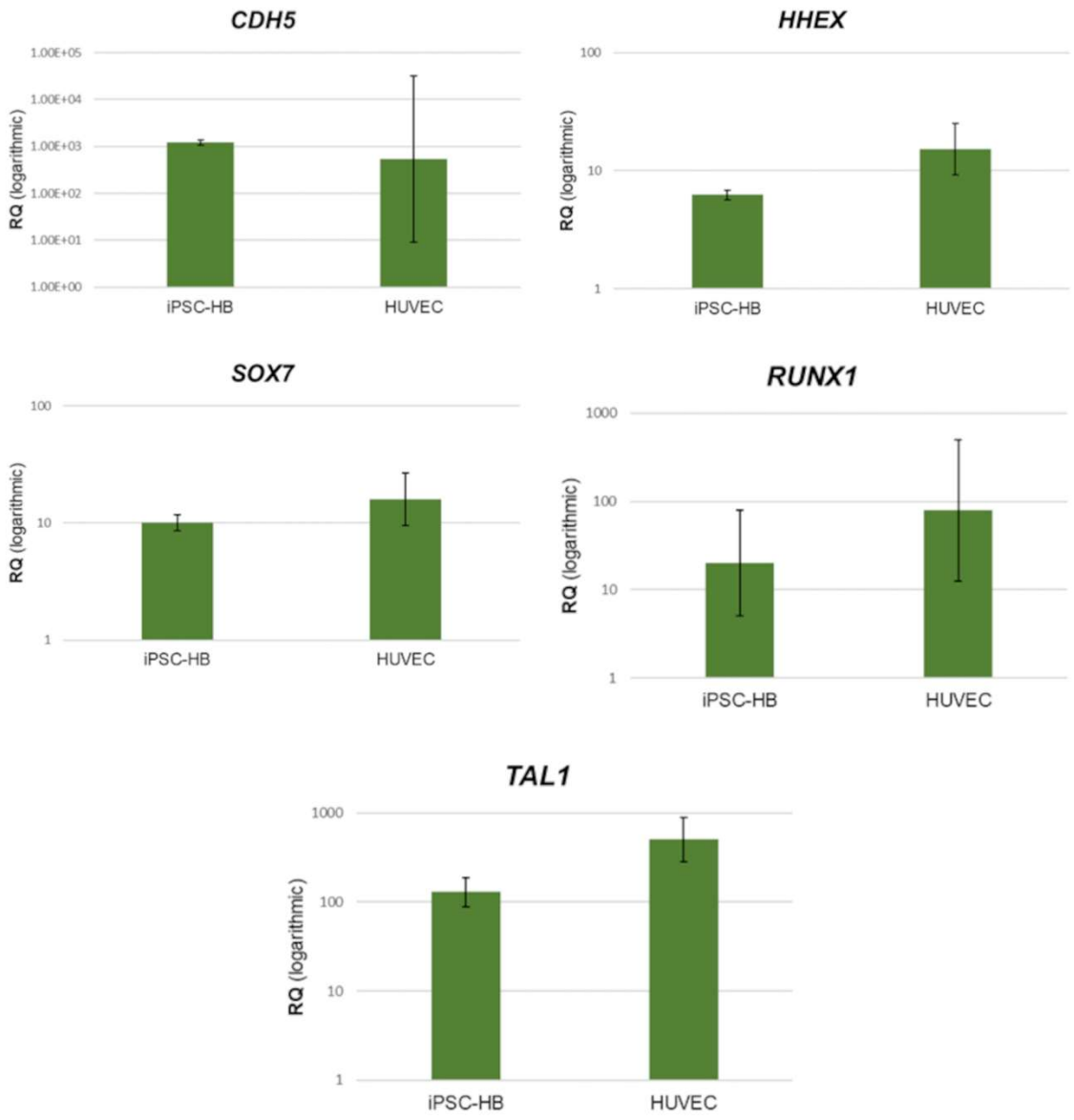

Figure 4.5 Increase in certain endothelial/hematopoietic genes in human iPSC-derived Hemangioblasts

Quantitative RT-PCR was used to detect expression of genes linked to hemangioblast development in our heterogenous cultures. We detected an increase in expression of *Cdh5, Hhex, Rux1, Sox7,* and *Tal1* in our cultures compared to undifferentiated human iPSCs. In addition, *Cdh5* had a higher expression in our culture than HUVEC. Samples were run in triplicate.

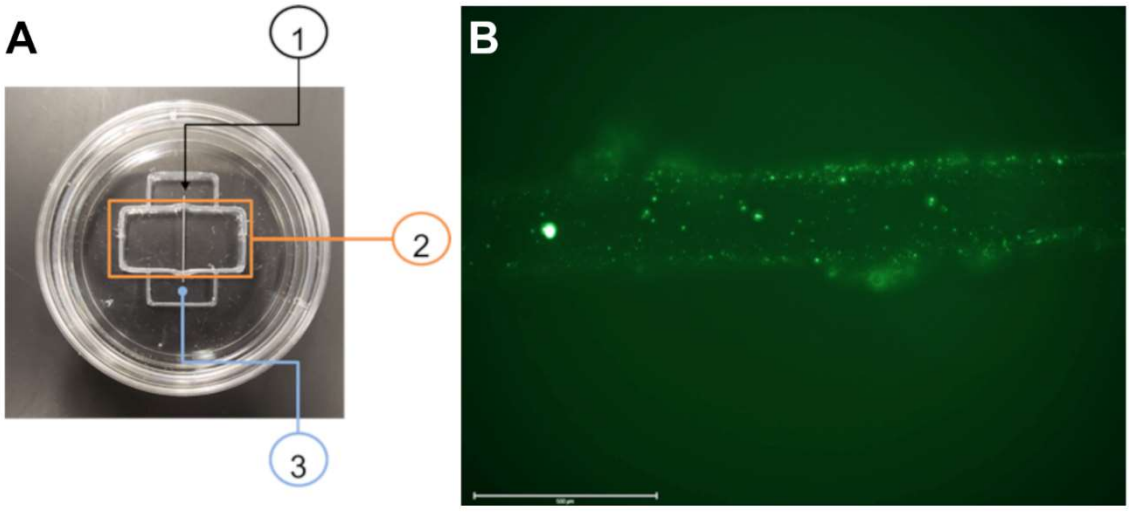

Figure 4.6 Hemangioblasts seed into Microchannel

A) Fibrin hydrogel layout. 300-micron pin for creation of microchannel (1), Silicone boundary for fibrin-endothelial media hydrogel (2), and silicone boundary for media reservoir (3). B) GFP-labeled hemangioblasts were seeded into microchannel left by removal of pin and cultured for 4-days.

Table 4.1 Recipe for IF9S Media

Base Media	
IMDM: F12 (1:1) – Life Technologies	
Component (Manufacture)	Concentration
L-ascorbic acid (Sigma-Aldrich)	10 mg/mL
Monothioglycerol (Sigma-Aldrich)	40 µL/L
Na-Selenite (Sigma-Aldrich)	8.5 µg/mL
Polyvinyl alcohol (Sigma-Aldrich)	10 g/L
GlutaMAX (Life Technologies)	1X
Nonessential amino acids (Life Technologies)	1X
Chemically defined lipid concentrate (Life Technologies)	0.1X
Holo-Transferrin (Sigma-Aldrich)	11 mg/L
Insulin (Life Technologies)	20 mg/L

Chapter 5

Summary, Conclusions, Perspectives and Outlook

Summary and Conclusions

The primary goal of this work was to address the need to develop functional vasculature within tissue-engineered lungs. We focused on the regeneration of vascular endothelium. Despite success in the development of acellular lung scaffolds and seeding them with multiple cell types for both cellular and functional regeneration, vascular complications (i.e., thromboses, hemorrhage, and dysfunctional permeability barrier) have led to their inability to be used clinically or for long-term studies. With this in mind, our aims were to

1. Determine the endothelial cell phenotype needed to generate functional, patent pulmonary vasculature using acellular whole-lung matrices.
2. Generate and compare proteomic data of arterial and venous extracellular matrix (ECM) from pulmonary vasculature and how these differences may affect endothelial progenitors as they become mature endothelial cells.
3. Determine the capability of human-iPSC derived hemangioblast to develop functional endothelium.

Addressing our first aim (**Chapter 2**), we used standard *in vitro* cell culture conditions and our bioreactor system to identify pulmonary endothelial cells from a single source that is capable of overcoming selective tropism displayed by other pulmonary endothelial cells. This subset of rat pulmonary microvascular endothelial progenitor cells (RMEPCs) were sourced from the rat pulmonary microvascular cells (MVECs) and were able to recellularize all vascular areas in an acellular lung scaffold as well as generate a functional barrier. For this project, we compared RMEPCs to MVECs and pulmonary arterial endothelial cells (PAECs) from rats. *In vitro* the RMEPCs were also able to produce more VEGF and TIMP1, endothelial mediators, than both PAECs and MVECs. Initially while being cultured *in vitro*, RMEPCs didn't display the same level of endothelial

markers as the other two EC types under flow, but this changed once they were seeded in acellular mouse lung scaffolds and cultured in our bioreactor system. RMEPCs began to express CD31 and VE-Cadherin within lung constructs, they also produced more VEGF, TIMP1, PAI1, and CXCL1 than PAECs, MVECs, and the combination of the two (PAECs + MVECs). Similar to PAECs and MVECs, RMEPCs were able to bind and uptake acetylated LDL, a function only seen in endothelial cells and macrophages. Finally, despite the lack of pericytes or other supporting cells, RMEPCs were able to create a functional barrier in the presence of flow. The presence, maturation, and function of RMEPCs in this study provides insight on resident pulmonary endothelial progenitors and their use in regenerating pulmonary endothelium for tissue-engineering purposes.

As for our second aim, addressed in **Chapter 3**, we used decellularized porcine pulmonary vascular arteries and veins for label-free liquid chromatography-mass spectrometry (LC/MS) to generate proteomic results of the protein components within each sample group. While unable to conduct direct quantitative comparisons, we observed higher protein diversity and abundance within pulmonary artery ECM proteins compared to vein ECM proteins. Furthermore, we created methacrylated gelatin (GelMA)-based hydrogels embedded with RMEPCs. Within the hydrogels, we were able to incorporate arterial or venous ECM (A-ECM and V-ECM, respectively) particles to observe the effect on RMEPC maturation. Within a week we observed increased gene expression of several endothelial genes within ECM hydrogels compared to RMEPC *in vitro* and GelMA. We were able to detect increased expression of several endothelial genes, one of which was *Ephnb4*, a gene that is highly expressed in venous ECs and was found to have a higher fold-change in RMEPCs cultured in V-ECM than A-ECM.

Finally addressing our third aim (**Chapter 4**), we adapted a protocol originally designed to generate hemogenic hemangioblasts to instead generate angiogenic hemangioblasts. Utilizing this new protocol and transient hypoxic incubation (5% O_2, 5% CO_2, 37°C), we were able to generate $CD31^+/VEGFR2^+$ and VE-$Cadherin^+/CD73^+$ subcultures. Though unconfirmed, we suspect that these two subcultures overlap, providing angiogenic hemangioblasts (HBs). We determined that success for generation of angiogenic HB subcultures was dependent on inclusion of tenascin-C and several growth factors (i.e., BMP4, Activin A, LiCl, FGF2, VEGF-A). Quantitative PCR data also revealed that after differentiation, several genes important in endothelial and hematopoietic differentiation are upregulated within our heterogeneous cultures in comparison to undifferentiated iPSCs. Last, we were able to observe our HBs seed along the luminal wall of a hydrogel microchannel and culture for several days afterwards. This provides us with some indication that our hiPSC-derived HBs are capable of seeding within the lumen of acellular vessels, a necessary function for re-endothelialization.

Perspectives and Outlook

Tissue resident progenitor cells have the ability to repair damaged endothelium, often forming a larger portion of new ECs than those derived from circulating EPCs (Zhang et al., 2014; Mao et al., 2015; Nishimura et al., 2015). Alvarez et al. initially identified the highly proliferative RMEPCs residing in the microvascular EC lung population (Alvarez et al., 2008) and we have confirmed their ability to re-endothelialize acellular lung scaffolds without vessel preference. In addition, we revealed that shortly after being cultured in acellular scaffolds, RMEPCs began to display characteristics and functions of mature ECs. These findings provide researchers in the field with a clear example of using tissue-specific resident EPCs in lieu of primary ECs for re-endothelization of an acellular organ. The next step towards generating functional pulmonary endothelium for

transplantable tissue-engineered lungs would be for identification and implementation of human lung-specific EPC in an acellular lung scaffold. If similar success is observed with such studies, the identified EPCs could be used with additional cell types for total regeneration of blood vessels and recellularization of the entire organ.

Quantitative proteomic analysis of unlabeled peptides from a complex heterogeneous mixture is a challenging task but has been accomplished with absolute and relative quantification of healthy, aged, pathologic and decellularized lungs and vasculature (Talusan et al., 2005; Calle et al., 2016; Godin et al., 2016; Lynch et al., 2016; Rosmark et al., 2018; Angelidis et al., 2019; Merl-Pham et al., 2019; Tian et al., 2019). The data we've acquired from our LC/MS analysis of unlabeled pulmonary arteries and veins will contribute to the current lack of knowledge of pulmonary vasculature ECM proteomics. Through the advice from our collaboration with UMN-CMSP, utilization of other proteomic software may allow us to conduct further quantitative analysis from the data we've already acquired. This may even provide the field with additional insight on intricate differences between ECM proteins between the two vessel types. Future proteomic work may also include processing and identification of proteins from our insoluble fraction as well as inclusion of microvessels.

Initially planned experiments for our A-ECM and V-ECM study included a 2D culture design for comparing the effects of A-ECM and V-ECM particles in an *in vivo* setting. This would be similar to the experimental design presented by Mesquita et al. in which they supplemented their culture media with ECM particles from either atrial or ventricular heart chambers to observe their effect on maturing iPSC-derived cardiomyocytes (Mesquita et al., 2021). We suggest that future experimental designs for ECM hydrogels can be improved by increasing the initial quantity of cells embedded in hydrogels, dialyzing ECM particles to remove any residual detergents from the decellularization

process and decreasing the concentration of ECM particles used in hydrogels. Previous studies on the effect of detergents on cells have described their potential alteration to ECM components and residual negative impacts on recellularization (Simsa et al., 2018). We predict that ECM concentration may inherently be cytotoxic to cells, and other groups have used lower concentrations of ECM particles in their 3D cell cultures (Beachley et al., 2015). Implementation of one or more of these suggestions in addition to broader genotyping of 3D cultured cells for mature, arterial-specific, and venous-specific endothelial genes will provide greater insight on the potential of vessel-specific ECM particle influence on the maturation of endothelial progenitor cells.

Identification of $CD31^+/VEGFR2^+$ and VE-$Cadherin^+/CD73^+$ subcultures from differentiated human iPSCs assures us in the success of differentiating our cells into hemangioblasts as seen similarly by Uenishi et al. Further genotyping and functional experiments should be conducted for verification of this process. Previous studies of hemangioblasts cultured *in vitro* have described the ability of $CD34^+/VEGFR^+$ hemangioblasts to continue forming blast colonies for up to 9 months (Pelosi et al., 2002). Hemangioblasts have also been defined by their ability to differentiate into hematopoietic cells or further mature into definitive vascular endothelial cells (Lu et al., 2007; Feng et al., 2010; Sun et al., 2010; Serrado Marques et al., 2018). We are currently in the process of using single cell RNA-seq of our iPSCs post-differentiation to identify the genomic profiles of the subcultures. This will provide more insight on the cells we hope to use in place of primary ECs for regenerating vasculature. Though we had difficulties in generating a large quantity of cells that would be needed for re-endothelialization of acellular lungs or other organ scaffolds, we believe that iPSC-derived hemangioblasts can still be used in conjunction with other EPCs or ECs for

tissue-engineering purposes or alone in site directed re-endothelialization of damaged endothelium.

References

Accinni, L., Natali, P. G., Silvestrini, M., and Martino, C. De (1983). Actin in the extracellular matrix of smooth muscle cells. An immunoelectron microscopic study. *Connect. Tissue Res.* 11, 69–78. doi:10.3109/03008208309015012.

Adamson, R. H., Sarai, R. K., Altangerel, A., Clark, J. F., Weinbaum, S., and Curry, F. E. (2013). Microvascular permeability to water is independent of shear stress, but dependent on flow direction. *Am J Physiol Hear. Circ Physiol* 304, H1077-84. doi:10.1152/ajpheart.00956.2012.

Ahya, V. N., and Diamond, J. M. (2019). Lung Transplantation. *Med. Clin. North Am.* 103, 425–433. doi:https://doi.org/10.1016/j.mcna.2018.12.003.

Aird, W. C. (2007). Phenotypic heterogeneity of the endothelium: I. Structure, function, and mechanisms. *Circ. Res.* doi:10.1161/01.RES.0000255691.76142.4a.

Aird, W. C. (2012). “Endothelial Cell Heterogeneity,” in *Cold Spring Harb Perspect Med* doi:10.1101/cshperspect.a006429.

Akinnola, I., Rossi, D. R., Meyer, C., Lindsey, A., Haase, D. R., Fogas, S., et al. (2021). Engineering Functional Vasculature in Decellularized Lungs Depends on Comprehensive Endothelial Cell Tropism. *Front. Bioeng. Biotechnol.* 0, 727. doi:10.3389/FBIOE.2021.727869.

Alvarez, D. F., Huang, L., King, J. A., ElZarrad, M. K., Yoder, M. C., and Stevens, T. (2008). Lung microvascular endothelium is enriched with progenitor cells that exhibit vasculogenic capacity. *Am J Physiol Lung Cell Mol Physiol* 294, L419-30. doi:10.1152/ajplung.00314.2007.

Amaya, E. (2013). The hemangioblast: a state of competence. *Blood* 122, 3853–3854. doi:10.1182/blood-2013-10-533075.

Angelidis, I., Simon, L. M., Fernandez, I. E., Strunz, M., Mayr, C. H., Greiffo, F. R., et al. (2019). An atlas of the aging lung mapped by single cell transcriptomics and deep tissue proteomics. *Nat. Commun.* 10. doi:10.1038/S41467-019-08831-9.

Aspalter, I., Gordon, E., Dubrac, A., Ragab, A., Narloch, J., Vizán, P., et al. (2015). Alk1 and Alk5 inhibition by Nrp1 controls vascular sprouting downstream of Notch. *Nat. Commun.* 6. doi:10.1038/NCOMMS8264.

Bach, P., and Bentley, J. (1980). Structural glycoprotein, fact or artefact. *Connect. Tissue Res.* 7, 185–196. doi:10.3109/03008208009152110.

Bahramsoltani, M., Slosarek, I., Spiegelaere, W. De, and Plendl, J. (2014). Angiogenesis and Collagen Type IV Expression in Different Endothelial Cell Culture Systems. *Anat. Histol. Embryol.* 43, 103–115. doi:10.1111/AHE.12052.

Balestrini, J. L., Gard, A. L., Gerhold, K. A., Wilcox, E. C., Liu, A., Schwan, J., et al. (2016). Comparative biology of decellularized lung matrix: Implications of species mismatch in regenerative medicine. *Biomaterials*. doi:10.1016/j.biomaterials.2016.06.025.

Ballard, V. L. T., Sharma, A., Duignan, I., Holm, J. M., Chin, A., Choi, R., et al. (2006). Vascular tenascin-C regulates cardiac endothelial phenotype and

neovascularization. *FASEB J.* 20, 717–719. doi:10.1096/fj.05-5131fje.

Barallobre-Barreiro, J., Loeys, B., Mayr, M., Rienks, M., Verstraeten, A., and Kovacic, J. (2020). Extracellular Matrix in Vascular Disease, Part 2/4: JACC Focus Seminar. *J. Am. Coll. Cardiol.* 75, 2189–2203. doi:10.1016/J.JACC.2020.03.018.

Baruah, J., and Wary, K. K. (2019). Exosomes in the Regulation of Vascular Endothelial Cell Regeneration. *Front. Cell Dev. Biol.* 7. doi:10.3389/fcell.2019.00353.

Beachley, V. Z., Wolf, M. T., Sadtler, K., Manda, S. S., Jacobs, H., Blatchley, M., et al. (2015). Tissue matrix arrays for high throughput screening and systems analysis of cell function. *Nat. Methods* 12, 1197. doi:10.1038/NMETH.3619.

Bella, J., and Hulmes, D. (2017). Fibrillar Collagens. *Subcell. Biochem.* 82, 457–490. doi:10.1007/978-3-319-49674-0_14.

Belloni, P. N., and Tressler, R. J. (1990). Microvascular endothelial cell heterogeneity: interactions with leukocytes and tumor cells. *Cancer Metastasis Rev* 8, 353–389. Available at: http://dx.doi.org/.

Bishop, E. S., Mostafa, S., Pakvasa, M., Luu, H. H., Lee, M. J., Wolf, J. M., et al. (2017). 3-D bioprinting technologies in tissue engineering and regenerative medicine: Current and future trends. *Genes Dis.* 4, 185–195. doi:10.1016/J.GENDIS.2017.10.002.

Bober, M., Enochsson, C., Collin, M., and Mörgelin, M. (2010). Collagen VI Is a Subepithelial Adhesive Target for Human Respiratory Tract Pathogens. *J. Innate Immun.* 2, 160–166. doi:10.1159/000232587.

Bonvillain, R. W., Danchuk, S., Sullivan, D. E., Betancourt, A. M., Semon, J. A., Eagle, M. E., et al. (2012). A nonhuman primate model of lung regeneration: detergent-mediated decellularization and initial in vitro recellularization with mesenchymal stem cells. *Tissue Eng Part A* 18, 2437–2452. doi:10.1089/ten.TEA.2011.0594.

Bonvillain, R. W., Scarritt, M. E., Pashos, N. C., Mayeux, J. P., Meshberger, C. L., Betancourt, A. M., et al. (2013). Nonhuman primate lung decellularization and recellularization using a specialized large-organ bioreactor. *J. Vis. Exp.*, 1–11. doi:10.3791/50825.

Boyd, N. L., Dhara, S. K., Rekaya, R., Godbey, E. A., Hasneen, K., Rao, R. R., et al. (2017). BMP4 Promotes Formation of Primitive Vascular Networks in Human Embryonic Stem Cell–Derived Embryoid Bodies. *Exp. Biol. Med.* 232, 833–843. doi:10.3181/00379727-232-2320833.

Burgess, J. K., Ge, Q., Poniris, M. H., Boustany, S., Twigg, S. M., Black, J. L., et al. (2006). Connective tissue growth factor and vascular endothelial growth factor from airway smooth muscle interact with the extracellular matrix. *Am. J. Physiol. - Lung Cell. Mol. Physiol.* 290. doi:10.1152/ajplung.00287.2005.

Calle, E. A., Ghaedi, M., Sundaram, S., Sivarapatna, A., Tseng, M. K., and Niklason, L. E. (2014). Strategies for Whole Lung Tissue Engineering. *IEEE Trans Biomed Eng* 61, 1482–1496. doi:10.1109/tbme.2014.2314261.

Calle, E. A., Hill, R. C., Leiby, K. L., Le, A. V., Gard, A. L., Madri, J. A., et al. (2016). Targeted proteomics effectively quantifies differences between native lung and detergent-decellularized lung extracellular matrices. *Acta Biomater.* 46, 91.

doi:10.1016/J.ACTBIO.2016.09.043.

Calle, E. A., Leiby, K. L., Raredon, M. B., and Niklason, L. E. (2017). Lung regeneration: Steps toward clinical implementation and use. *Curr. Opin. Anaesthesiol.* doi:10.1097/ACO.0000000000000425.

Calnek, D. S., and Grinnell, B. W. (1998). Thrombomodulin-Dependent Anticoagulant Activity Is Regulated by Vascular Endothelial Growth Factor. *Exp. Cell Res.* 238, 294–298. doi:10.1006/excr.1997.3812.

Cao, J., Navis, A., Cox, B. D., Dickson, A. L., Gemberling, M., Karra, R., et al. (2016). Single epicardial cell transcriptome sequencing identifies Caveolin 1 as an essential factor in zebrafish heart regeneration. *Development* 143, 232–243. doi:10.1242/dev.130534.

Cao, N., and Yao, Z. (2011). The hemangioblast: from concept to authentication. *Anat. Rec. (Hoboken).* 294, 580–588. doi:10.1002/AR.21360.

Castellon, R., Caballero, S., Hamdi, H. K., Atilano, S. R., Aoki, A. M., Tarnuzzer, R. W., et al. (2002). Effects of Tenascin-C on Normal and Diabetic Retinal Endothelial Cells in Culture. *Investig. Ophthalmol. Vis. Sci.* 43, 2758–2766.

Chai, D., Zhang, L., Xi, S., Cheng, Y., Jiang, H., and Hu, R. (2018). Nrf2 Activation Induced by Sirt1 Ameliorates Acute Lung Injury After Intestinal Ischemia/Reperfusion Through NOX4-Mediated Gene Regulation. *Cell. Physiol. Biochem.* 46, 781–792. doi:10.1159/000488736.

Chang, E. I., Bonillas, R. G., El-ftesi, S., Ceradini, D. J., Vial, I. N., Chan, D. A., et al. (2009). Tissue engineering using autologous microcirculatory beds as vascularized bioscaffolds. *Faseb j* 23, 906–915. doi:10.1096/fj.08-114868.

Chen, L., Murray, A., Segal, R., Bushnell, A., and Walsh, M. (1978). Studies on intercellular LETS glycoprotein matrices. *Cell* 14, 377–391. doi:10.1016/0092-8674(78)90123-X.

Chen, P., Cescon, M., and Bonaldo, P. (2013). Collagen VI in cancer and its biological mechanisms. *Trends Mol. Med.* 19, 410–417. doi:10.1016/J.MOLMED.2013.04.001.

Cheresh, D. A., and Stupack, D. G. (2008). Regulation of angiogenesis: Apoptotic cues from the ECM. *Oncogene* 27, 6285–6298. doi:10.1038/onc.2008.304.

Chiu, J. J., and Chien, S. (2011). Effects of disturbed flow on vascular endothelium: pathophysiological basis and clinical perspectives. *Physiol Rev* 91, 327–387. doi:10.1152/physrev.00047.2009.

Choi, K., Kennedy, M., Kazarov, A., Papadimitriou, J. C., and Keller, G. (1998). A common precursor for hematopoietic and endothelial cells. *Development* 125, 725–732. Available at: http://dx.doi.org/.

Chung-Welch, N., Patton, W. F., Yen-Patton, G. P., Hechtman, H. B., and Shepro, D. (1989). Phenotypic comparison between mesothelial and microvascular endothelial cell lineages using conventional endothelial cell markers, cytoskeletal protein markers and in vitro assays of angiogenic potential. *Differentiation* 42, 44–53. Available at: http://dx.doi.org/.

Clark, J., Alvarez, D. F., Alexeyev, M., King, J. A., Huang, L., Yoder, M. C., et al. (2008). Regulatory role for nucleosome assembly protein-1 in the proliferative and vasculogenic phenotype of pulmonary endothelium. *Am J Physiol Lung Cell Mol Physiol* 294, L431-9. doi:10.1152/ajplung.00316.2007.

Claudio-Rizo, J. A., Mendoza-Novelo, B., Delgado, J., Castellano, L. E., and Mata-Mata, J. L. (2016). A new method for the preparation of biomedical hydrogels comprised of extracellular matrix and oligourethanes. *Biomed. Mater.* 11, 035016. doi:10.1088/1748-6041/11/3/035016.

Colorado, P. C., Torre, A., Kamphaus, G., Maeshima, Y., Hopfer, H., Takahashi, K., et al. (2000). Anti-angiogenic Cues from Vascular Basement Membrane Collagen. *Cancer Res.* 60.

Conway, E., Collen, D., and Carmeliet, P. (2001). Molecular mechanisms of blood vessel growth. *Cardiovasc. Res.* 49, 507–521. doi:10.1016/S0008-6363(00)00281-9.

Crabbe, A., Liu, Y., Sarker, S. F., Bonenfant, N. R., Barrila, J., Borg, Z. D., et al. (2015). Recellularization of decellularized lung scaffolds is enhanced by dynamic suspension culture. *PLoS One* 10, e0126846. doi:10.1371/journal.pone.0126846.

Crapo, P. M., Gilbert, T. W., and Badylak, S. F. (2011). An overview of tissue and whole organ decellularization processes. *Biomaterials* 32, 3233–3243. doi:10.1016/j.biomaterials.2011.01.057.

Cui, X., Lu, Y. W., Lee, V., Kim, D., Dorsey, T., Wang, Q., et al. (2015). Venous Endothelial Marker COUP-TFII Regulates the Distinct Pathologic Potentials of Adult Arteries and Veins. *Sci. Rep.* 5, 16193. doi:10.1038/SREP16193.

Daly, A. B., Wallis, J. M., Borg, Z. D., Bonvillain, R. W., Deng, B., Ballif, B. A., et al. (2012). Initial binding and recellularization of decellularized mouse lung scaffolds with bone marrow-derived mesenchymal stromal cells. *Tissue Eng Part A* 18, 1–16. doi:10.1089/ten.TEA.2011.0301.

Damodarasamy, M., Vernon, R. B., Chan, C. K., Plymate, S. R., Wight, T. N., and Reed, M. J. (2015). Hyaluronan in aged collagen matrix increases prostate epithelial cell proliferation. *In Vitro Cell. Dev. Biol. Anim.* 51, 50. doi:10.1007/S11626-014-9800-Z.

Damodarasamy, M., Vernon, R. B., Karres, N., Chang, C. H., Bianchi-Frias, D., Nelson, P. S., et al. (2010). Collagen Extracts Derived From Young and Aged Mice Demonstrate Different Structural Properties and Cellular Effects in Three-Dimensional Gels. *Journals Gerontol. Ser. A Biol. Sci. Med. Sci.* 65A, 209. doi:10.1093/GERONA/GLP202.

Davies, P. F., Robotewskyj, A., and Griem, M. L. (1994). Quantitative studies of endothelial cell adhesion. Directional remodeling of focal adhesion sites in response to flow forces. *J Clin Invest* 93, 2031–2038. doi:10.1172/jci117197.

Davis, G. E., and Senger, D. R. (2005). Endothelial extracellular matrix: biosynthesis, remodeling, and functions during vascular morphogenesis and neovessel stabilization. *Circ Res* 97, 1093–1107. doi:10.1161/01.RES.0000191547.64391.e3.

Dawson, D., Pearce, S., Zhong, R., Silverstein, R., Frazier, W., and Bouck, N. (1997). CD36 mediates the In vitro inhibitory effects of thrombospondin-1 on endothelial cells. *J. Cell Biol.* 138, 707–717. doi:10.1083/JCB.138.3.707.

Dawson, D., Volpert, O., Pearce, S., Schneider, A., Silverstein, R., Henkin, J., et al. (1999). Three distinct D-amino acid substitutions confer potent antiangiogenic activity on an inactive peptide derived from a thrombospondin-1 type 1 repeat. *Mol. Pharmacol.* 55, 332–338. doi:10.1124/MOL.55.2.332.

De Jong, O. G., Van Balkom, B. W. M., Schiffelers, R. M., Bouten, C. V. C., and Verhaar, M. C. (2014). Extracellular vesicles: potential roles in regenerative medicine. *Front. Immunol.* 5, 608. doi:10.3389/fimmu.2014.00608.

de la Puente, P., Muz, B., Azab, F., and Azab, A. (2013). Cell trafficking of endothelial progenitor cells in tumor progression. *Clin. Cancer Res.* 19, 3360–3368. doi:10.1158/1078-0432.CCR-13-0462.

Del Sorbo, L., Parotto, M., and Slutsky, A. (2014). Increasing the number of lungs available for transplantation. *Minerva Anestesiol.* 80, 942–953. Available at: https://pubmed.ncbi.nlm.nih.gov/24280815/ [Accessed August 19, 2021].

dela Paz, N. G., and D'Amore, P. A. (2009). Arterial versus venous endothelial cells. *Cell Tissue Res* 335, 5–16. doi:10.1007/s00441-008-0706-5.

Deregibus, M. C., Cantaluppi, V., Calogero, R., Lo Iacono, M., Tetta, C., Biancone, L., et al. (2007). Endothelial progenitor cell - Derived microvesicles activate an angiogenic program in endothelial cells by a horizontal transfer of mRNA. *Blood* 110, 2440–2448. doi:10.1182/blood-2007-03-078709.

Deutsch, M., Meinhart, J., Zilla, P., Howanietz, N., Gorlitzer, M., Froeschl, A., et al. (2009). Long-term experience in autologous in vitro endothelialization of infrainguinal ePTFE grafts. *J Vasc Surg* 49, 352–62; discussion 362. doi:10.1016/j.jvs.2008.08.101.

Di Russo, J., Luik, A., Yousif, L., Budny, S., Oberleithner, H., Hofschröer, V., et al. (2017). Endothelial basement membrane laminin 511 is essential for shear stress response. *EMBO J.* 36, 183–201. doi:10.15252/embj.201694756.

Doi, M., Thyboll, J., Kortesmaa, J., Jansson, K., Iivanainen, A., Parvardeh, M., et al. (2002). Recombinant Human Laminin-10 (α5β1γ1): PRODUCTION, PURIFICATION, AND MIGRATION-PROMOTING ACTIVITY ON VASCULAR ENDOTHELIAL CELLS. *J. Biol. Chem.* 277, 12741–12748. doi:10.1074/JBC.M111228200.

Doi, R., Tsuchiya, T., Mitsutake, N., Nishimura, S., Matsuu-Matsuyama, M., Nakazawa, Y., et al. (2017). Transplantation of bioengineered rat lungs recellularized with endothelial and adipose-derived stromal cells. *Sci Rep* 7, 8447. doi:10.1038/s41598-017-09115-2.

Dumas, S., Meta, E., Borri, M., Luo, Y., Li, Y., Rabelink, T., et al. (2021). Phenotypic diversity and metabolic specialization of renal endothelial cells. *Nat. Rev. Nephrol.* 17, 441–464. doi:10.1038/S41581-021-00411-9.

Fagerholm, S. C., Guenther, C., Asens, M. L., Savinko, T., and Uotila, L. M. (2019). Beta2-Integins and interacting proteins in leukocyte trafficking, immune supression, and immunodeficiency disease. *Front. Immunol.* 10, 254. doi:10.3389/fimmu.2019.00254.

Faury, G., Usson, Y., Robert-Nicoud, M., Robert, L., and Verdetti, J. (1998). Nuclear and

cytoplasmic free calcium level changes induced by elastin peptides in human endothelial cells. *Cell Biol.* 95, 2967–2972. Available at: www.pnas.org. [Accessed August 9, 2021].

Feletou, M., and Vanhoutte, P. M. (2006). Endothelial dysfunction: a multifaceted disorder (The Wiggers Award Lecture). *Am J Physiol Hear. Circ Physiol* 291, H985-1002. doi:10.1152/ajpheart.00292.2006.

Feng, H., Xu, Y., Luo, S., Dang, H., Liu, K., and Sun, W. Q. (2020). Evaluation and preservation of vascular architectures in decellularized whole rat kidneys. *Cryobiology* 95, 72–79. doi:10.1016/J.CRYOBIOL.2020.06.003.

Feng, Q., Lu, S. J., Klimanskaya, I., Gomes, I., Kim, D., Chung, Y., et al. (2010). Hemangioblastic derivatives from human induced pluripotent stem cells exhibit limited expansion and early senescence. *Stem Cells* 28, 704–712. doi:10.1002/stem.321.

Ferkowicz, M. J., and Yoder, M. C. (2005). Blood island formation: Longstanding observations and modern interpretations. *Exp. Hematol.* 33, 1041–1047. doi:10.1016/j.exphem.2005.06.006.

Ferrara, N., Gerber, H., and LeCouter, J. (2003). The biology of VEGF and its receptors. *Nat. Med.* 9, 669–676. doi:10.1038/NM0603-669.

Florczyk, U., Jazwa, A., Maleszewska, M., Mendel, M., Szade, K., Kozakowska, M., et al. (2014). Nrf2 regulates angiogenesis: effect on endothelial cells, bone marrow-derived proangiogenic cells and hind limb ischemia. *Antioxid. Redox Signal.* 20, 1693–1708. doi:https://dx.doi.org/10.1089/ars.2013.5219.

Gadue, P., Huber, T., Nostro, M., Kattman, S., and Keller, G. (2005). Germ layer induction from embryonic stem cells. *Exp. Hematol.* 33, 955–964. doi:10.1016/J.EXPHEM.2005.06.009.

Gao, Y., and Raj, J. (2005). Role of veins in regulation of pulmonary circulation. *Am. J. Physiol. Lung Cell. Mol. Physiol.* 288. doi:10.1152/AJPLUNG.00103.2004.

Giblin, S. P., and Midwood, K. S. (2015). Tenascin-C: Form versus function. *Cell Adhes. Migr.* 9, 48–82. doi:10.4161/19336918.2014.987587.

Gilbert-Honick, J., and Grayson, W. (2020). Vascularized and Innervated Skeletal Muscle Tissue Engineering. *Adv. Healthc. Mater.* 9. doi:10.1002/adhm.201900626.

Gilbert, T. W., Sellaro, T. L., and Badylak, S. F. (2006). Decellularization of tissues and organs. *Biomaterials* 27, 3675–3683. doi:10.1016/j.biomaterials.2006.02.014.

Gille, H., Kowalski, J., Li, B., LeCouter, J., Moffat, B., Zioncheck, T., et al. (2001). Analysis of biological effects and signaling properties of Flt-1 (VEGFR-1) and KDR (VEGFR-2). A reassessment using novel receptor-specific vascular endothelial growth factor mutants. *J. Biol. Chem.* 276, 3222–3230. doi:10.1074/JBC.M002016200.

Gilpin, S. E., Charest, J. M., Ren, X., and Ott, H. C. (2016). Bioengineering Lungs for Transplantation. *Thorac. Surg. Clin.* 26, 163–171. doi:10.1016/j.thorsurg.2015.12.004.

Giobbe, G. G., Crowley, C., Luni, C., Campinoti, S., Khedr, M., Kretzschmar, K., et al.

(2019). Extracellular matrix hydrogel derived from decellularized tissues enables endodermal organoid culture. *Nat. Commun.* 10. doi:10.1038/s41467-019-13605-4.

Godin, L. M., Sandri, B. J., Wagner, D. E., Meyer, C. M., Price, A. P., Akinnola, I., et al. (2016). Decreased laminin expression by human lung epithelial cells and fibroblasts cultured in acellular lung scaffolds from aged mice. *PLoS One*. doi:10.1371/journal.pone.0150966.

Goldman, O., Feraud, O., Boyer-Di Ponio, J., Driancourt, C., Clay, D., Le Bousse-Kerdiles, M., et al. (2009). A boost of BMP4 accelerates the commitment of human embryonic stem cells to the endothelial lineage. *Stem Cells* 27, 1750–1759. doi:10.1002/STEM.100.

Goveia, J., Rohlenova, K., Taverna, F., Treps, L., Conradi, L. C., Pircher, A., et al. (2020). An Integrated Gene Expression Landscape Profiling Approach to Identify Lung Tumor Endothelial Cell Heterogeneity and Angiogenic Candidates. *Cancer Cell* 37, 21-36.e13. doi:10.1016/j.ccell.2019.12.001.

Gramann, M., Wendler, O., Haeberle, L., and Schick, B. (2009). Prominent collagen type VI expression in juvenile angiofibromas. *Histochem. Cell Biol.* 131, 155–164. doi:10.1007/S00418-008-0501-0.

Greenlee, T. K., Ross, R., and Hartman, J. L. (1966). THE FINE STRUCTURE OF ELASTIC FIBERS. *J. Cell Biol.* 30, 59–71. doi:10.1083/JCB.30.1.59.

Gross, P. M. (1992). Chapter 31: Circumventricular organ capillaries. *Prog. Brain Res.* 91, 219–233. doi:10.1016/S0079-6123(08)62338-9.

Guo, Z., and Mo, Z. (2020). Keap1-Nrf2 signaling pathway in angiogenesis and vascular diseases. *J. Tissue Eng. Regen. Med.* 14, 869–883. doi:10.1002/TERM.3053.

Hayden, M. R., Sowers, J. R., and Tyagi, S. C. (2005). The central role of vascular extracellular matrix and basement membrane remodeling in metabolic syndrome and type 2 diabetes: the matrix preloaded. *Cardiovasc. Diabetol.* 4, 9. doi:10.1186/1475-2840-4-9.

Herzog, Y., Guttmann-Raviv, N., and Neufeld, G. (2005). Segregation of arterial and venous markers in subpopulations of blood islands before vessel formation. *Dev. Dyn.* 232, 1047–1055. doi:10.1002/DVDY.20257.

Howell, S., and Doane, K. (1998). Type VI collagen increases cell survival and prevents anti-beta 1 integrin-mediated apoptosis. *Exp. Cell Res.* 241, 230–241. doi:10.1006/EXCR.1998.4051.

Hsieh, S. H., Ying, N. W., Wu, M. H., Chiang, W. F., Hsu, C. L., Wong, T. Y., et al. (2008). Galectin-1, a novel ligand of neuropilin-1, activates VEGFR-2 signaling and modulates the migration of vascular endothelial cells. *Oncogene 2008 2726* 27, 3746–3753. doi:10.1038/sj.onc.1211029.

Hu, G., Strydom, D., Fett, J., Riordan, J., and Vallee, B. (1993). Actin is a binding protein for angiogenin. *Proc. Natl. Acad. Sci. U. S. A.* 90, 1217–1221. doi:10.1073/PNAS.90.4.1217.

Hu, H., Jiang, C., Li, R., and Zhao, J. (2019). Comparison of endothelial cell- and endothelial progenitor cell-derived exosomes in promoting vascular endothelial cell repair. *Int. J. Clin. Exp. Pathol.* 12, 2793–2800. Available at:

http://www.ncbi.nlm.nih.gov/pubmed/31934115 [Accessed April 29, 2020].

Huleihel, L., Hussey, G. S., Naranjo, J. D., Zhang, L., Dziki, J. L., Turner, N. J., et al. (2016). Matrix-bound nanovesicles within ECM bioscaffolds. *Sci. Adv.* 2, e1600502–e1600502. doi:10.1126/sciadv.1600502.

Hynes, R., and Naba, A. (2012). Overview of the matrisome--an inventory of extracellular matrix constituents and functions. *Cold Spring Harb. Perspect. Biol.* 4. doi:10.1101/CSHPERSPECT.A004903.

Ibrahim, S., and Ramamurthi, A. (2008). Hyaluronic acid cues for functional endothelialization of vascular constructs. *J Tissue Eng Regen Med* 2, 22–32. doi:10.1002/term.61.

Iozzo, R. V., and Schaefer, L. (2015). Proteoglycan form and function: A comprehensive nomenclature of proteoglycans. *Matrix Biol.* 42, 11–55. doi:10.1016/j.matbio.2015.02.003.

Ishihara, J., Ishihara, A., Fukunaga, K., Sasaki, K., White, M. J. V., Briquez, P. S., et al. (2018). Laminin heparin-binding peptides bind to several growth factors and enhance diabetic wound healing. *Nat. Commun.* 9. doi:10.1038/s41467-018-04525-w.

Jain, V., Bordes, S., and Bhardwaj, A. (2021). Physiology, Pulmonary Circulatory System. *StatPearls*. Available at: https://www.ncbi.nlm.nih.gov/books/NBK525948/ [Accessed September 17, 2021].

Jiang, X., Li, T., Li, B., Wei, W., Li, F., Chen, S., et al. (2021). SOX7 suppresses endothelial-to-mesenchymal transitions by enhancing VE-cadherin expression during outflow tract development. *Clin. Sci. (Lond).* 135, 829–846. doi:10.1042/CS20201496.

Joddar, B., Kumar, S. A., and Kumar, A. (2018). A Contact-Based Method for Differentiation of Human Mesenchymal Stem Cells into an Endothelial Cell-Phenotype. *Cell Biochem Biophys* 76, 187–195. doi:10.1007/s12013-017-0828-z.

Jones, P., Scott-Burden, T., and Gevers, W. (1979). Glycoprotein, elastin, and collagen secretion by rat smooth muscle cells. *Proc. Natl. Acad. Sci. U. S. A.* 76, 353–357. doi:10.1073/PNAS.76.1.353.

Jourde-Chiche, N., Fakhouri, F., Dou, L., Bellien, J., Burtey, S., Frimat, M., et al. (2019). Endothelium structure and function in kidney health and disease. *Nat. Rev. Nephrol.* 15, 87–108. doi:10.1038/S41581-018-0098-Z.

Kallianpur, A. R., Jordan, J. E., and Brandt, S. J. (1994). The SCL/TAL-1 Gene Is Expressed in Progenitors of Both the Hematopoietic and Vascular Systems During Embryogenesis. *Blood* 83, 1200–1208. doi:10.1182/BLOOD.V83.5.1200.1200.

Kalucka, J., de Rooij, L. P. M. H., Goveia, J., Rohlenova, K., Dumas, S. J., Meta, E., et al. (2020). Single-Cell Transcriptome Atlas of Murine Endothelial Cells. *Cell* 180, 764-779.e20. doi:10.1016/j.cell.2020.01.015.

Kamphaus, G. D., Colorado, P. C., Panka, D. J., Hopfer, H., Ramchandran, R., Torre, A., et al. (2000). Canstatin, a Novel Matrix-derived Inhibitor of Angiogenesis and Tumor Growth *. *J. Biol. Chem.* 275, 1209–1215. doi:10.1074/JBC.275.2.1209.

Kataoka, H., Hayashi, M., Nakagawa, R., Tanaka, Y., Izumi, N., Nishikawa, S., et al. (2011). Etv2/ER71 induces vascular mesoderm from Flk1+PDGFRα+ primitive mesoderm. *Blood* 118, 6975–6986. doi:10.1182/BLOOD-2011-05-352658.

Kim, D., Lee, V., Dorsey, T. B., Niklason, L. E., Gui, L., and Dai, G. (2018). Neuropilin-1 Mediated Arterial Differentiation of Murine Pluripotent Stem Cells. *Stem Cells Dev.* 27, 441. doi:10.1089/SCD.2017.0240.

King, J., Hamil, T., Creighton, J., Wu, S., Bhat, P., McDonald, F., et al. (2004a). Structural and functional characteristics of lung macro- and microvascular endothelial cell phenotypes. *Microvasc. Res.* 67, 139–151. doi:10.1016/J.MVR.2003.11.006.

King, J., Hamil, T., Creighton, J., Wu, S., Bhat, P., McDonald, F., et al. (2004b). Structural and functional characteristics of lung macro- and microvascular endothelial cell phenotypes. *Microvasc Res* 67, 139–151. doi:10.1016/j.mvr.2003.11.006.

Klomp, J., Hyun, J., Klomp, J., Pajcini, K., Rehman, J., and Malik, A. (2020). Comprehensive transcriptomic profiling reveals SOX7 as an early regulator of angiogenesis in hypoxic human endothelial cells. *J. Biol. Chem.* 295, 4796–4808. doi:10.1074/JBC.RA119.011822.

Knust, J., Ochs, M., Jørgen, H., Gundersen, G., and Nyengaard, J. R. (2009). Stereological Estimates of Alveolar Number and Size and Capillary Length and Surface Area in Mice Lungs. 292, 113–122. doi:10.1002/ar.20747.

Koffler, J., Kaufman-Francis, K., Shandalov, Y., Egozi, D., Pavlov, D. A., Landesberg, A., et al. (2011). Improved vascular organization enhances functional integration of engineered skeletal muscle grafts. *Proc Natl Acad Sci USA*, 14789–14794. doi:10.1073/pnas.1017825108/-/DCSupplemental.

Kotloff, R. M., and Thabut, G. (2011). Lung transplantation. *Am J Respir Crit Care Med* 184, 159–171. doi:10.1164/rccm.201101-0134CI.

Krock, B., Skuli, N., and Simon, M. (2011). Hypoxia-induced angiogenesis: good and evil. *Genes Cancer* 2, 1117–1133. doi:10.1177/1947601911423654.

Kuijper, S., Turner, C., and Adams, R. (2007). Regulation of angiogenesis by Eph-ephrin interactions. *Trends Cardiovasc. Med.* 17, 145–151. doi:10.1016/J.TCM.2007.03.003.

Kular, J., Basu, S., and Sharma, R. (2014). The extracellular matrix: Structure, composition, age-related differences, tools for analysis and applications for tissue engineering. *J. Tissue Eng.* 5. doi:10.1177/2041731414557112.

Kurobe, H., Maxfield, M. W., Breuer, C. K., and Shinoka, T. (2012). Concise review: tissue-engineered vascular grafts for cardiac surgery: past, present, and future. *Stem Cells Transl Med* 1, 566–571. doi:10.5966/sctm.2012-0044.

Kyriakides, T. R., Zhu, Y. H., Smith, L. T., Bain, S. D., Yang, Z., Lin, M. T., et al. (1998). Mice that lack thrombospondin 2 display connective tissue abnormalities that are associated with disordered collagen fibrillogenesis, an increased vascular density, and a bleeding diathesis. *J. Cell Biol.* 140, 419–430. doi:10.1083/jcb.140.2.419.

Lamandé, S., Mörgelin, M., Adams, N., Selan, C., and Allen, J. (2006). The C5 domain

of the collagen VI alpha3(VI) chain is critical for extracellular microfibril formation and is present in the extracellular matrix of cultured cells. *J. Biol. Chem.* 281, 16607–16614. doi:10.1074/JBC.M510192200.

Lawler, P. R., and Lawler, J. (2012). Molecular basis for the regulation of angiogenesis by thrombospondin-1 and -2. *Cold Spring Harb. Perspect. Med.* 2. doi:10.1101/cshperspect.a006627.

Le, A., Hatachi, G., Beloiartsev, A., Ghaedi, M., Engler, A., Baevova, P., et al. (2017). Efficient and Functional Endothelial Repopulation of Whole Lung Organ Scaffolds. *ACS Biomater. Sci. Eng.* 3, 2000–2010. doi:10.1021/ACSBIOMATERIALS.6B00784.

Leiby, K. L., Raredon, M. S. B., and Niklason, L. E. (2020). Bioengineering the Blood-gas Barrier. *Compr. Physiol.* 10, 415. doi:10.1002/CPHY.C190026.

Lepedda, A. J., Nieddu, G., Formato, M., Baker, M. B., Fernández-Pérez, J., and Moroni, L. (2021). Glycosaminoglycans: From Vascular Physiology to Tissue Engineering Applications. *Front. Chem.* 9. doi:10.3389/fchem.2021.680836.

Liao, E. C., Paw, B. H., Oates, A. C., Pratt, S. J., Postlethwait, J. H., and Zon, L. I. (1998). SCL/Tal-1 transcription factor acts downstream of cloche to specify hematopoietic and vascular progenitors in zebrafish. *Genes Dev.* 12, 621. doi:10.1101/GAD.12.5.621.

Liao, W., Ho, C. Y., Yan, Y. L., Postlethwait, J., and Stainier, D. Y. (2000). Hhex and scl function in parallel to regulate early endothelial and blood differentiation in zebrafish. *Development* 127, 4303–4313. doi:10.1242/DEV.127.20.4303.

Lilly, A., Lacaud, G., and Kouskoff, V. (2017). SOXF transcription factors in cardiovascular development. *Semin. Cell Dev. Biol.* 63, 50–57. doi:10.1016/J.SEMCDB.2016.07.021.

Liu, G., Wu, R., Yang, B., Deng, C., Lu, X., Walker, S. J., et al. (2018). Human Urine-Derived Stem Cell Differentiation to Endothelial Cells with Barrier Function and Nitric Oxide Production. *Stem Cells Transl. Med.* 7, 686–698. doi:https://dx.doi.org/10.1002/sctm.18-0040.

Liu, J., Hao, H., Xia, L., Ti, D., Huang, H., Dong, L., et al. (2015). Hypoxia Pretreatment of Bone Marrow Mesenchymal Stem Cells Facilitates Angiogenesis by Improving the Function of Endothelial Cells in Diabetic Rats with Lower Ischemia. *PLoS One* 10, e0126715. doi:10.1371/JOURNAL.PONE.0126715.

Liu, X., Cai, Y., Xia, C., Wu, H., Li, Q., Xu, Z., et al. (2019). An innovative method to obtain porous porcine aorta scaffolds for tissue engineering. *Artif. Organs* 43, 1162–1169. doi:10.1111/aor.13519.

Liu, Y., Cai, S., Shu, X. Z., Shelby, J., and Prestwich, G. D. (2007). Release of basic fibroblast growth factor from a crosslinked glycosaminoglycan hydrogel promotes wound healing. *Wound Repair Regen.* 15, 245–251. doi:10.1111/J.1524-475X.2007.00211.X.

Lowe, K., Alvarez, D. F., King, J. A., and Stevens, T. (2010). Perivascular fluid cuffs decrease lung compliance by increasing tissue resistance. *Crit Care Med* 38, 1458–1466. doi:10.1097/CCM.0b013e3181de18f0.

Lu, S. J., Feng, Q., Caballero, S., Chen, Y., Moore, M. A., Grant, M. B., et al. (2007). Generation of functional hemangioblasts from human embryonic stem cells. *Nat Methods* 4, 501–509. doi:10.1038/nmeth1041.

Luxey, M., Laussu, J., Jungas, T., and Davy, A. (2011). Generation of transgenic mice overexpressing EfnB2 in endothelial cells. *genesis* 49, 811–820. doi:10.1002/DVG.20785.

Lynch, M., Barallobre-Barreiro, J., Jahangiri, M., and Mayr, M. (2016). Vascular proteomics in metabolic and cardiovascular diseases. *J. Intern. Med.* 280, 325. doi:10.1111/JOIM.12486.

Ma, B., Zhang, K., Hendrie, C., Liang, C., Li, M., Doherty-Kirby, A., et al. (2003). PEAKS: powerful software for peptide de novo sequencing by tandem mass spectrometry. *Rapid Commun. Mass Spectrom.* 17, 2337–2342. doi:10.1002/RCM.1196.

Maeshima, Y., Sudhakar, A., Lively, J., Ueki, K., Kharbanda, S., Kahn, C., et al. (2002). Tumstatin, an endothelial cell-specific inhibitor of protein synthesis. *Science* 295, 140–143. doi:10.1126/SCIENCE.1065298.

Malek, A. M., and Izumo, S. (1996). Mechanism of endothelial cell shape change and cytoskeletal remodeling in response to fluid shear stress. *J Cell Sci* 109 (Pt 4, 713–726. Available at: http://dx.doi.org/.

Mammoto, A., and Mammoto, T. (2019). Vascular Niche in Lung Alveolar Development, Homeostasis, and Regeneration. *Front. Bioeng. Biotechnol.* doi:10.3389/fbioe.2019.00318.

Mao, S., Ye, X., Liu, G., Song, D., and Liu, S. (2015). Resident Endothelial Cells and Endothelial Progenitor Cells Restore Endothelial Barrier Function After Inflammatory Lung Injury. *Arterioscler. Thromb. Vasc. Biol.* 35, 1635–1644. doi:10.1161/ATVBAHA.115.305519.

Marchand, M., Monnot, C., Muller, L., and Germain, S. (2019). Extracellular matrix scaffolding in angiogenesis and capillary homeostasis. *Semin. Cell Dev. Biol.* 89, 147–156. doi:10.1016/j.semcdb.2018.08.007.

Marcu, R., Choi, Y. J., Xue, J., Fortin, C. L., Wang, Y., Nagao, R. J., et al. (2018). Human Organ-Specific Endothelial Cell Heterogeneity. *iScience* 4, 20–35. doi:10.1016/j.isci.2018.05.003.

Martino, M. M., Brkic, S., Bovo, E., Burger, M., Schaefer, D. J., Wolff, T., et al. (2015). Extracellular Matrix and Growth Factor Engineering for Controlled Angiogenesis in Regenerative Medicine. *Front. Bioeng. Biotechnol.* 0, 45. doi:10.3389/FBIOE.2015.00045.

McCarron, J. G., Lee, M. D., and Wilson, C. (2017). The Endothelium Solves Problems That Endothelial Cells Do Not Know Exist. *Trends Pharmacol. Sci.* 38, 322. doi:10.1016/J.TIPS.2017.01.008.

Meng, F., Meyer, C. M., Joung, D., Vallera, D. A., McAlpine, M. C., and Panoskaltsis-Mortari, A. (2019). 3D Bioprinted In Vitro Metastatic Models via Reconstruction of Tumor Microenvironments. *Adv. Mater.* 31, 1806899. doi:10.1002/adma.201806899.

Merl-Pham, J., Basak, T., Knüppel, L., Ramanujam, D., Athanason, M., Behr, J., et al. (2019). Quantitative proteomic profiling of extracellular matrix and site-specific collagen post-translational modifications in an in vitro model of lung fibrosis. *Matrix Biol. Plus* 1. doi:10.1016/J.MBPLUS.2019.04.002.

Mesquita, F. C. P., Morrissey, J., Lee, P.-F., Monnerat, G., Xi, Y., Andersson, H., et al. (2021). Cues from human atrial extracellular matrix enrich the atrial differentiation of human induced pluripotent stem cell-derived cardiomyocytes. *Biomater. Sci.* 9, 3737–3749. doi:10.1039/D0BM01686A.

Michel, R. (1982). Arteries and veins of the normal dog lung: qualitative and quantitative structural differences. *Am. J. Anat.* 164, 227–241. doi:10.1002/AJA.1001640304.

Mogaldea, A., Theodoridis, K., Goecke, T., Tudorache, I., Haverich, A., Cebotari, S., et al. (2019). Assessment of cytocompatibility and mechanical properties of detergent-decellularized ovine pericardial tissue. *Int. J. Artif. Organs*. doi:10.1177/0391398819850583.

Molnar, C., and Gair, J. (2015). 20.2 Gas Exchange across Respiratory Surfaces.

Mongiat, M., Andreuzzi, E., Tarticchio, G., and Paulitti, A. (2016). Extracellular matrix, a hard player in angiogenesis. *Int. J. Mol. Sci.* 17. doi:10.3390/ijms17111822.

Moroianu, J., Fett, J., Riordan, J., and Vallee, B. (1993). Actin is a surface component of calf pulmonary artery endothelial cells in culture. *Proc. Natl. Acad. Sci. U. S. A.* 90, 3815–3819. doi:10.1073/PNAS.90.9.3815.

Murray, J. F. (2010). The structure and function of the Lung. *Internatoinal J. Tuberc. Lung Dis.* 14, 391–96.

Nagao, R. J., Ouyang, Y., Keller, R., Nam, S. Y., Malik, G. R., Emelianov, S. Y., et al. (2016). Ultrasound-guided photoacoustic imaging-directed re-endothelialization of acellular vasculature leads to improved vascular performance. *Acta Biomater.* 32, 35–45. doi:10.1016/j.actbio.2015.12.029.

Neve, A., Cantatore, F. P., Maruotti, N., Corrado, A., and Ribatti, D. (2014). Extracellular Matrix Modulates Angiogenesis in Physiological and Pathological Conditions. *Biomed Res. Int.* 2014. doi:10.1155/2014/756078.

Nichols, J. E., La Francesca, S., Niles, J. A., Vega, S. P., Argueta, L. B., Frank, L., et al. (2018). Production and transplantation of bioengineered lung into a large-animal model. *Sci. Transl. Med.* 10. doi:10.1126/scitranslmed.aao3926.

Niklason, L., and Dai, G. (2018). Arterial Venous Differentiation for Vascular Bioengineering. *Annu Rev Biomed Eng* 20, 431–447. doi:10.1146/annurev-bioeng-062117-121231.

Nishimura, R., Nishiwaki, T., Kawasaki, T., Sekine, A., Suda, R., Urushibara, T., et al. (2015). Hypoxia-induced proliferation of tissue-resident endothelial progenitor cells in the lung. *Am. J. Physiol. Lung Cell. Mol. Physiol.* 308, L746–L758. doi:10.1152/AJPLUNG.00243.2014.

Nourse, M. B., Halpin, D. E., Scatena, M., Mortisen, D. J., Tulloch, N. L., Hauch, K. D., et al. (2010). VEGF induces differentiation of functional endothelium from human embryonic stem cells: implications for tissue engineering. *Arterioscler. Thromb. Vasc. Biol.* 30, 80–89. doi:https://dx.doi.org/10.1161/ATVBAHA.109.194233.

O'Brien, M. F., Goldstein, S., Walsh, S., Black, K. S., Elkins, R., and Clarke, D. (1999). The SynerGraft valve: a new acellular (nonglutaraldehyde-fixed) tissue heart valve for autologous recellularization first experimental studies before clinical implantation. *Semin. Thorac. Cardiovasc. Surg.* 11, 194–200.

O'Neill, J. D., Anfang, R., Anandappa, A., Costa, J., Javidfar, J., Wobma, H. M., et al. (2013). Decellularization of human and porcine lung tissues for pulmonary tissue engineering. in *Annals of Thoracic Surgery* doi:10.1016/j.athoracsur.2013.04.022.

Oh, S.-Y., Kim, J. Y., and Park, C. (2015). The ETS Factor, ETV2: a Master Regulator for Vascular Endothelial Cell Development. *Mol. Cells* 38, 1029. doi:10.14348/MOLCELLS.2015.0331.

Ohata, K., and Ott, H. C. (2000). Human-scale lung regeneration based on decellularized matrix scaffolds as a biologic platform. *Surg. Today* 50, 633–643. doi:10.1007/s00595-020-02000-y.

Okada, H., Takemura, G., Suzuki, K., Oda, K., Takada, C., Hotta, Y., et al. (2017). Three-dimensional ultrastructure of capillary endothelial glycocalyx under normal and experimental endotoxemic conditions. *Crit. Care 2017 211* 21, 1–10. doi:10.1186/S13054-017-1841-8.

Ott, H. C., Matthiesen, T. S., Goh, S. K., Black, L. D., Kren, S. M., Netoff, T. I., et al. (2008). Perfusion-decellularized matrix: using nature's platform to engineer a bioartificial heart. *Nat Med* 14, 213–221. doi:10.1038/nm1684.

Pankov, R., and Yamada, K. M. (2002). Fibronectin at a glance. *J. Cell Sci.* 115, 3861–3863. doi:10.1242/jcs.00059.

Park, J., and Scherer, P. E. (2012). Adipocyte-derived endotrophin promotes malignant tumor progression. *J. Clin. Invest.* 122, 4243. doi:10.1172/JCI63930.

Pashneh-Tala, S., MacNeil, S., and Claeyssens, F. (2016). The tissue-engineered vascular graft - Past, present, and future. *Tissue Eng. - Part B Rev.* 22, 68–100. doi:10.1089/ten.teb.2015.0100.

Patarroyo, M., Tryggvason, K., and Virtanen, I. (2002). Laminin isoforms in tumor invasion, angiogenesis and metastasis. *Semin. Cancer Biol.* 12, 197–207. doi:10.1016/S1044-579X(02)00023-8.

Patten, D. A. (2018). SCARF1: a multifaceted, yet largely understudied, scavenger receptor. *Inflamm. Res.* 67, 627–632. doi:10.1007/s00011-018-1154-7.

Pelosi, E., Valtieri, M., Coppola, S., Botta, R., Gabbianelli, M., Lulli, V., et al. (2002). Identification of the hemangioblast in postnatal life. *Blood* 100, 3203–3208. doi:10.1182/blood-2002-05-1511.

Petersen, T. H., Calle, E. A., Zhao, L., Lee, E. J., Gui, L., Raredon, M. B., et al. (2010). Tissue-engineered lungs for in vivo implantation. *Science (80-.).* 329, 538–541. doi:10.1126/science.1189345.

Petitclerc, E., Boutaud, A., Prestayko, A., Xu, J., Sado, Y., Ninomiya, Y., et al. (2000). New functions for non-collagenous domains of human collagen type IV. Novel integrin ligands inhibiting angiogenesis and tumor growth in vivo. *J. Biol. Chem.* 275, 8051–8061. doi:10.1074/jbc.275.11.8051.

Powers, K. A., and Dhamoon, A. S. (2021). Physiology, Pulmonary Ventilation and Perfusion. *StatPearls*. Available at: https://www.ncbi.nlm.nih.gov/books/NBK539907/ [Accessed September 17, 2021].

Price, A. P., England, K. A., Matson, A. M., Blazar, B. R., and Panoskaltsis-Mortari, A. (2010). Development of a decellularized lung bioreactor system for bioengineering the lung: the matrix reloaded. *Tissue Eng Part A* 16, 2581–2591. doi:10.1089/ten.TEA.2009.0659.

Price, A. P., Godin, L. M., Domek, A., Cotter, T., D'Cunha, J., Taylor, D. A., et al. (2015). Automated Decellularization of Intact, Human-Sized Lungs for Tissue Engineering. *Tissue Eng. Part C. Methods* 21, 94. doi:10.1089/TEN.TEC.2013.0756.

Pries, A., and Kuebler, W. (2006). Normal endothelium. *Handb. Exp. Pharmacol.* 176, 1–40. doi:10.1007/3-540-32967-6_1.

Przysinda, A., Feng, W., and Li, G. (2020). Diversity of Organism-Wide and Organ-Specific Endothelial Cells. *Curr. Cardiol. Rep.* 22, 19. doi:10.1007/s11886-020-1275-9.

Pugsley, M. K., and Tabrizchi, R. (2000). The vascular system: An overview of structure and function. *J. Pharmacol. Toxicol. Methods* 44, 333–340. doi:10.1016/S1056-8719(00)00125-8.

Rajendran, P., Rengarajan, T., Thangavel, J., Nishigaki, Y., Sakthisekaran, D., Sethi, G., et al. (2013). The vascular endothelium and human diseases. *Int. J. Biol. Sci.* 9, 1057–1069. doi:10.7150/ijbs.7502.

Ramos, A. L., Darabi, R., Akbarloo, N., Borges, L., Catanese, J., Dineen, S. P., et al. (2010). Clonal analysis reveals a common progenitor for endothelial, myeloid, and lymphoid precursors in umbilical cord blood. *Circ. Res.* 107, 1460–1469. doi:https://dx.doi.org/10.1161/CIRCRESAHA.110.223669.

Raposo, G., and Stoorvogel, W. (2013). Extracellular vesicles: Exosomes, microvesicles, and friends. *J. Cell Biol.* 200, 373–383. doi:10.1083/jcb.201211138.

Ren, X., Moser, P. T., Gilpin, S. E., Okamoto, T., Wu, T., Tapias, L. F., et al. (2015). Engineering pulmonary vasculature in decellularized rat and human lungs. *Nat. Biotechnol.* 33, 1097. doi:doi:10.1038/nbt.3354.

Risau, W., and Flamme, I. (1995). Vasculogenesis. *Annu. Rev. Cell Dev. Biol.* 11, 73–91. doi:10.1146/annurev.cb.11.110195.000445.

Ritter, E. F., Vann, R. D., Wyble, C., Barwick, W. J., and Klitzman, B. (1989). Hydrostatic pressure reduces thrombogenicity of polytetrafluoroethylene vascular grafts. *Am J Physiol* 257, H1076-81. doi:10.1152/ajpheart.1989.257.4.H1076.

Robertson, M. J., Dries-Devlin, J. L., Kren, S. M., Burchfield, J. S., and Taylor, D. A. (2014). Optimizing recellularization of whole decellularized heart extracellular matrix. *PLoS One* 9, e90406. doi:10.1371/journal.pone.0090406.

Robinet, A., Fahem, A., Cauchard, J.-H., Huet, E., Vincent, L., Lorimier, S., et al. (2005). Elastin-derived peptides enhance angiogenesis by promoting endothelial cell migration and tubulogenesis through upregulation of MT1-MMP. *J. Cell Sci.* 118, 343–356. doi:10.1242/JCS.01613.

Rosmark, O., Åhrman, E., Müller, C., Rendin, L. E., Eriksson, L., Malmström, A., et al. (2018). Quantifying extracellular matrix turnover in human lung scaffold cultures. *Sci. Rep.* 8. doi:10.1038/S41598-018-23702-X.

Rozario, T., and DeSimone, D. (2010). The extracellular matrix in development and morphogenesis: a dynamic view. *Dev. Biol.* 341, 126–140. doi:10.1016/J.YDBIO.2009.10.026.

Rubiś, P., Wiśniowska-Śmialek, S., Wypasek, E., Biernacka-Fijalkowska, B., Rudnicka-Sosin, L., Dziewiecka, E., et al. (2016). Fibrosis of extracellular matrix is related to the duration of the disease but is unrelated to the dynamics of collagen metabolism in dilated cardiomyopathy. *Inflamm. Res.* 65, 941. doi:10.1007/S00011-016-0977-3.

Sackett, S. D., Tremmel, D. M., Ma, F., Feeney, A. K., Maguire, R. M., Brown, M. E., et al. (2018). Extracellular matrix scaffold and hydrogel derived from decellularized and delipidized human pancreas. *Sci. Rep.* 8, 1–16. doi:10.1038/s41598-018-28857-1.

Saldin, L. T., Cramer, M. C., Velankar, S. S., White, L. J., and Badylak, S. F. (2017). Extracellular matrix hydrogels from decellularized tissues: Structure and function. *Acta Biomater.* 49, 1–15. doi:10.1016/j.actbio.2016.11.068.

Sandoo, A., Veldhuijzen van Zanten, J. J. C. ., Metsios, G. S., Carroll, D., and Kitas, G. D. (2010). The Endothelium and Its Role in Regulating Vascular Tone. *Open Cardiovasc. Med. J.* 4, 302–312. doi:10.2174/1874192401004010302.

Scarritt, M. E., Bonvillain, R. W., Burkett, B. J., Wang, G., Glotser, E. Y., Zhang, Q., et al. (2014). Hypertensive Rat Lungs Retain Hallmarks of Vascular Disease upon Decellularization but Support the Growth of Mesenchymal Stem Cells. *Tissue Eng. Part A* 20, 1426. doi:10.1089/TEN.TEA.2013.0438.

Scarritt, M. E., Pashos, N. C., Motherwell, J. M., Eagle, Z. R., Burkett, B. J., Gregory, A. N., et al. (2018). Re-endothelialization of rat lung scaffolds through passive, gravity-driven seeding of segment-specific pulmonary endothelial cells. *J. Tissue Eng. Regen. Med.* 12, e786–e806. doi:10.1002/term.2382.

Schaefer, L., and Schaefer, R. M. (2010). Proteoglycans: From structural compounds to signaling molecules. *Cell Tissue Res.* 339, 237–246. doi:10.1007/s00441-009-0821-y.

Schultz, G. S., and Wysocki, A. (2009). Interactions between extracellular matrix and growth factors in wound healing. *Wound Repair Regen.* 17, 153–162. doi:10.1111/j.1524-475X.2009.00466.x.

Seo, H.-R., Jeong, H. E., Joo, H. J., Choi, S.-C., Park, C.-Y., Kim, J.-H., et al. (2016). Intrinsic FGF2 and FGF5 promotes angiogenesis of human aortic endothelial cells in 3D microfluidic angiogenesis system. *Sci. Reports 2016 61* 6, 1–11. doi:10.1038/srep28832.

Serrado Marques, J., Teixeira, V., Jacinto, A., and Tavares, A. T. (2018). Identification of Novel Hemangioblast Genes in the Early Chick Embryo. *Cells* 7. doi:10.3390/cells7020009.

Shin, D., and Anderson, D. J. (2005). Isolation of arterial-specific genes by subtractive hybridization reveals molecular heterogeneity among arterial endothelial cells. *Dev.*

Dyn. 233, 1589–1604. doi:10.1002/DVDY.20479.

Shin, D., Garcia-Cardena, G., Hayashi, S. I., Gerety, S., Asahara, T., Stavrakis, G., et al. (2001). Expression of EphrinB2 Identifies a Stable Genetic Difference Between Arterial and Venous Vascular Smooth Muscle as Well as Endothelial Cells, and Marks Subsets of Microvessels at Sites of Adult Neovascularization. *Dev. Biol.* 230, 139–150. doi:10.1006/DBIO.2000.9957.

Siavashi, V., Nassiri, S. M., Rahbarghazi, R., Vafaei, R., and Sariri, R. (2016). ECM-Dependence of Endothelial Progenitor Cell Features. *J. Cell. Biochem.* 117, 1934–1946. doi:10.1002/JCB.25492.

Sieminski, A. L., Hebbel, R. P., and Gooch, K. J. (2005). Improved microvascular network in vitro by human blood outgrowth endothelial cells relative to vessel-derived endothelial cells. *Tissue Eng* 11, 1332–1345. doi:10.1089/ten.2005.11.1332.

Simsa, R., Padma, A. M., Heher, P., Hellström, M., Teuschl, A., Jenndahl, L., et al. (2018). Systematic in vitro comparison of decellularization protocols for blood vessels. *PLoS One*. doi:10.1371/journal.pone.0209269.

Song, J., Guyette, J., Gilpin, S., Gonzalez, G., Vacanti, J., and Ott, H. (2013). Regeneration and experimental orthotopic transplantation of a bioengineered kidney. *Nat. Med.* 19, 646–651. doi:10.1038/NM.3154.

Song, J. J., Kim, S. S., Liu, Z., Madsen, J. C., Mathisen, D. J., Vacanti, J. P., et al. (2011). Enhanced in vivo function of bioartificial lungs in rats. *Ann Thorac Surg* 92, 996–998. doi:10.1016/j.athoracsur.2011.05.018.

Song, J., Zhang, X., Buscher, K., Wang, Y., Wang, H., Russo, J. Di, et al. (2017). Endothelial Basement Membrane Laminin 511 Contributes to Endothelial Junctional Tightness and Thereby Inhibits Leukocyte Transmigration. *Cell Rep.* 18, 1256–1269. doi:10.1016/J.CELREP.2016.12.092.

Sorenson, R. L., and Brelje, T. C. (2014). *Atlas of Human Histology*. 3rd ed. Minneapolis: University of Minnesota.

Sottile, J. (2004). Regulation of angiogenesis by extracellular matrix. *Biochim. Biophys. Acta - Rev. Cancer* 1654, 13–22. doi:10.1016/j.bbcan.2003.07.002.

Stabler, C. T., Caires, L. C., Jr., Mondrinos, M. J., Marcinkiewicz, C., Lazarovici, P., et al. (2016a). Enhanced Re-Endothelialization of Decellularized Rat Lungs. *Tissue Eng. Part C. Methods* 22, 439. doi:10.1089/TEN.TEC.2016.0012.

Stabler, C. T., Caires, L. C., Mondrinos, M. J., Marcinkiewicz, C., Lazarovici, P., Wolfson, M. R., et al. (2016b). Enhanced Re-Endothelialization of Decellularized Rat Lungs. *Tissue Eng. - Part C Methods*. doi:10.1089/ten.tec.2016.0012.

Stary, H. C., Blankenhorn, D. H., Chandler, A. B., Glagov, S., W Insull, J., Richardson, M., et al. (1992). A definition of the intima of human arteries and of its atherosclerosis-prone regions. A report from the Committee on Vascular Lesions of the Council on Arteriosclerosis, American Heart Association. *Circulation* 85, 391–405. doi:10.1161/01.CIR.85.1.391.

Steinle, J., Meininger, C., Chowdhury, U., Wu, G., and Granger, H. (2003). Role of ephrin B2 in human retinal endothelial cell proliferation and migration. *Cell. Signal.*

15, 1011–1017. doi:10.1016/S0898-6568(03)00072-X.

Stenzel, D., Franco, C. A., Estrach, S., Mettouchi, A., Sauvaget, D., Rosewell, I., et al. (2011). Endothelial basement membrane limits tip cell formation by inducing Dll4/Notch signalling in vivo. *EMBO Rep.* 12, 1135–1143. doi:10.1038/embor.2011.194.

Sterzel, R. B., Hartner, A., Schlötzer-Schrehardt, U., Voit, S., Hausknecht, B., Doliana, R., et al. (2000). Elastic fiber proteins in the glomerular mesangium in vivo and in cell culture. *Kidney Int.* 58, 1588–1602. doi:10.1046/J.1523-1755.2000.00320.X.

Stevens, T. (2011). Functional and molecular heterogeneity of pulmonary endothelial cells. *Proc Am Thorac Soc* 8, 453–457. doi:10.1513/pats.201101-004MW.

Sudhakar, A., Sugimoto, H., Yang, C., Lively, J., Zeisberg, M., and Kalluri, R. (2003). Human tumstatin and human endostatin exhibit distinct antiangiogenic activities mediated by αvβ3 and α5β1 integrins. *Proc. Natl. Acad. Sci. U. S. A.* 100, 4766. doi:10.1073/PNAS.0730882100.

Sumanas, S., Jorniak, T., and Lin, S. (2005). Identification of novel vascular endothelial–specific genes by the microarray analysis of the zebrafish cloche mutants. *Blood* 106, 534. doi:10.1182/BLOOD-2004-12-4653.

Sun, Y., Li, W., Lu, Z., Chen, R., Ling, J., Ran, Q., et al. (2011). Rescuing replication and osteogenesis of aged mesenchymal stem cells by exposure to a young extracellular matrix. *FASEB J.* 25, 1474. doi:10.1096/FJ.10-161497.

Sun, Z., Zhang, Y., Brunt, K. R., Wu, J., Li, S. H., Fazel, S., et al. (2010). An adult uterine hemangioblast: evidence for extramedullary self-renewal and clonal bilineage potential. *Blood* 116, 2932–2941. doi:10.1182/blood-2010-01-266882.

Suresh, K., and Shimoda, L. (2016). Lung Circulation. *Compr. Physiol.* 6, 897–943. doi:10.1002/CPHY.C140049.

Talusan, P., Bedri, S., Yang, S., Kattapuram, T., Silva, N., Roughley, P. J., et al. (2005). Analysis of Intimal Proteoglycans in Atherosclerosis-prone and Atherosclerosis-resistant Human Arteries by Mass Spectrometry. *Mol. Cell. Proteomics* 4, 1350. doi:10.1074/MCP.M500088-MCP200.

Thabut, G., and Mal, H. (2017). “Outcomes after lung transplantation,” in *J Thorac Dis*, 2684–2691. doi:10.21037/jtd.2017.07.85.

Thyboll, J., Kortesmaa, J., Cao, R., Soininen, R., Wang, L., Iivanainen, A., et al. (2002). Deletion of the Laminin α4 Chain Leads to Impaired Microvessel Maturation. *Mol. Cell. Biol.* 22, 1194–1202. doi:10.1128/mcb.22.4.1194-1202.2002.

Tian, Y., Li, H., Gao, Y., Liu, C., Qiu, T., Wu, H., et al. (2019). Quantitative proteomic characterization of lung tissue in idiopathic pulmonary fibrosis. *Clin. Proteomics* 16, 1–11. doi:10.1186/S12014-019-9226-4.

Tolsma, S. S., Volpert, O. V, Good, D. J., Frazier, W. A., Polverini, P. J., and Bouck, N. (1993). Peptides derived from two separate domains of the matrix protein thrombospondin-1 have anti-angiogenic activity. *J. Cell Biol.* 122, 497–511. doi:10.1083/jcb.122.2.497.

Townsley, M. I. (2012). Structure and composition of pulmonary arteries, capillaries, and

veins. *Compr. Physiol.* 2, 675–709. doi:10.1002/CPHY.C100081.

Tsang, K. M., Hyun, J. S., Cheng, K. T., Vargas, M., Mehta, D., Ushio-Fukai, M., et al. (2017). Embryonic Stem Cell Differentiation to Functional Arterial Endothelial Cells through Sequential Activation of ETV2 and NOTCH1 Signaling by HIF1alpha. *Stem cell reports* 9, 796–806. doi:https://dx.doi.org/10.1016/j.stemcr.2017.07.001.

Tucker, R. P., Spring, J., Baumgartner, S., Martin, D., Hagios, C., Poss, P. M., et al. (1994). Novel tenascin variants with a distinctive pattern of expression in the avian embryo. *Development* 120, 637–647. doi:10.1242/DEV.120.3.637.

Turner, K., Adams, C., Staelens, S., Deckmyn, H., and San Antonio, J. (2020). Crucial Role for Endothelial Cell α2β1 Integrin Receptor Clustering in Collagen-Induced Angiogenesis. *Anat. Rec. (Hoboken).* 303, 1604–1618. doi:10.1002/AR.24277.

Twardowski, T., Fertalam, A., Orgel, J., and San Antonio, J. (2007). Type I collagen and collagen mimetics as angiogenesis promoting superpolymers. *Curr. Pharm. Des.* 13, 3608–3621. doi:10.2174/138161207782794176.

Uenishi, G., Theisen, D., Lee, J. H., Kumar, A., Raymond, M., Vodyanik, M., et al. (2014). Tenascin C promotes hematoendothelial development and T lymphoid commitment from human pluripotent stem cells in chemically defined conditions. *Stem Cell Reports* 3, 1073–1084. doi:10.1016/j.stemcr.2014.09.014.

van der Merwe, Y., Faust, A. E., Sakalli, E. T., Westrick, C. C., Hussey, G., Conner, I. P., et al. (2019). Matrix-bound nanovesicles prevent ischemia-induced retinal ganglion cell axon degeneration and death and preserve visual function. *Sci. Rep.* 9, 1–15. doi:10.1038/s41598-019-39861-4.

Van Pham, P., Vu, N., Nguyen, H., Dao, T., Le, H., Phi, L., et al. (2017). ETV-2 activated proliferation of endothelial cells and attenuated acute hindlimb ischemia in mice. *In Vitro Cell. Dev. Biol. Anim.* 53, 616–625. doi:10.1007/S11626-017-0151-4.

Veikkola, T., and Alitalo, K. (1999). VEGFs, receptors and angiogenesis. *Semin. Cancer Biol.* 9, 211–220. doi:10.1006/SCBI.1998.0091.

Verhamme, P., and Hoylaerts, M. F. (2006). The pivotal role of the endothelium in haemostasis and thrombosis. *Acta Clin Belg* 61, 213–219. doi:10.1179/acb.2006.036.

Viale, G., Castellani, P., Dorcaratto, A., Pau, A., Sehrbundt, E., Siri, A., et al. (2002). Occurrence of a glioblastoma-associated tenascin-C isoform in cerebral cavernomas and neighboring vessels. *Neurosurgery* 50, 838–842. doi:10.1097/00006123-200204000-00028.

von Drygalski, A., Furlan-Freguia, C., Mosnier, L. O., Yegneswaran, S., Ruf, W., and Griffin, J. H. (2012). Infrared fluorescence for vascular barrier breach in vivo--a novel method for quantitation of albumin efflux. *Thromb Haemost* 108, 981–991. doi:10.1160/th12-03-0196.

Walluscheck, K. P., Steinhoff, G., and Haverich, A. (1996). Endothelial cell seeding of de-endothelialised human arteries: improvement by adhesion molecule induction and flow-seeding technology. *Eur J Vasc Endovasc Surg* 12, 46–53. Available at: http://dx.doi.org/.

Wang, H. U., Chen, Z.-F., and Anderson, D. J. (1998). Molecular Distinction and

Angiogenic Interaction between Embryonic Arteries and Veins Revealed by ephrin-B2 and Its Receptor Eph-B4. *Cell* 93, 741–753. doi:10.1016/S0092-8674(00)81436-1.

Wang, K., Lin, R. Z., Hong, X., Ng, A. H., Lee, C. N., Neumeyer, J., et al. (2020). Robust differentiation of human pluripotent stem cells into endothelial cells via temporal modulation of ETV2 with modified mRNA. *Sci. Adv.* 6. doi:10.1126/SCIADV.ABA7606.

Wei, Y., Gong, J., Xu, Z., and Duh, E. (2016). Nrf2 promotes reparative angiogenesis through regulation of NADPH oxidase-2 in oxygen-induced retinopathy. *Free Radic. Biol. Med.* 99, 234–243. doi:10.1016/J.FREERADBIOMED.2016.08.013.

Weibel, E. R. (2016). Lung morphometry: the link between structure and function. *Cell Tissue Res. 2016 3673* 367, 413–426. doi:10.1007/S00441-016-2541-4.

Weibel, E. R. (2017). Lung morphometry: the link between structure and function Introduction: searching for the structural basis of lung physiology. *Cell Tissue Res.*, 413–426. doi:10.1007/s00441-016-2541-4.

West, J. B. (2009). Comparative physiology of the pulmonary blood-gas barrier: the unique avian solution. *Am J Physiol Regul Integr Comp Physiol* 297, 1625–1634. doi:10.1152/ajpregu.00459.2009.-Two.

Wijelath, E. S., Murray, J., Rahman, S., Patel, Y., Ishida, A., Strand, K., et al. (2002). Novel Vascular Endothelial Growth Factor Binding Domains of Fibronectin Enhance Vascular Endothelial Growth Factor Biological Activity. *Circ. Res.* 91, 25–31. doi:10.1161/01.RES.0000026420.22406.79.

Woldhuis, R. R., Vries, M. de, Timens, W., Berge, M. van den, Demaria, M., Oliver, B. G. G., et al. (2020). Link between increased cellular senescence and extracellular matrix changes in COPD. *https://doi.org/10.1152/ajplung.00028.2020* 319, L48–L60. doi:10.1152/AJPLUNG.00028.2020.

Xu, H., Pumiglia, K., and LaFlamme, S. (2020). Laminin-511 and α6 integrins regulate the expression of CXCR4 to promote endothelial morphogenesis. *J. Cell Sci.* 133. doi:10.1242/JCS.246595.

Xu, L., Huang, Y., Wang, D., Zhu, S., Wang, Z., Yang, Y., et al. (2019). Reseeding endothelial cells with fibroblasts to improve the re-endothelialization of pancreatic acellular scaffolds. *J. Mater. Sci. Mater. Med.* 30. doi:10.1007/S10856-019-6287-X.

Yao, Y., Yao, J., and Boström, K. I. (2019). SOX Transcription Factors in Endothelial Differentiation and Endothelial-Mesenchymal Transitions. *Front. Cardiovasc. Med.* 6, 30. doi:10.3389/FCVM.2019.00030.

Ye, L., Zhang, S., Greder, L., Dutton, J., Keirstead, S. A., Lepley, M., et al. (2013). Effective Cardiac Myocyte Differentiation of Human Induced Pluripotent Stem Cells Requires VEGF. *PLoS One* 8, 53764. doi:10.1371/JOURNAL.PONE.0053764.

Yi, S., Ding, F., Gong, L., and Gu, X. (2017). Extracellular Matrix Scaffolds for Tissue Engineering and Regenerative Medicine. *Curr. Stem Cell Res. Ther.* 12, 233–246. doi:10.2174/1574888X11666160905092513.

You, L.-R., Lin, F.-J., Lee, C. T., DeMayo, F. J., Tsai, M.-J., and Tsai, S. Y. (2005). Suppression of Notch signalling by the COUP-TFII transcription factor regulates

vein identity. *Nat. 2005 4357038* 435, 98–104. doi:10.1038/nature03511.

Young, K. A., and Dilling, D. F. (2019). The Future of Lung Transplantation. *Chest* 155, 465–473. doi:10.1016/j.chest.2018.08.1036.

Yousif, L. F., Di Russo, J., and Sorokin, L. (2013). Laminin isoforms in endothelial and perivascular basement membranes. *Cell Adhes. Migr.* 7, 101–110. doi:10.4161/cam.22680.

Zhang, M., Rehman, J., and Malik, A. B. (2014). Endothelial Progenitor Cells and Vascular Repair. *Curr. Opin. Hematol.* 21, 224. doi:10.1097/MOH.0000000000000041.

Zhao, Y., and Young, S. (1995). Tenascin in rat lung development: in situ localization and cellular sources. *Am. J. Physiol.* 269. doi:10.1152/AJPLUNG.1995.269.4.L482.